# Some Mathematical Challenges from Life Sciences

## Part III

Peter Schuster, Universität Wien
Peter F.Stadler, Universität Leipzig
Günter Wagner, Yale University, New Haven, CT
Angela Stevens, Max-Planck-Institut für Mathematik in den Naturwissenschaften, Leipzig
and
Ivo L. Hofacker, Universität Wien

Oberwolfach, GE, 16.-21.11.2003

1. Mathematics and the life sciences in the 21st century

2. Selection dynamics

**3. RNA evolution *in silico* and optimization of structure and properties**

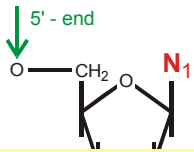


5'-end GCGGAUUUAGCUCAGUUGGGAGAGCGCCAGACUGAAGAUCUGGAGGUCCUGUGUUCGAUCCACAGAAUUCGCACCA 3'-end

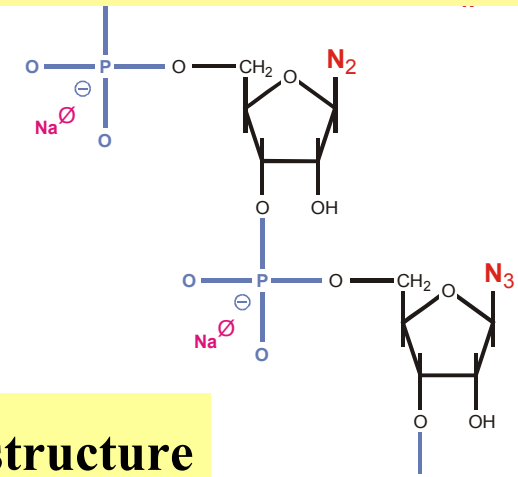


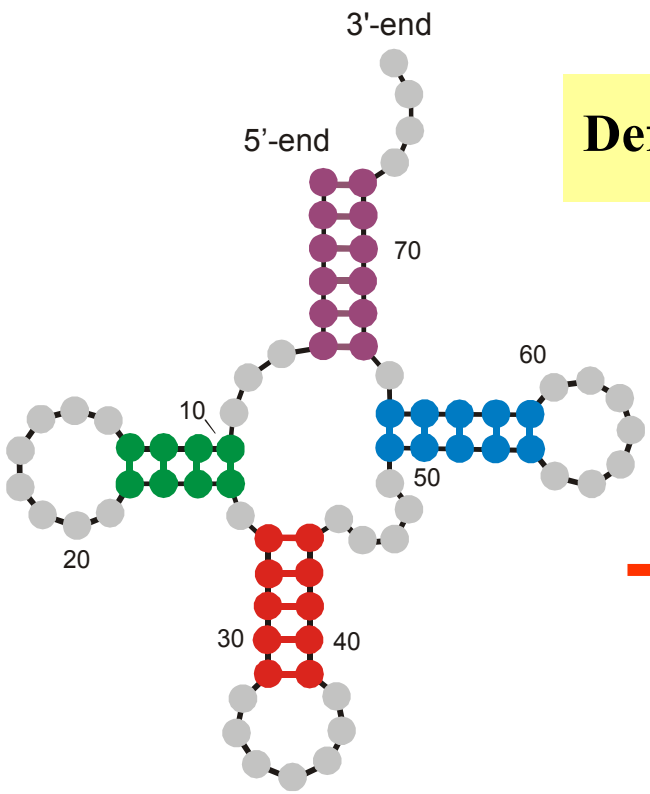


**Definition of RNA structure**

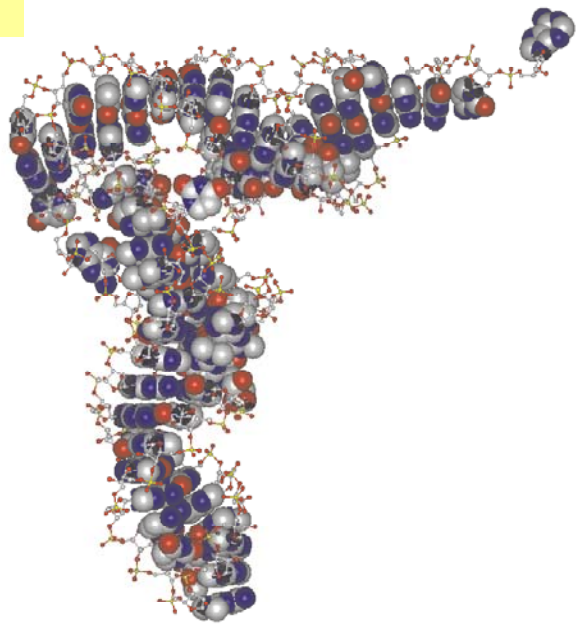

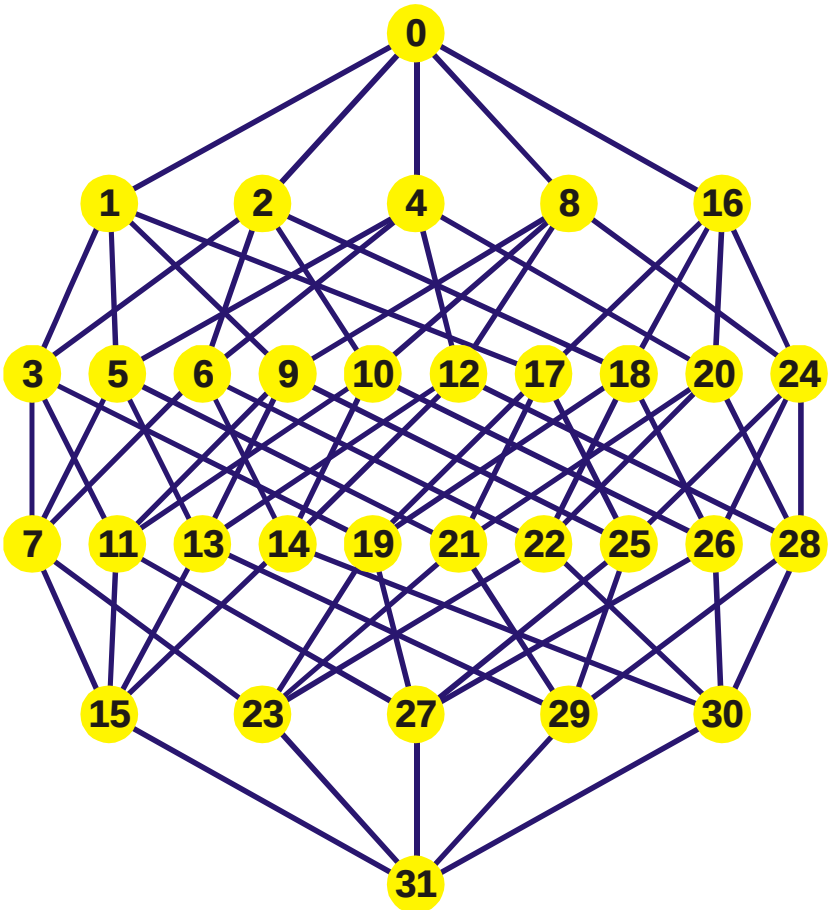


**Mutant class**

0

1

2

3

4

5

**Binary sequences are encoded by their decimal equivalents:**

**C = 0 and G = 1, for example,**

**"0" ≡ 00000 = CCCCC,**

**"14" ≡ 01110 = CGGGC,**

**"29" ≡ 11101 = GGGCG, etc.**

Sequence space of binary sequences of chain lenght n=5

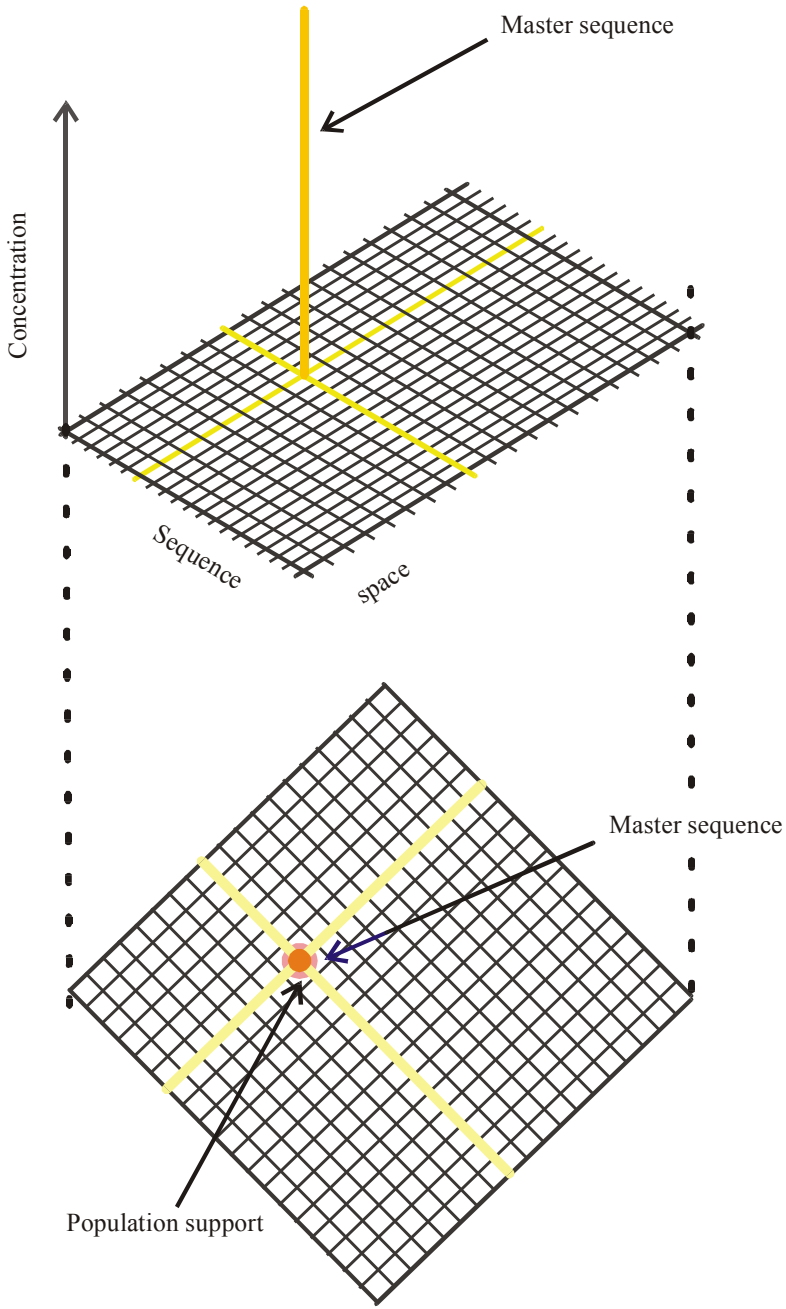


Population and population support in sequence space: The master sequence

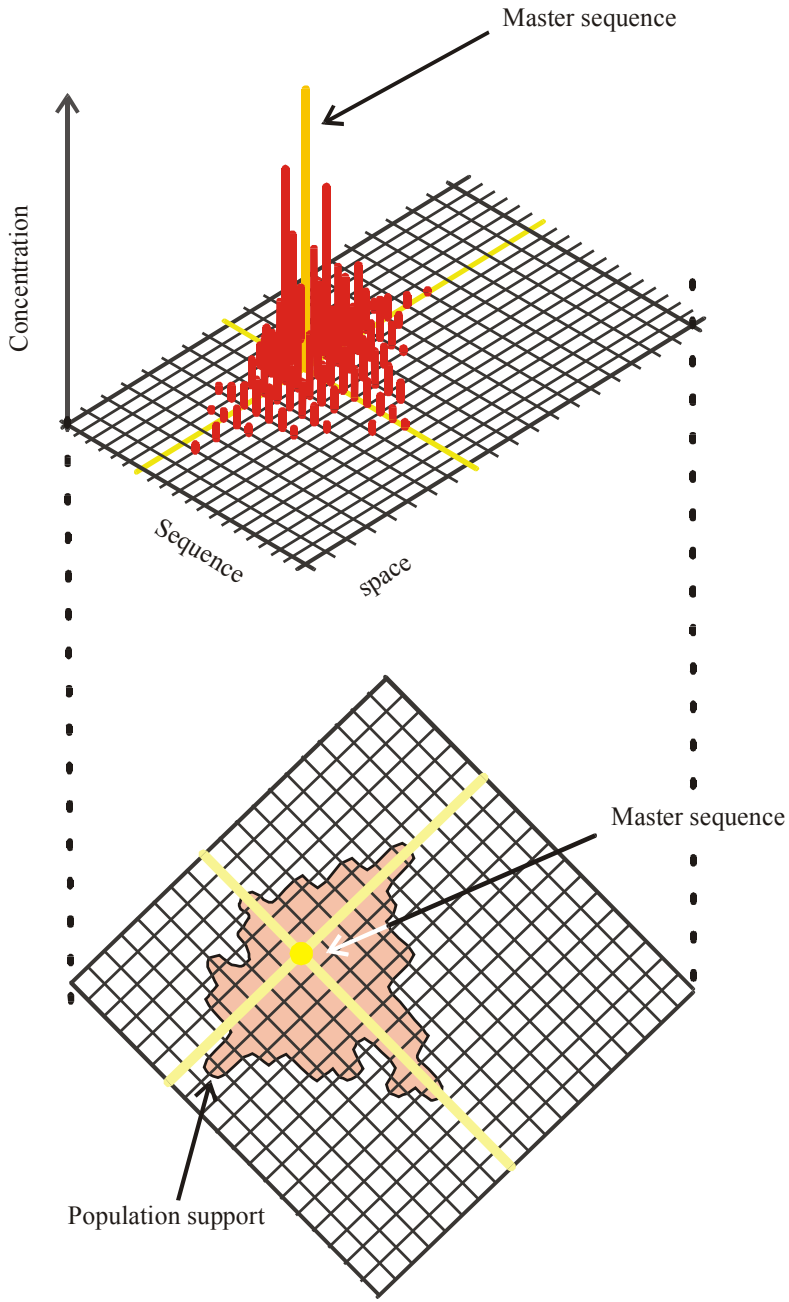


Population and population support in sequence space: The quasi-species

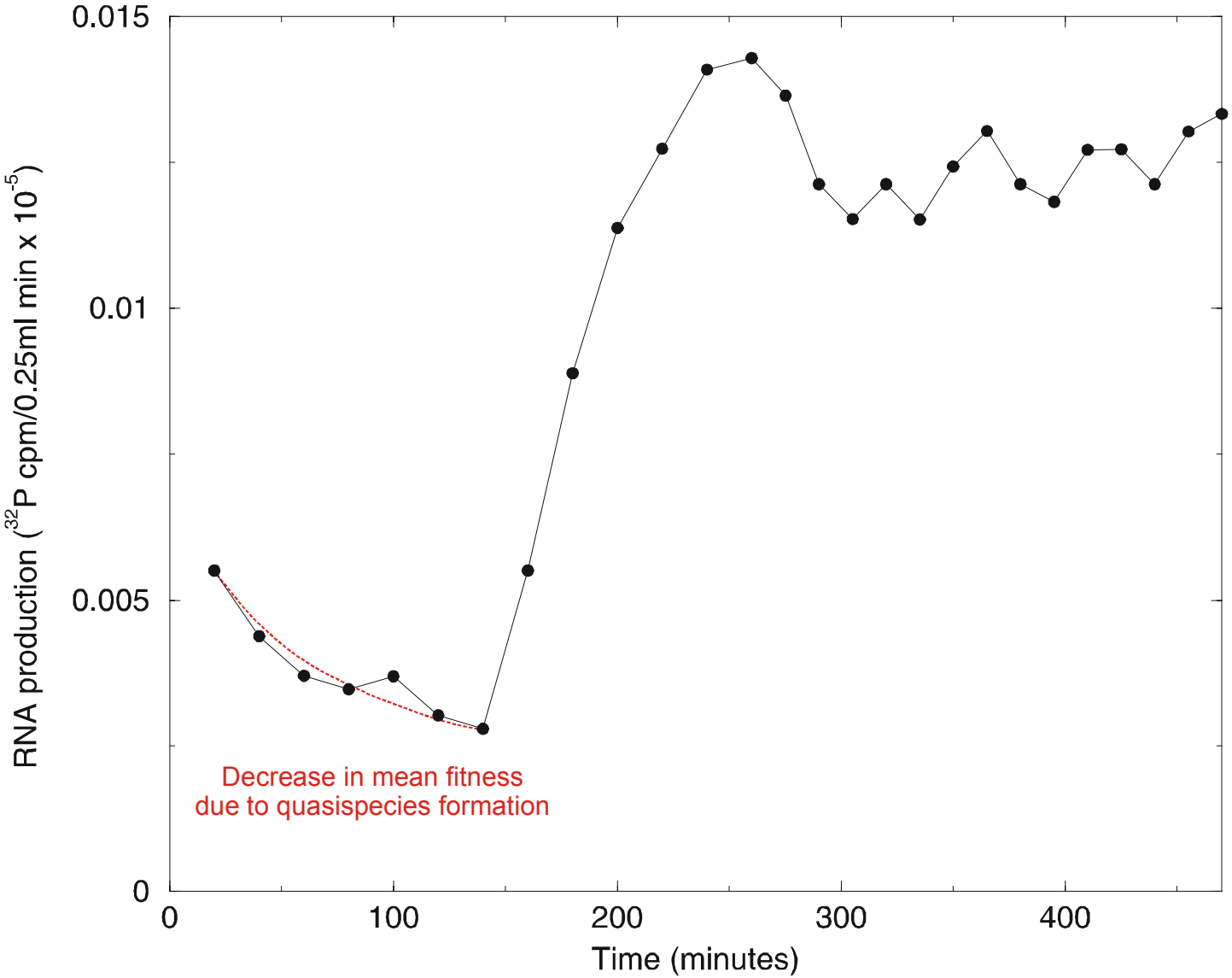


The increase in RNA production rate during a serial transfer experiment

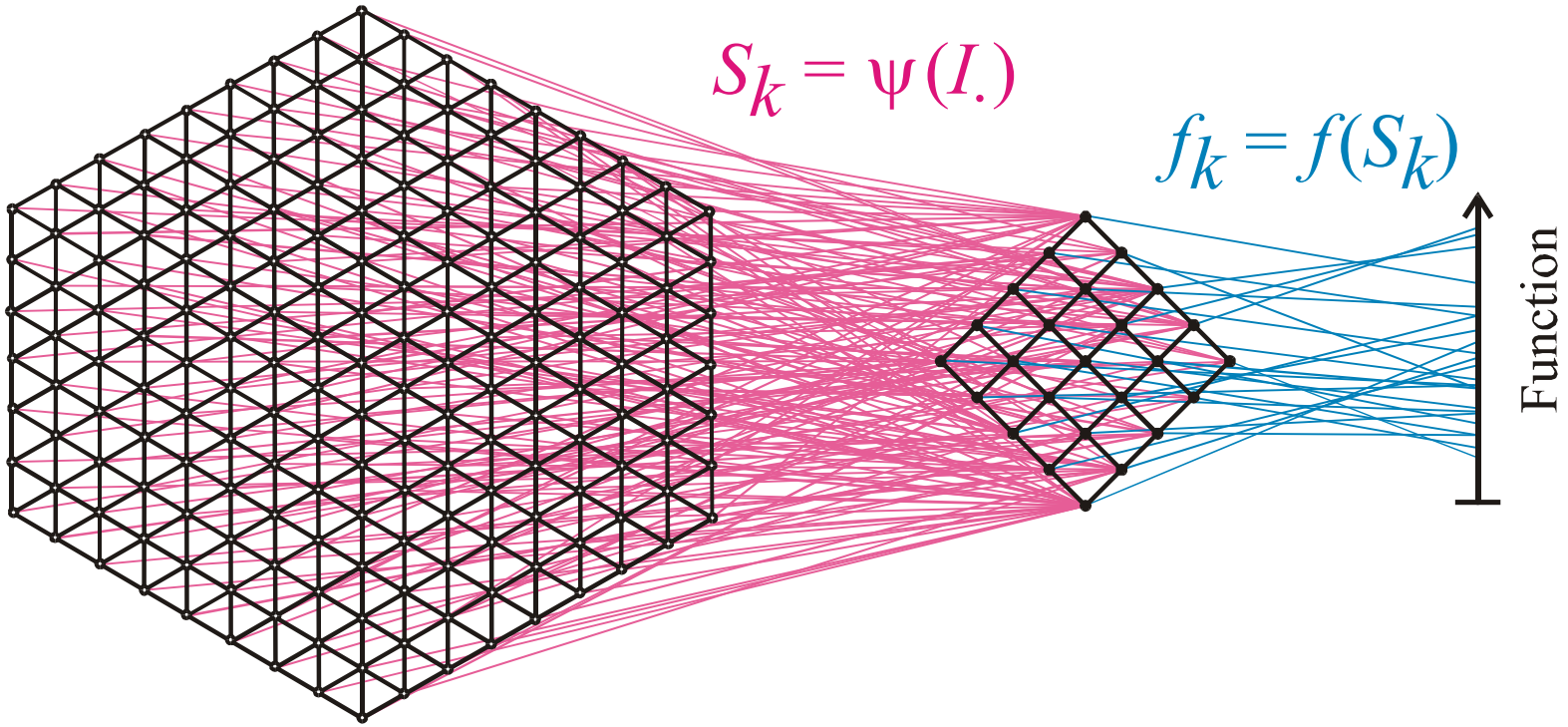


Mapping from sequence space into structure space and into function

5’-end

3’-end

GUAUCGAAAUACGUAGCGUAUGGGGAUGCUGGACGGUCCCAUCGGUACUCCA

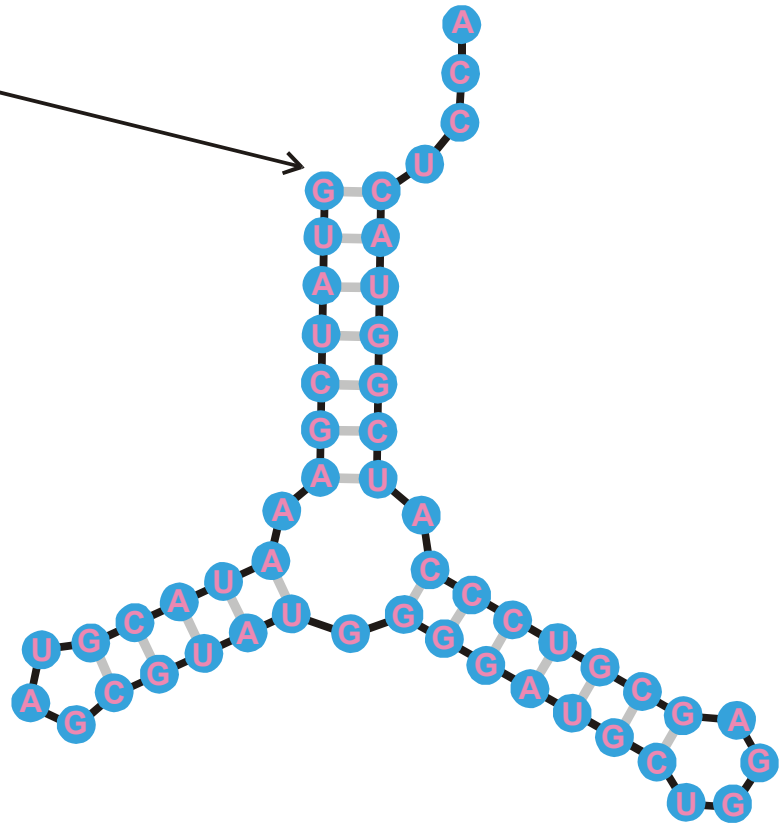

RNAStudio.lnk

GGCGCGCCCGGCGCC

GUAUCGAAAUACGUAGCGUAUGGGGAUGCUGGACGGUCCCAUCGGUACUCCA

UGGUUACGCGUUGGGGUAACGAAGAUUCCGAGAGGAGUUUAGUGACUAGAGG

Folding of RNA sequences into secondary structures of minimal free energy, $DG_0^{300}$

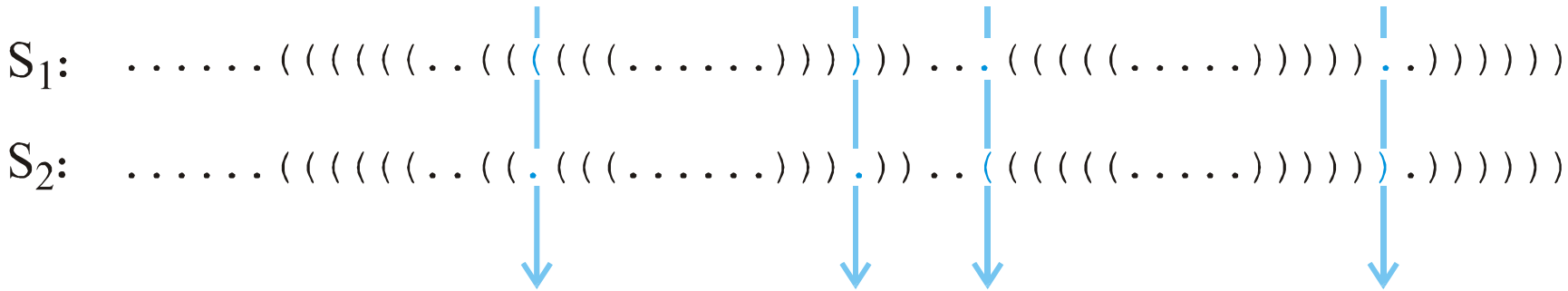


Hamming distance $d_H(S_1,S_2) = 4$

(i) $d_H(S_1,S_1) = 0$

(ii) $d_H(S_1,S_2) = d_H(S_2,S_1)$

(iii) $d_H(S_1,S_3) \P d_H(S_1,S_2) + d_H(S_2,S_3)$

The Hamming distance between structures in parentheses notation forms a metric in structure space

Replication rate constant:

$$f_k = g / [a + Dd_S^{(k)}]$$

$$Dd_S^{(k)} = d_H(S_k, S_t)$$

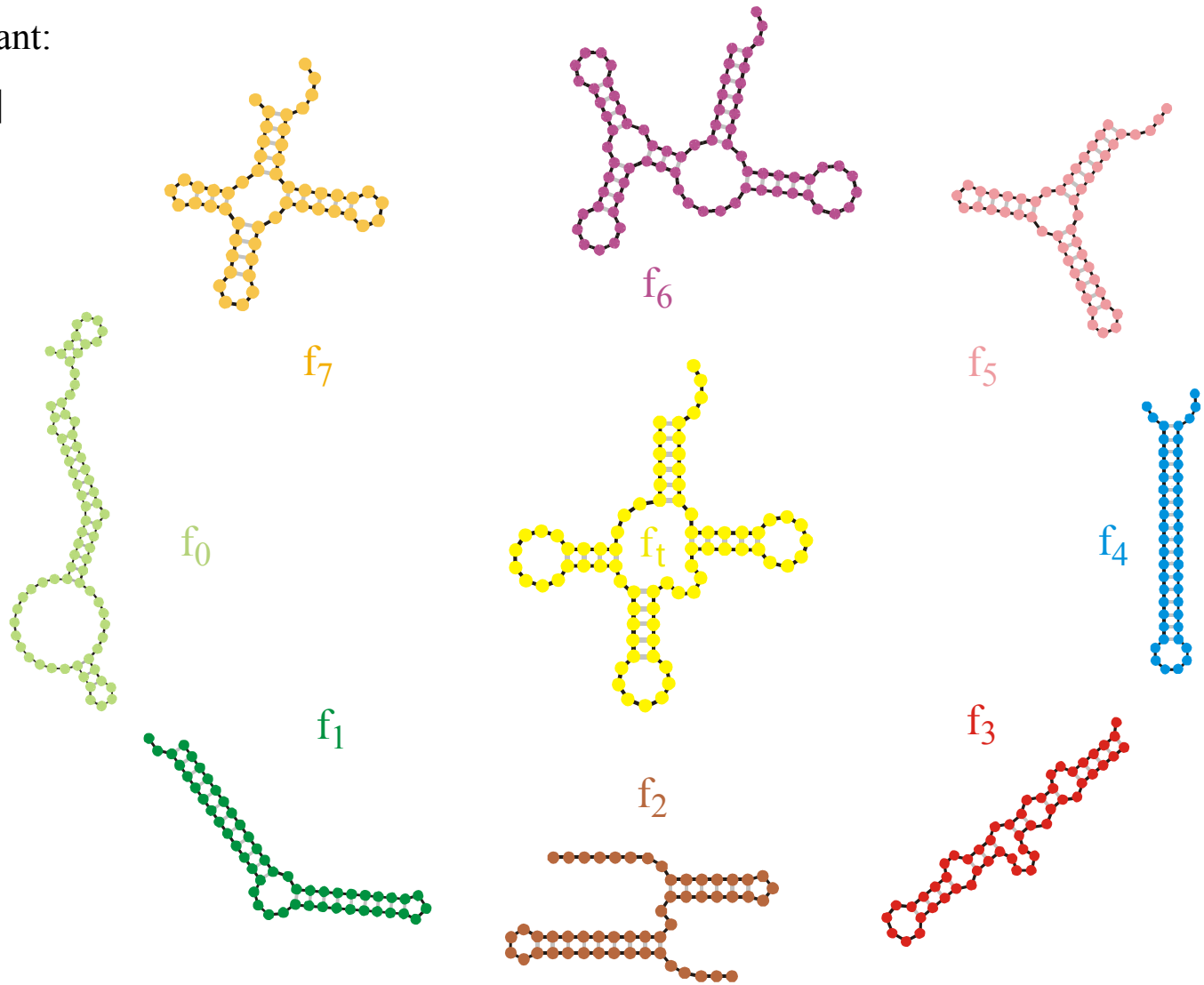


Evaluation of RNA secondary structures yields replication rate constants

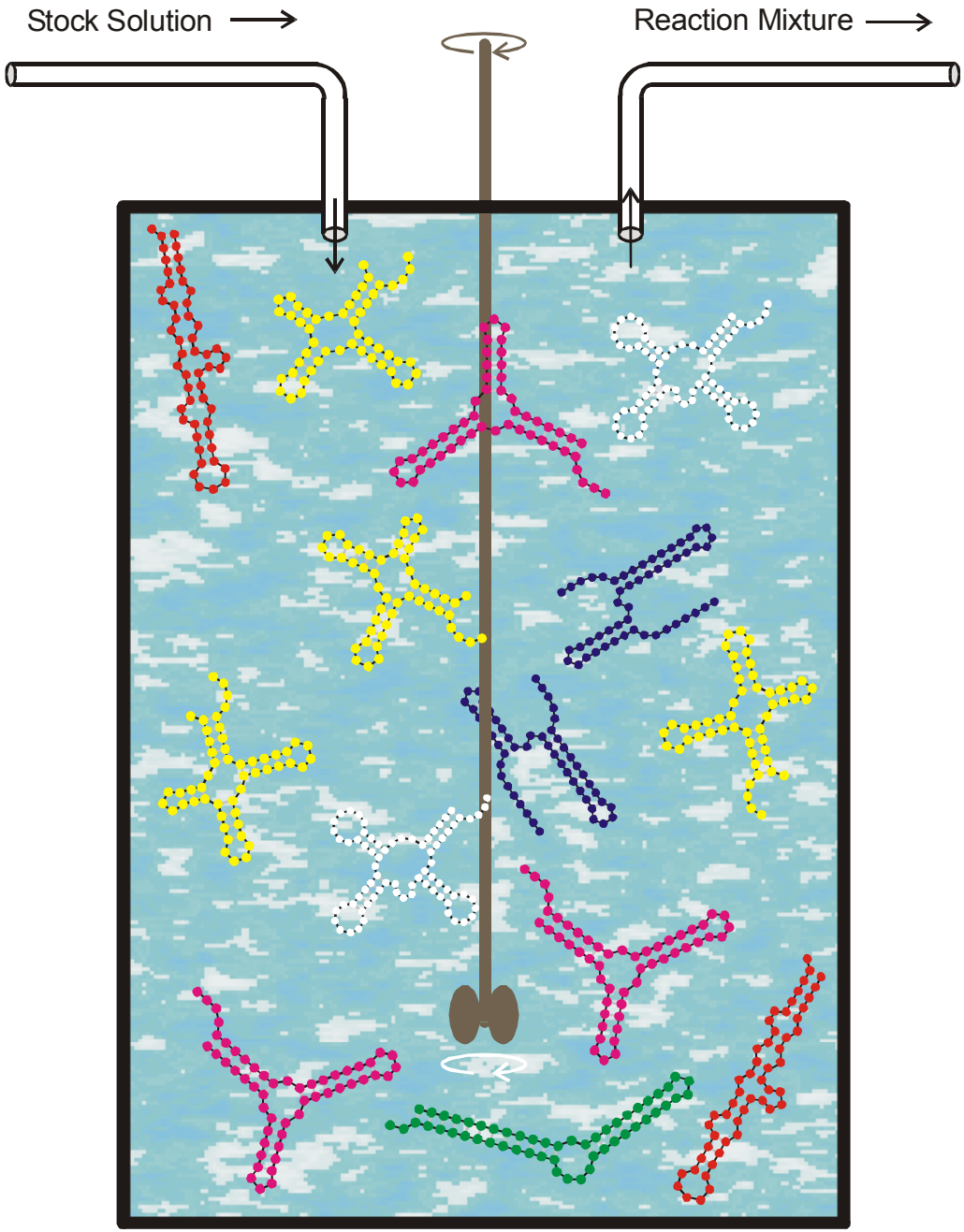


Replication rate constant:

$$f_k = g / [a + Dd_S^{(k)}]$$

$$Dd_S^{(k)} = d_H(S_k, S_t)$$

Selection constraint:

# RNA molecules is controlled by the flow

$$N(t) \approx \overline{N} \pm \sqrt{\overline{N}}$$

The flowreactor as a device for studies of evolution ***in vitro*** and ***in silico***

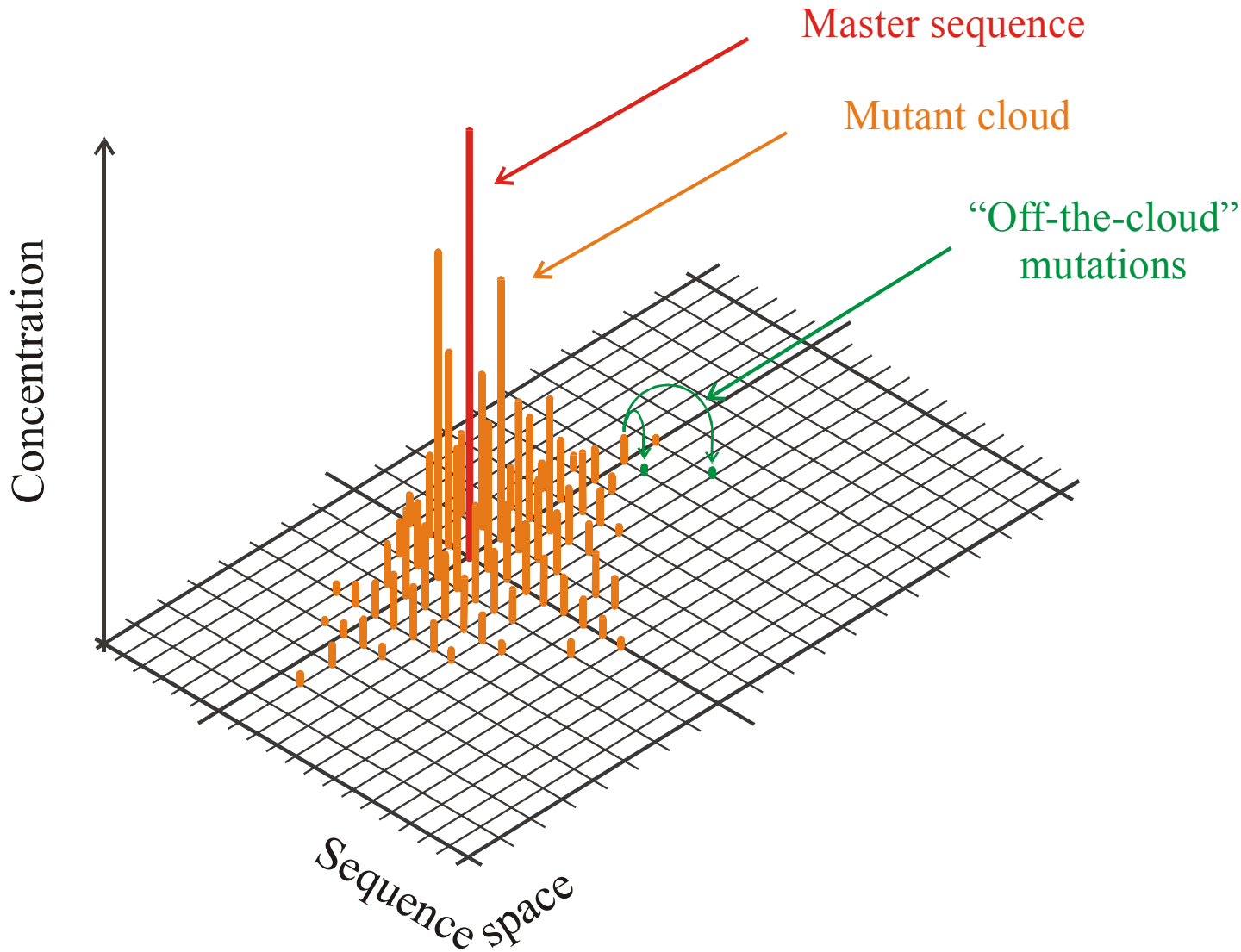


The molecular quasispecies
in sequence space

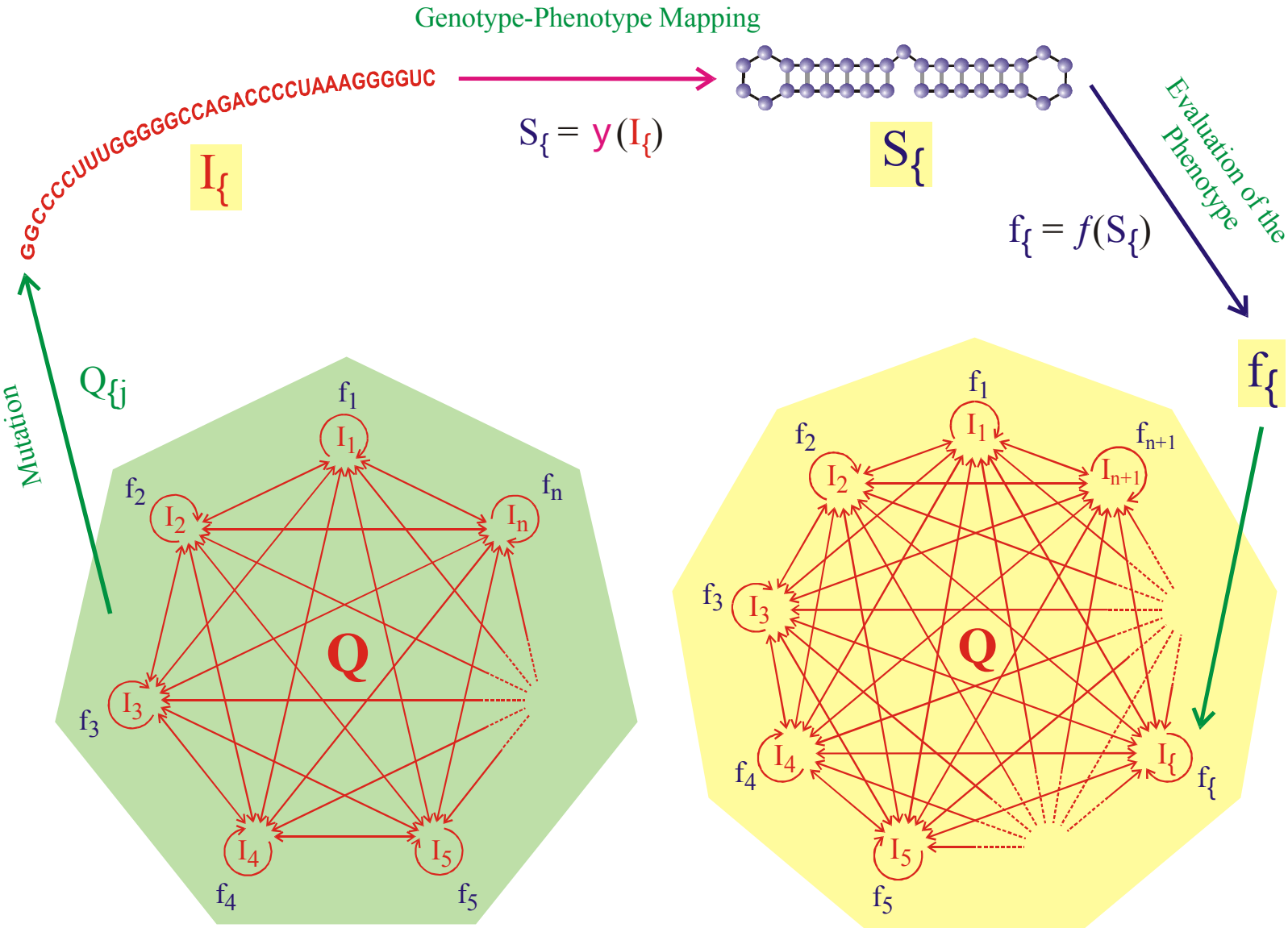


Evolutionary dynamics
including molecular phenotypes

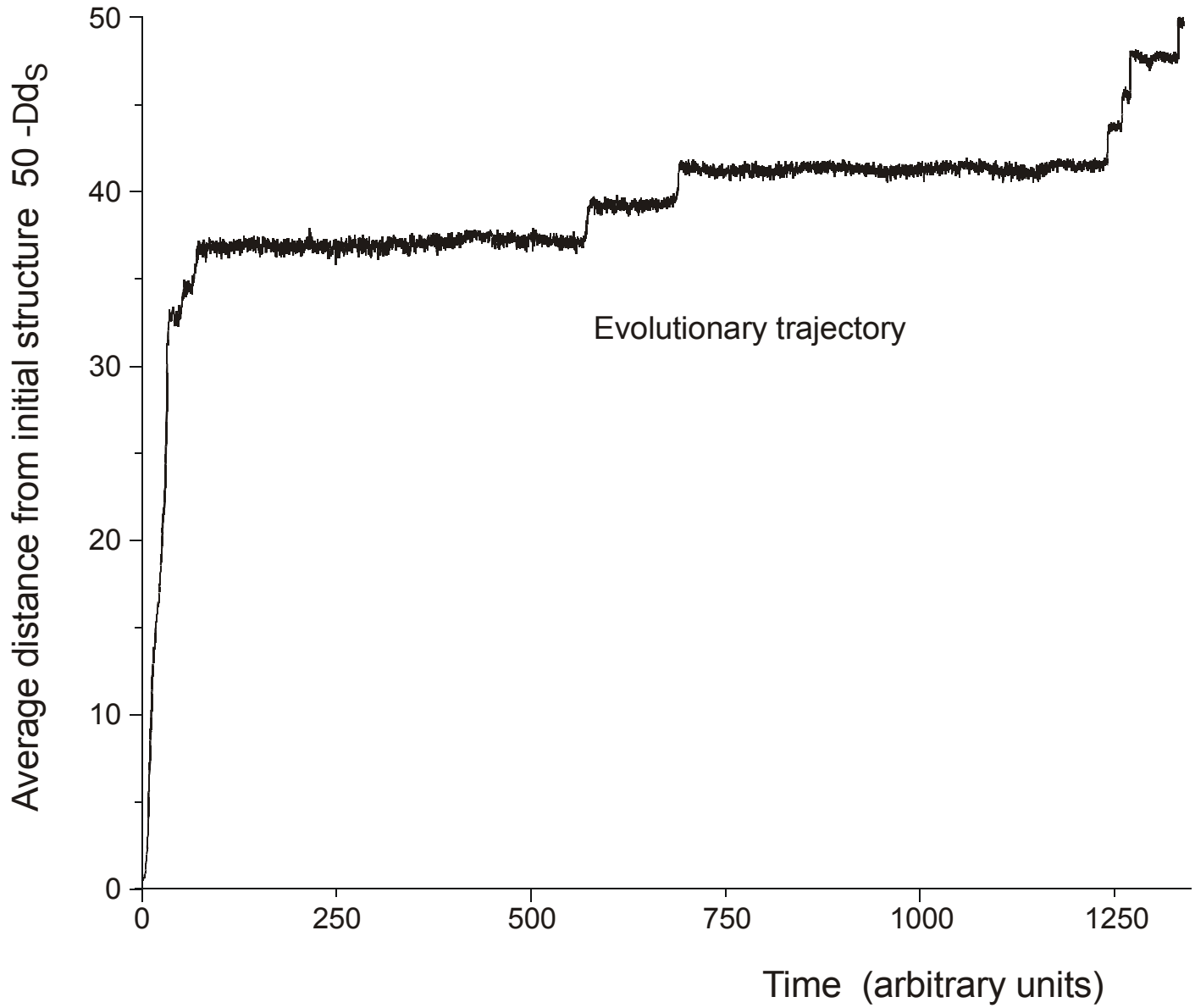


***In silico*** optimization in the flow reactor: Trajectory (**biologists‘ view**)

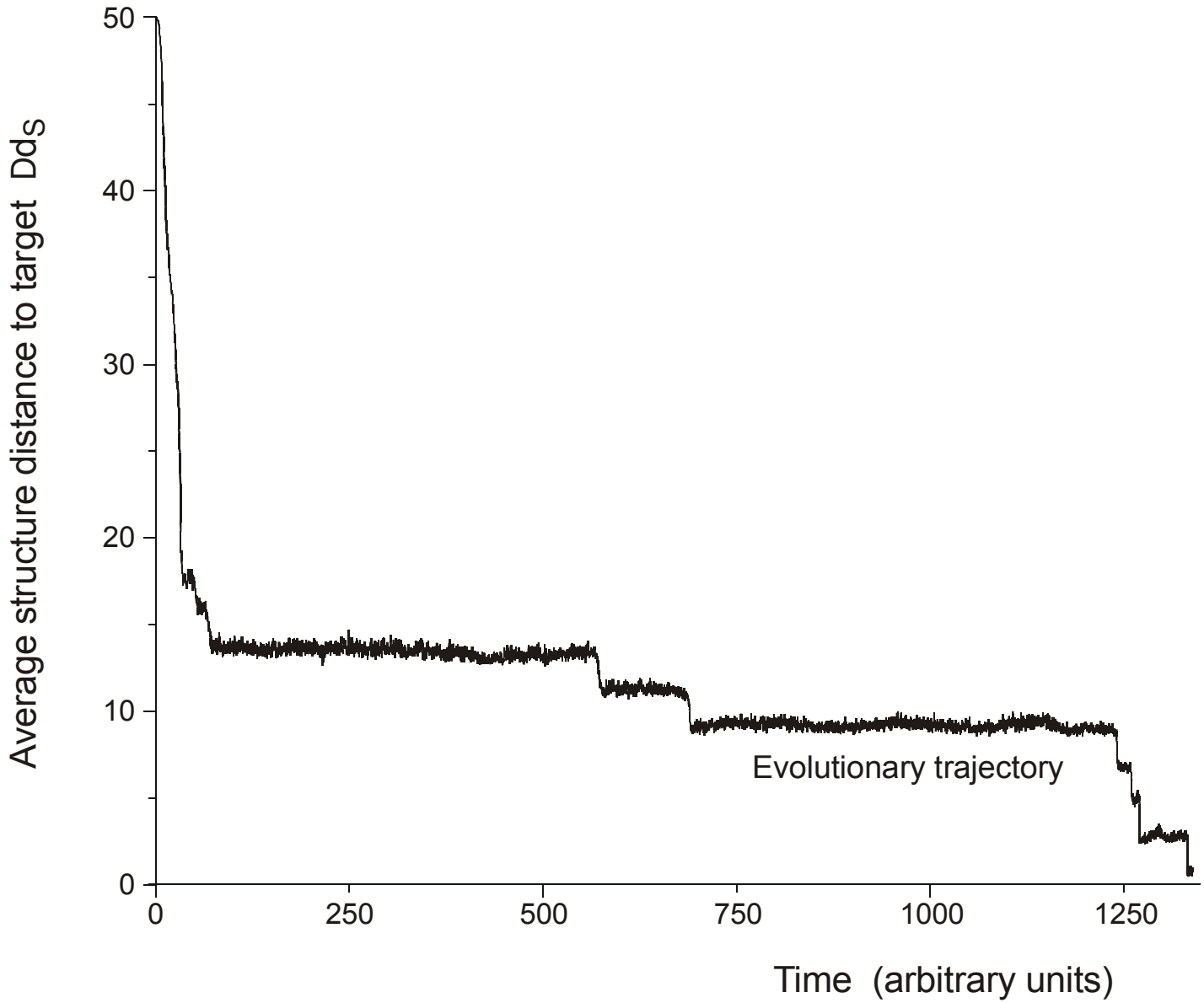


***In silico*** optimization in the flow reactor: Trajectory (**physicists‘ view**)

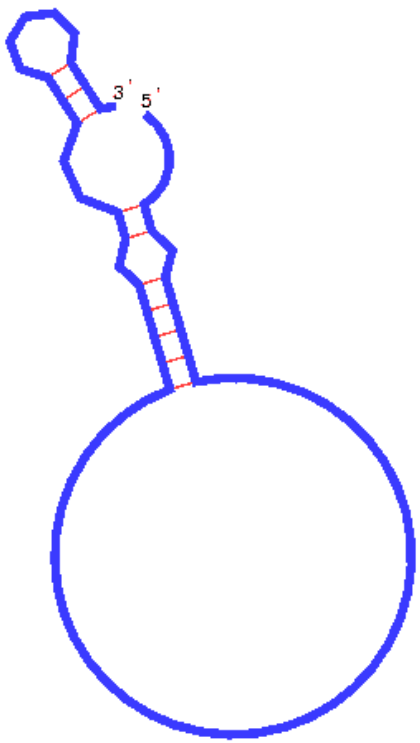


**AUGC**

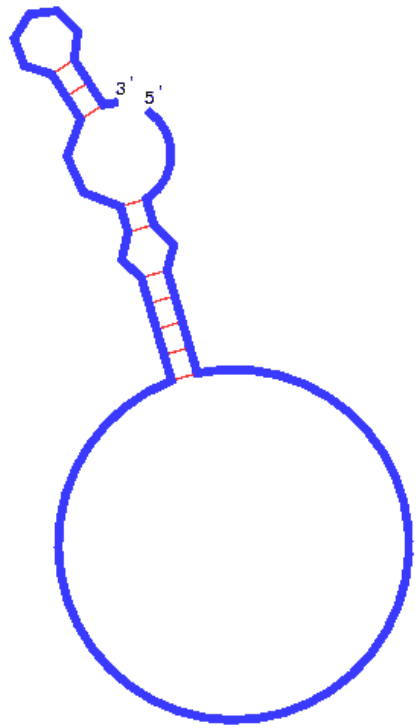


**GC**

Movies of optimization trajectories over the **AUGC** and the **GC** alphabet

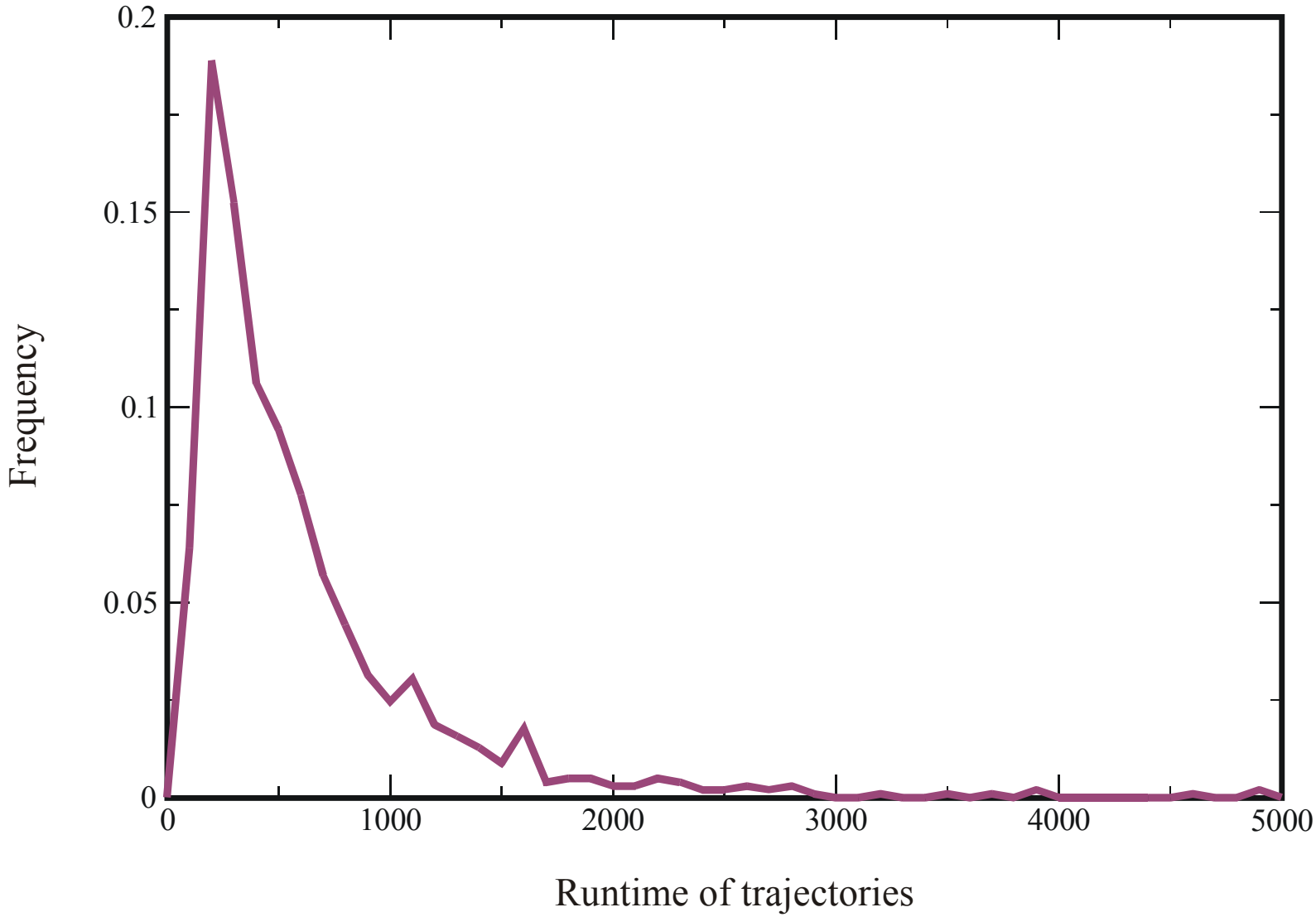


Statistics of the lengths of trajectories from initial structure to target (**AUGC**-sequences)

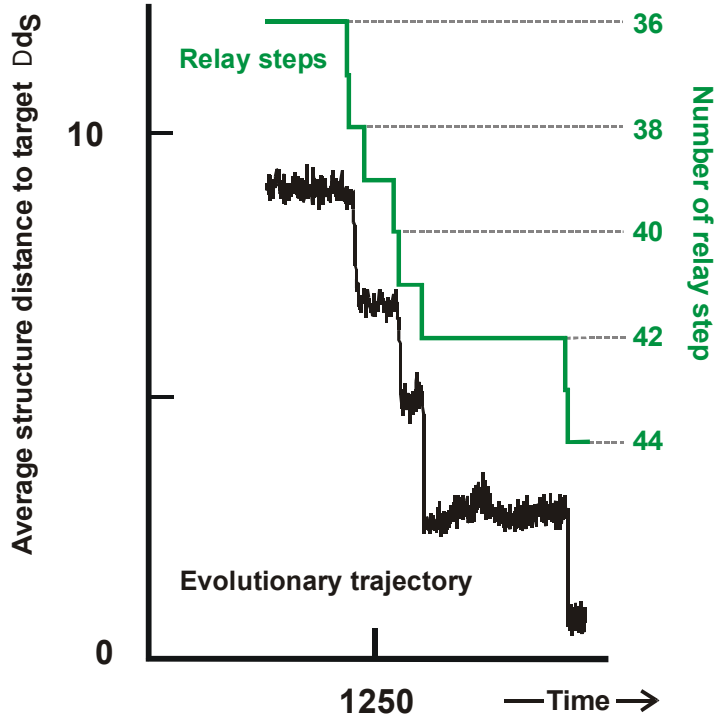


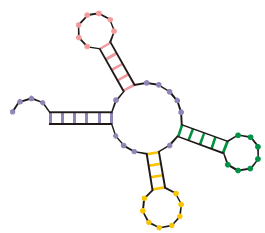

44

Endconformation of optimization

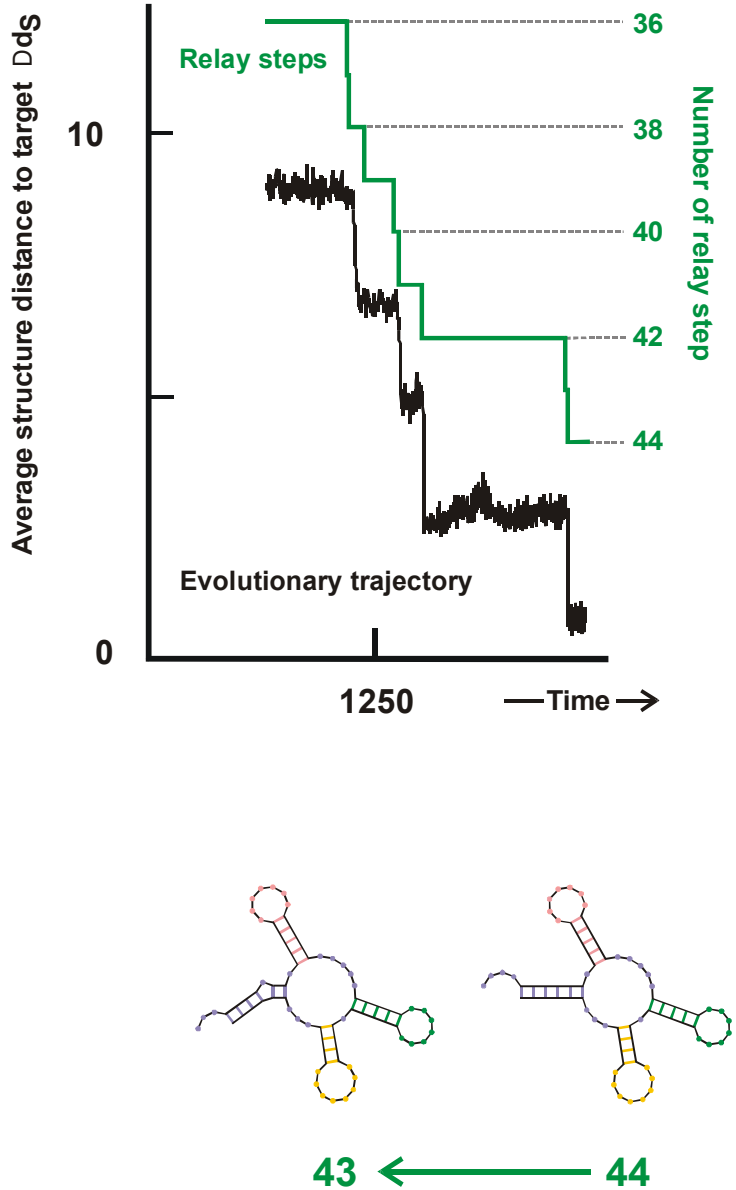


Reconstruction of the last step 43 Á 44

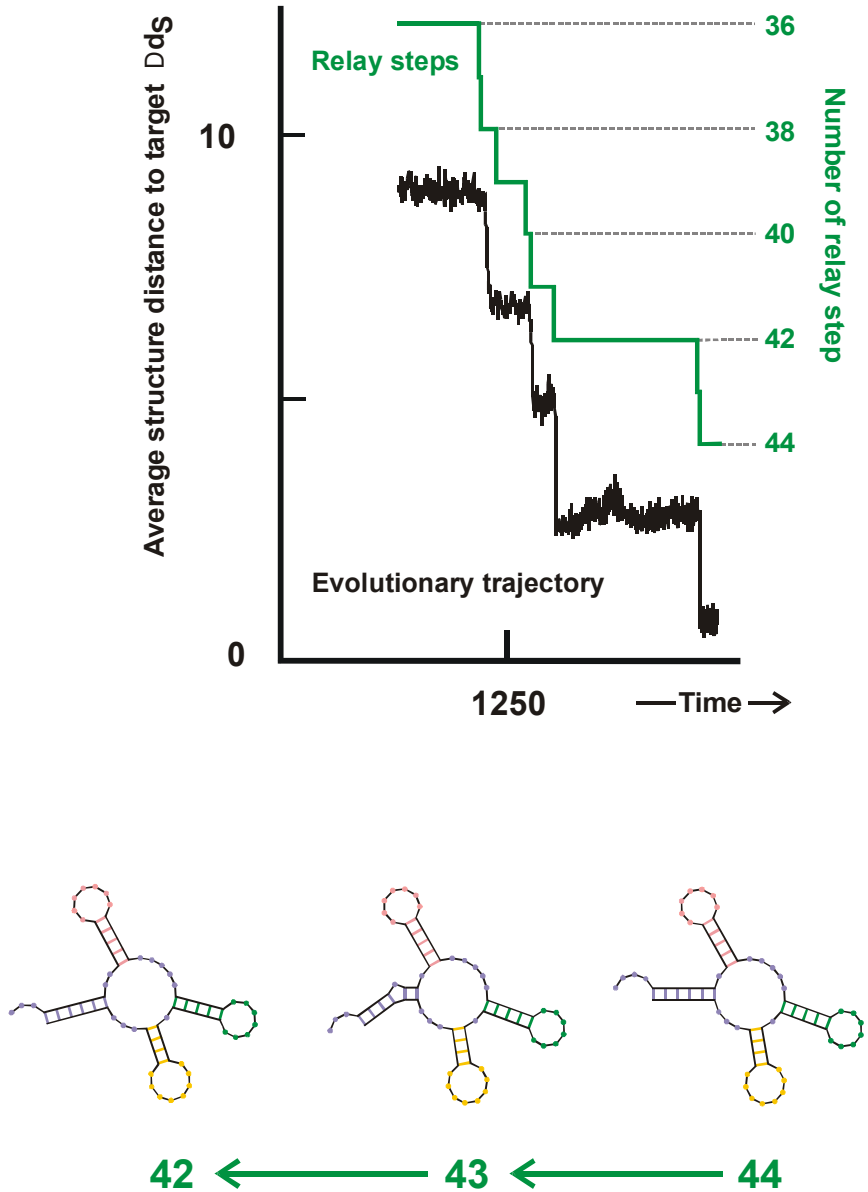


Reconstruction of last-but-one step 42 Á 43 ( Á 44)

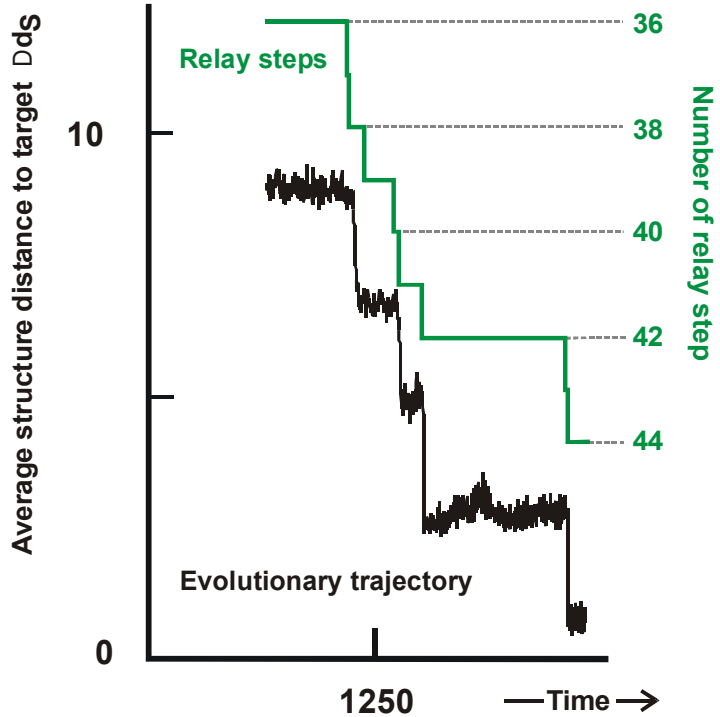


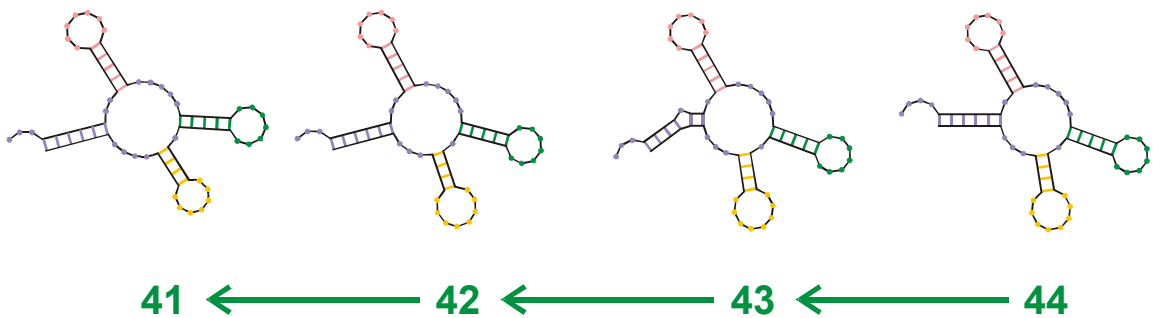


Reconstruction of step 41 Á 42 ( Á 43 Á 44)

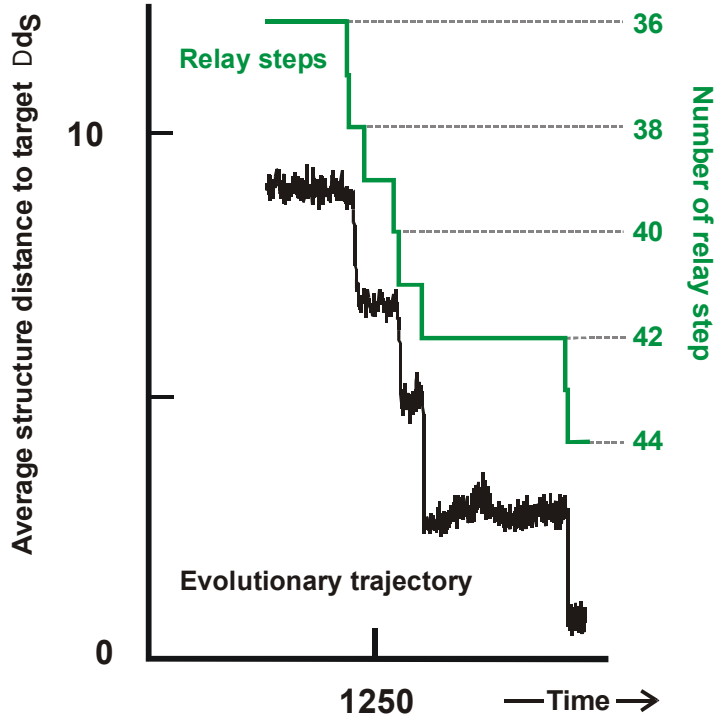


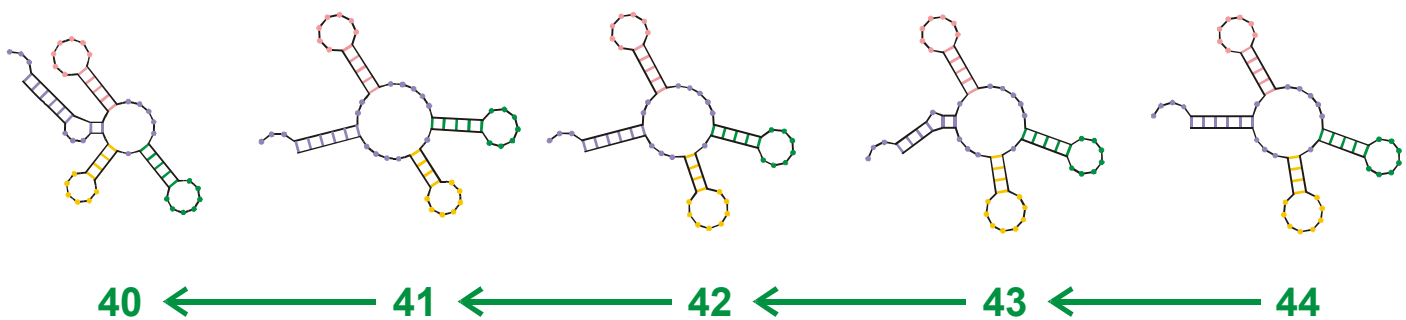


Reconstruction of step 40 Á 41 ( Á 42 Á 43 Á 44)

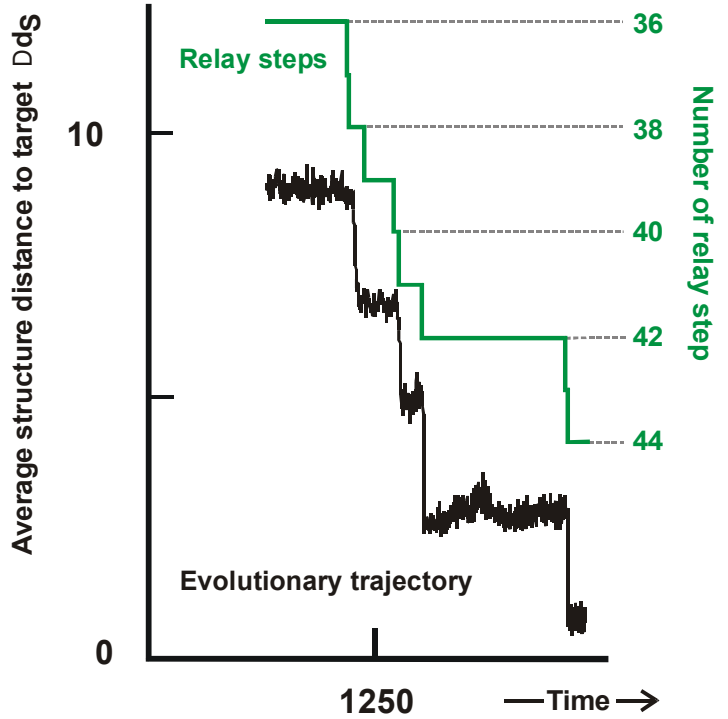


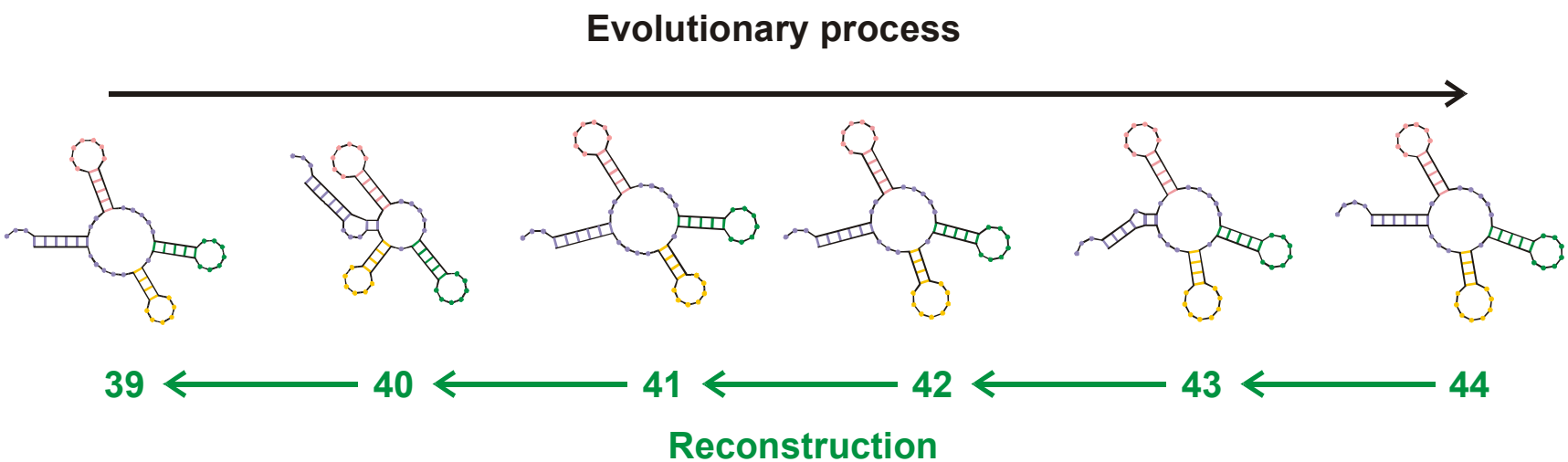


Reconstruction of the relay series

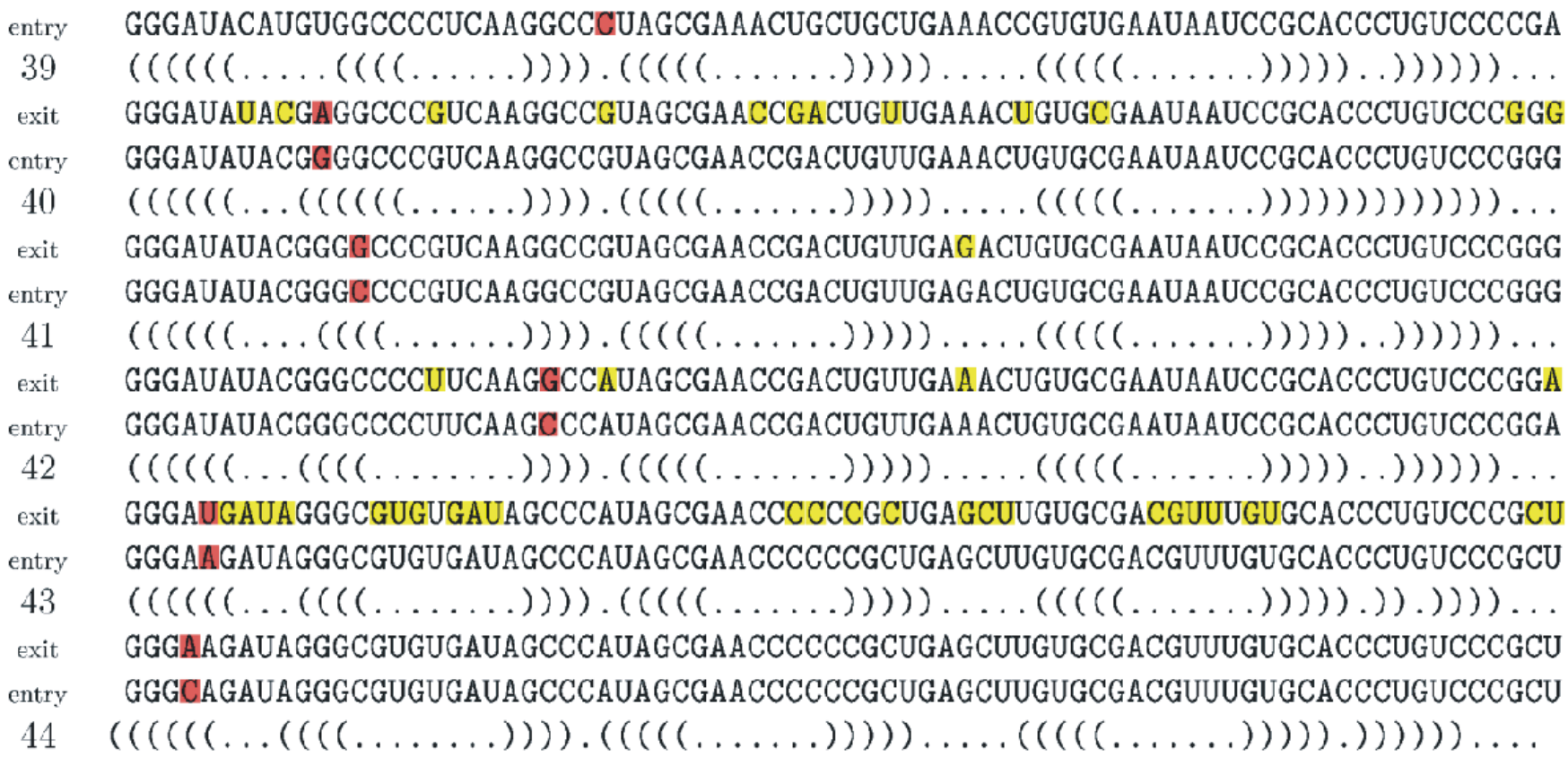


**Transition inducing point mutations** **Neutral point mutations**

Change in RNA sequences during the final five relay steps 39 Á 44

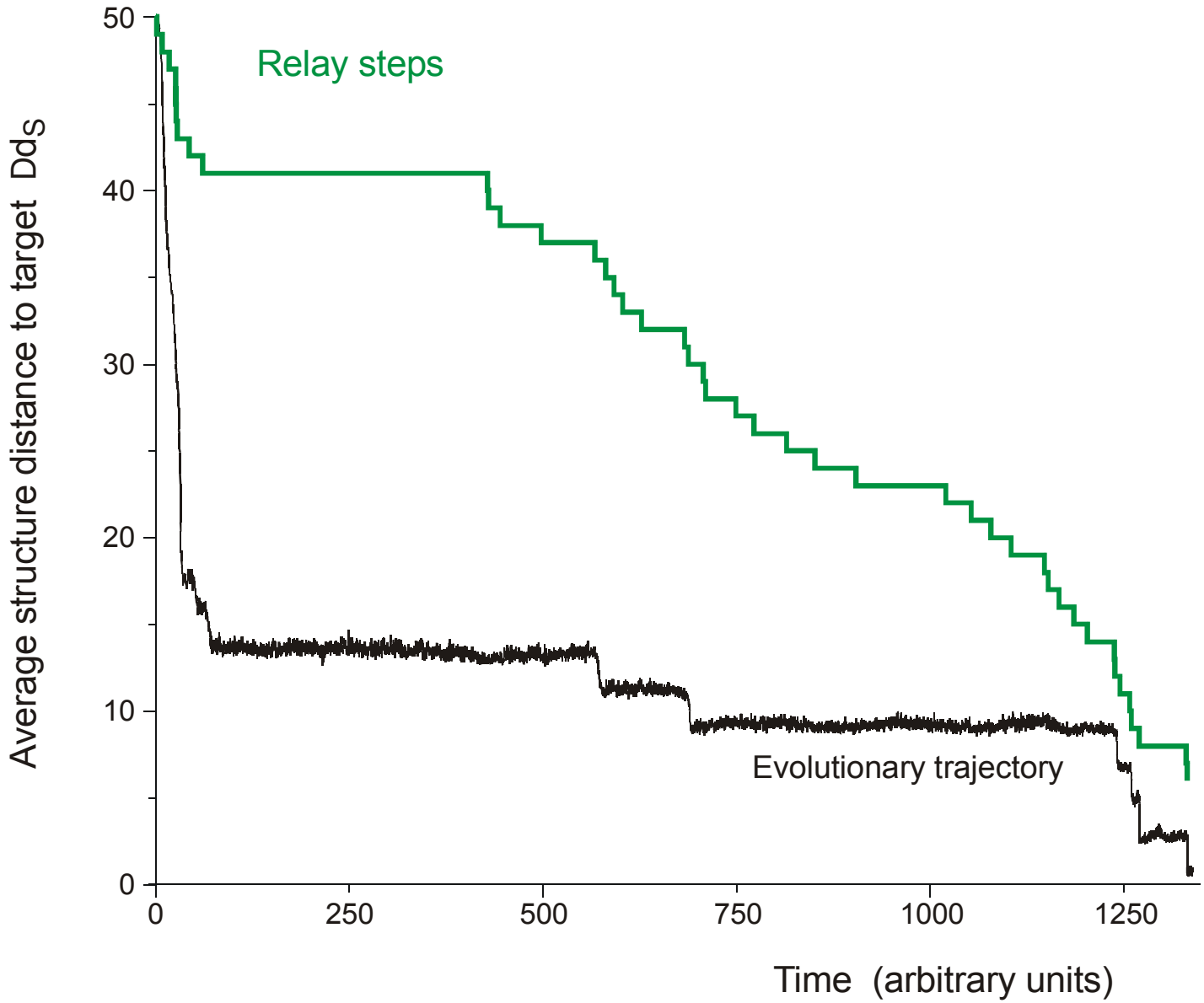


***In silico*** optimization in the flow reactor: Trajectory and relay steps

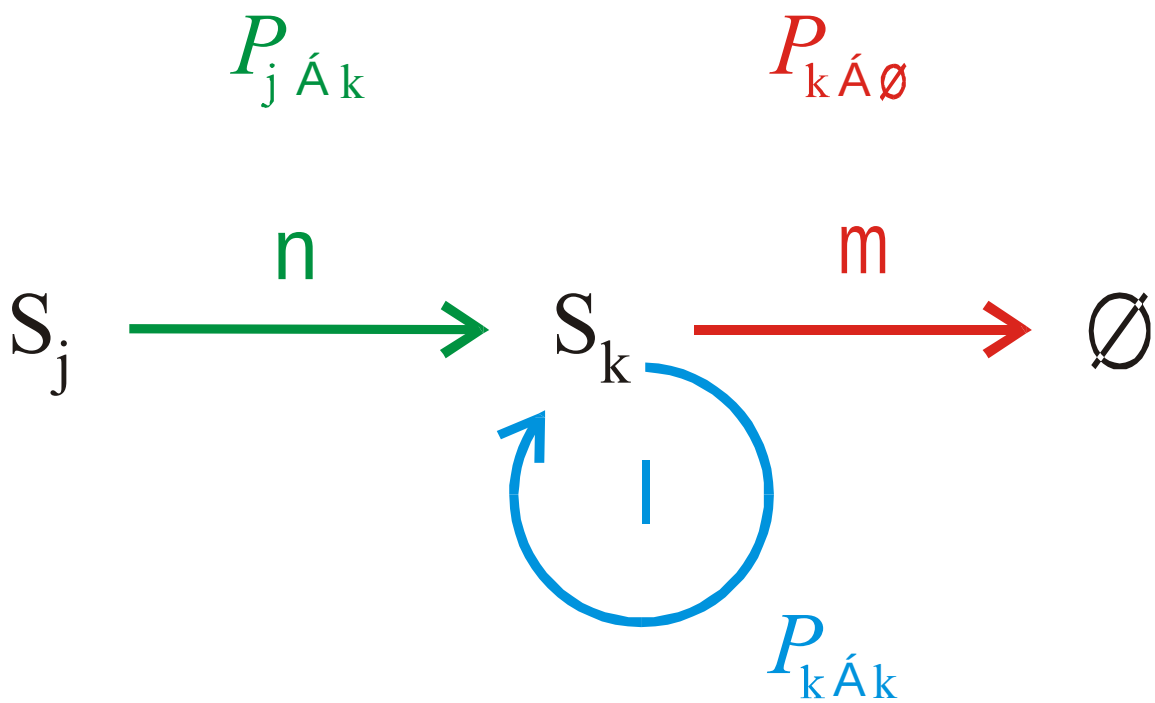


Birth-and-death process with immigration

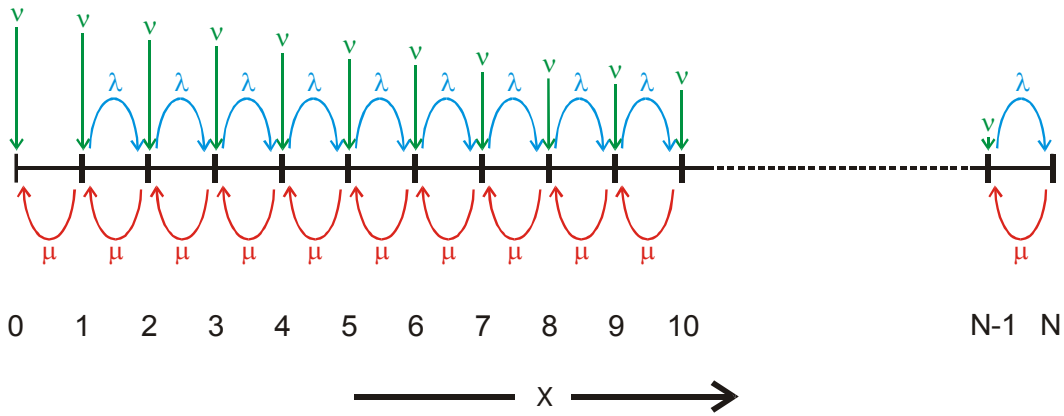


$\lambda(x) = \lambda x + \nu (N-x)$ $\mu(x) = \mu x$

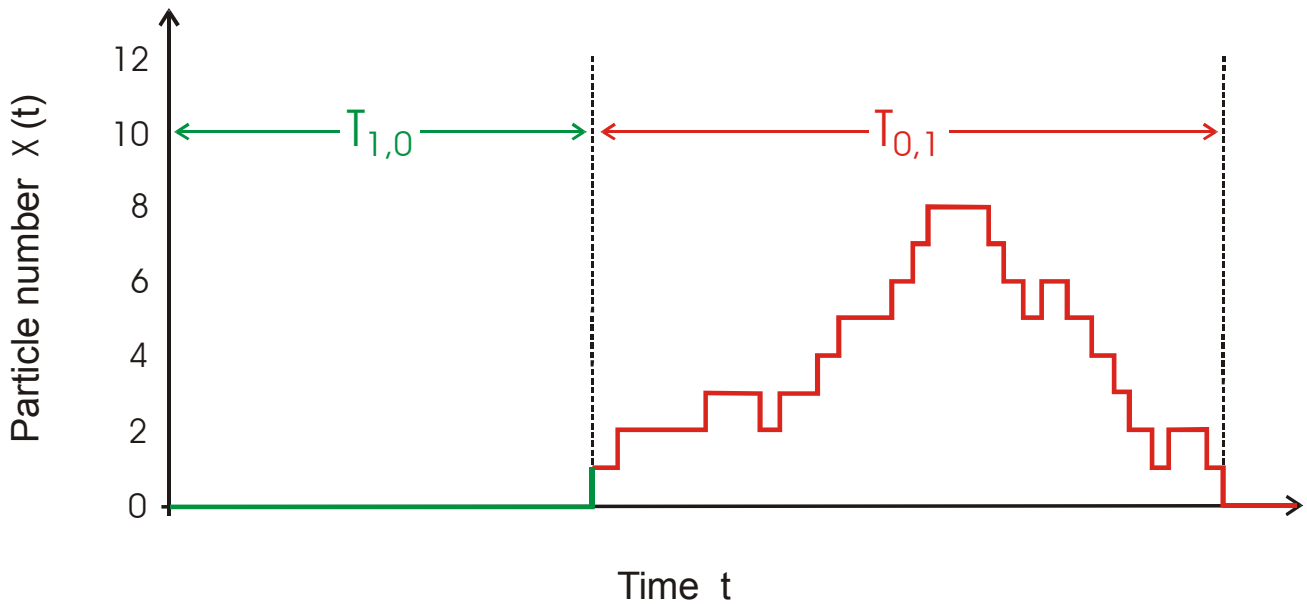


Calculation of transition probabilities by means of a birth-and-death process with immigration

**28 neutral point mutations** during a long quasi-stationary epoch

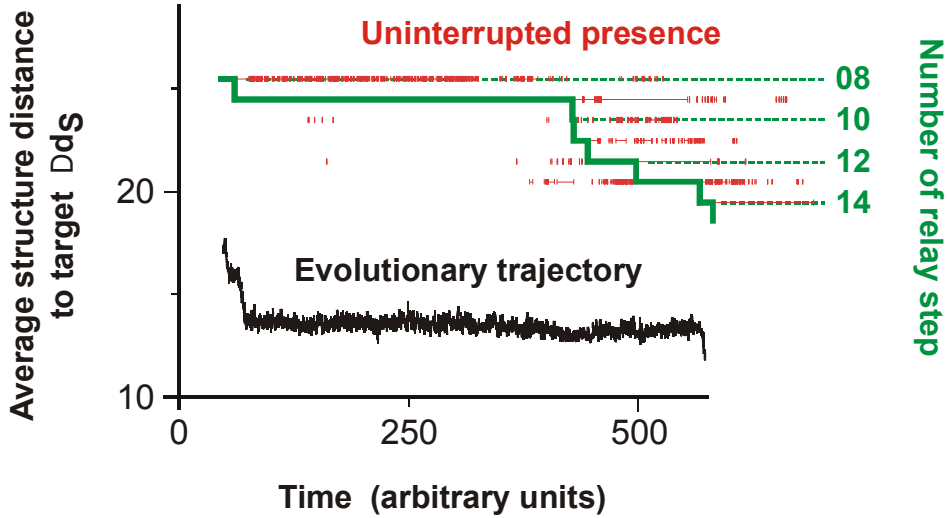


```
entry  GGUAUGGGCGUUGAAUAGUAGGGUUUAAACCAAUCGGCCAACGAUCUCGUGUGCGCAUUUCAUAUCCCGUACAGAA
8      .((((((((((((.........(((....)))........)))))).....((((.........))))))))))....
exit   GGUAUGGGCGUUGAAUAAUAGGGUUUAAACCAAUCGGCCAACGAUCUCGUGUGCGCAUUUCAUAUCCCAUACAGAA
entry  GGUAUGGGCGUUGAAUAAUAGGGUUUAAACCAAUCGGCCAACGAUCUCGUGUGCGCAUUUCAUAUACCAUACAGAA
9      .((((((.((((.........(((....)))........)))))).....((((.........)))))..))))))....
exit   UGGAUGGACGUUGAAUAACAAGGUAUCGACCAAACAACCAACGAGUAAGUGUGUACGCCCCACACACCGUCCCAAG
entry  UGGAUGGACGUUGAAUAACAAGGUAUCGACCAAACAACCAACGAGUAAGUGUGUACGCCCCACACAGCGUCCCAAG
10     .(((((..((((.........(((....)))........)))))).....((((.........))))..)))))....
exit   UGGAUGGACGUUGAAUAACAAGGUAUCGACCAAACAACCAACGAGUAAGUGUGUACGCCCCACACAGCGUCCCAAG
```

**Transition inducing point mutations** **Neutral point mutations**

**Neutral genotype evolution** during phenotypic stasis

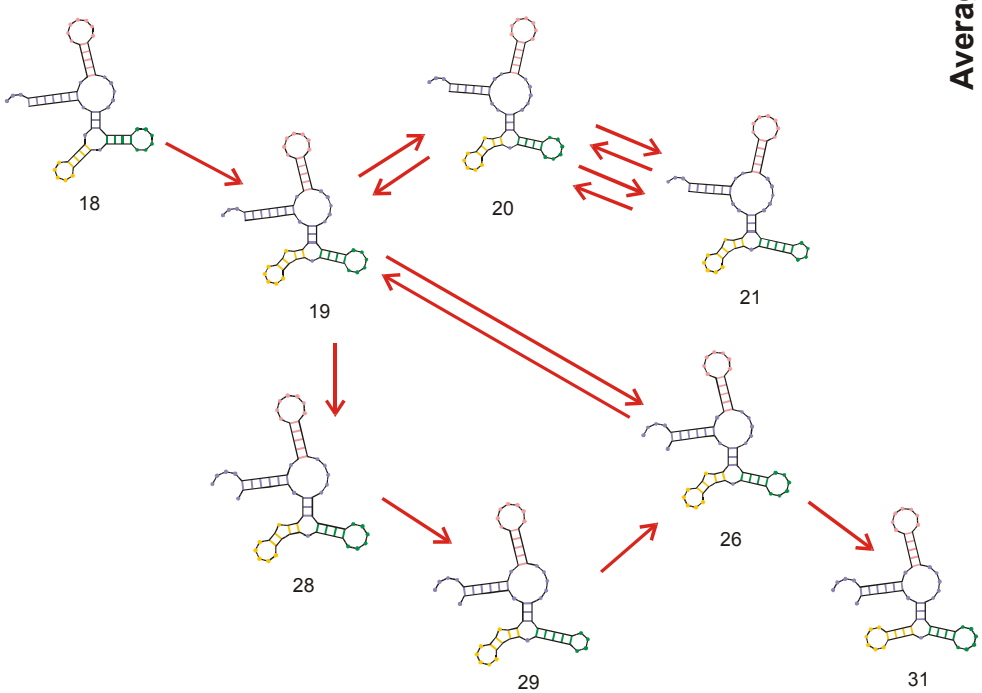


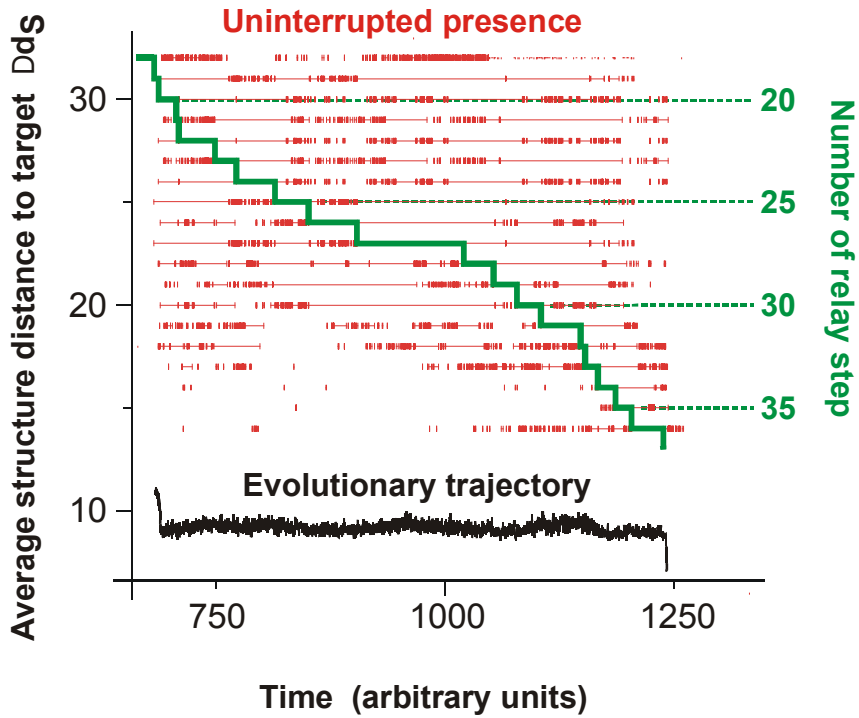


A random sequence of **minor** or continuous **transitions** in the relay series

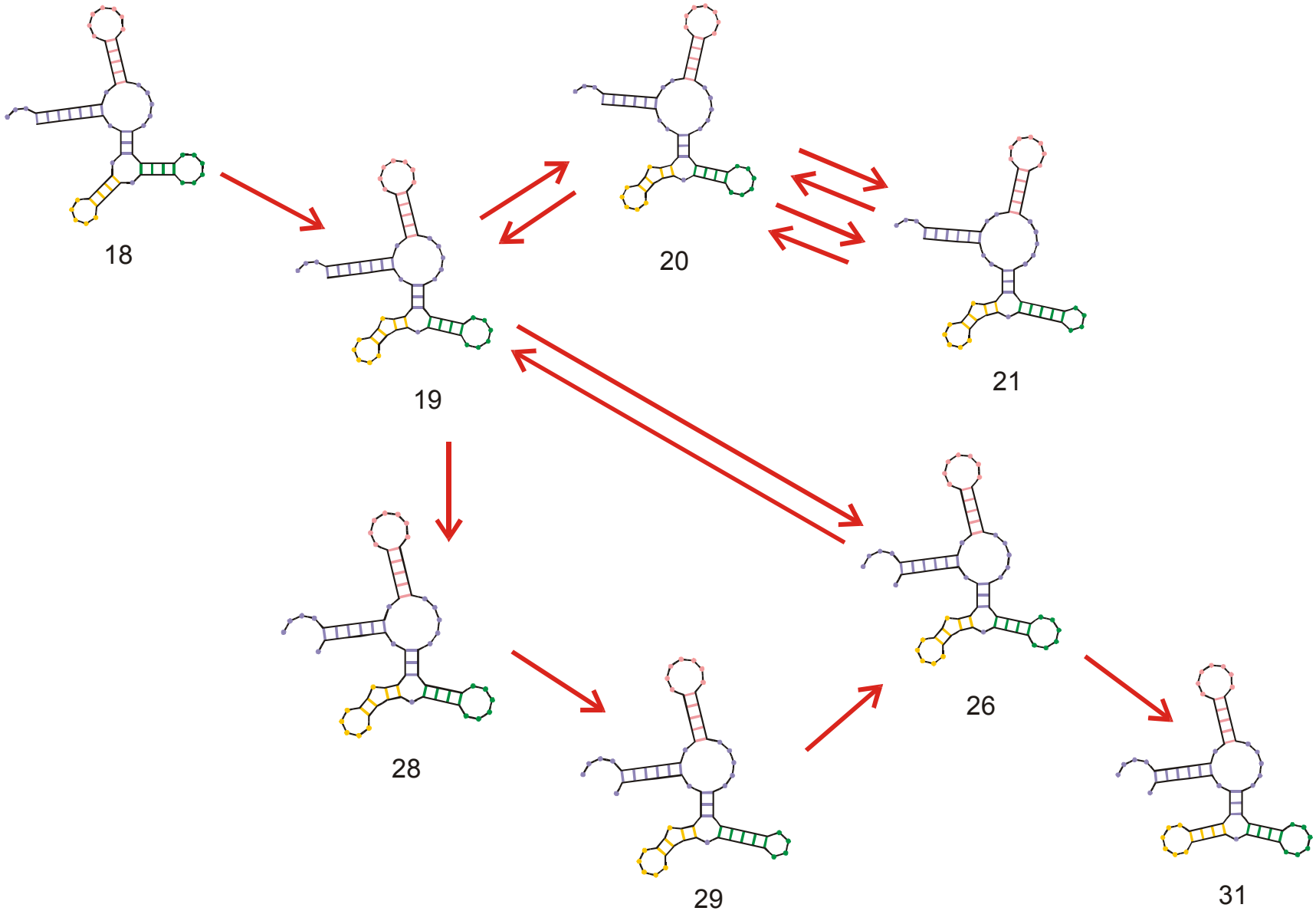


A random sequence of **minor** or continuous **transitions** in the relay series


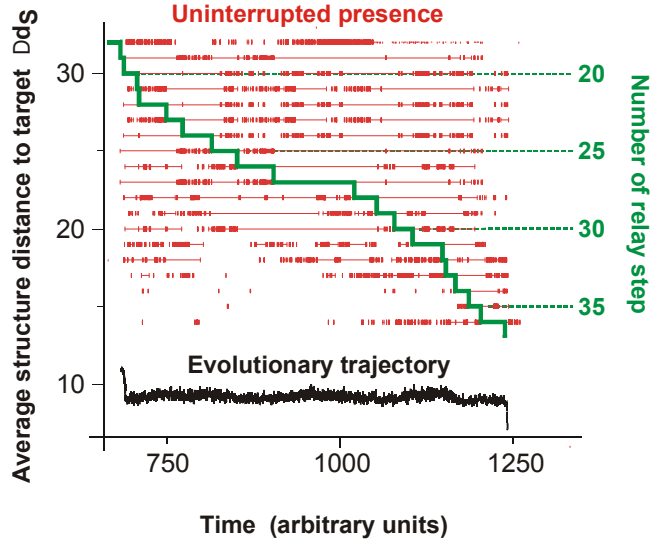


A random sequence of **minor** or continuous **transitions** in the relay series

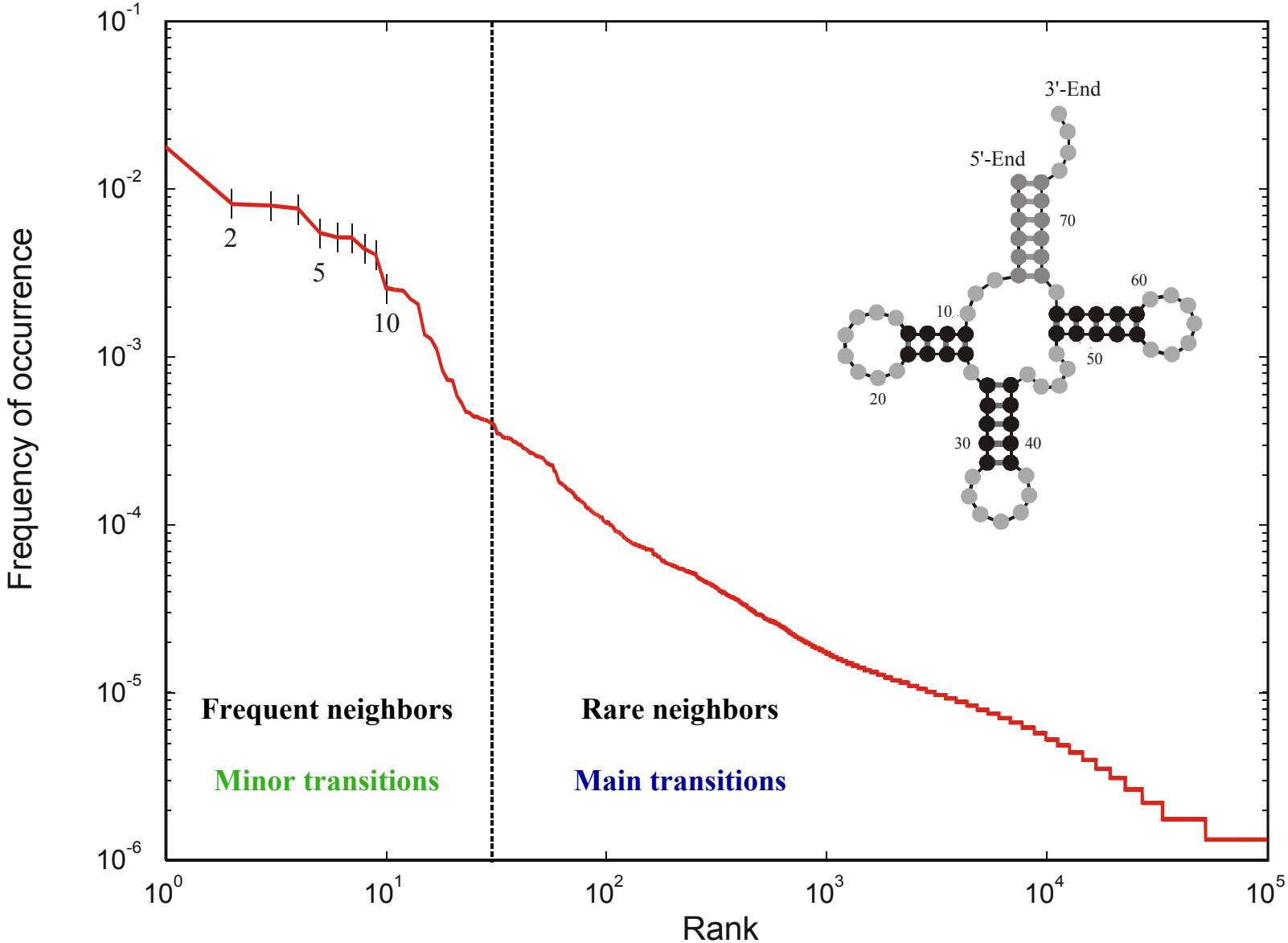


Probability of occurrence of different structures in the mutational neighborhood of $tRNA^{phe}$

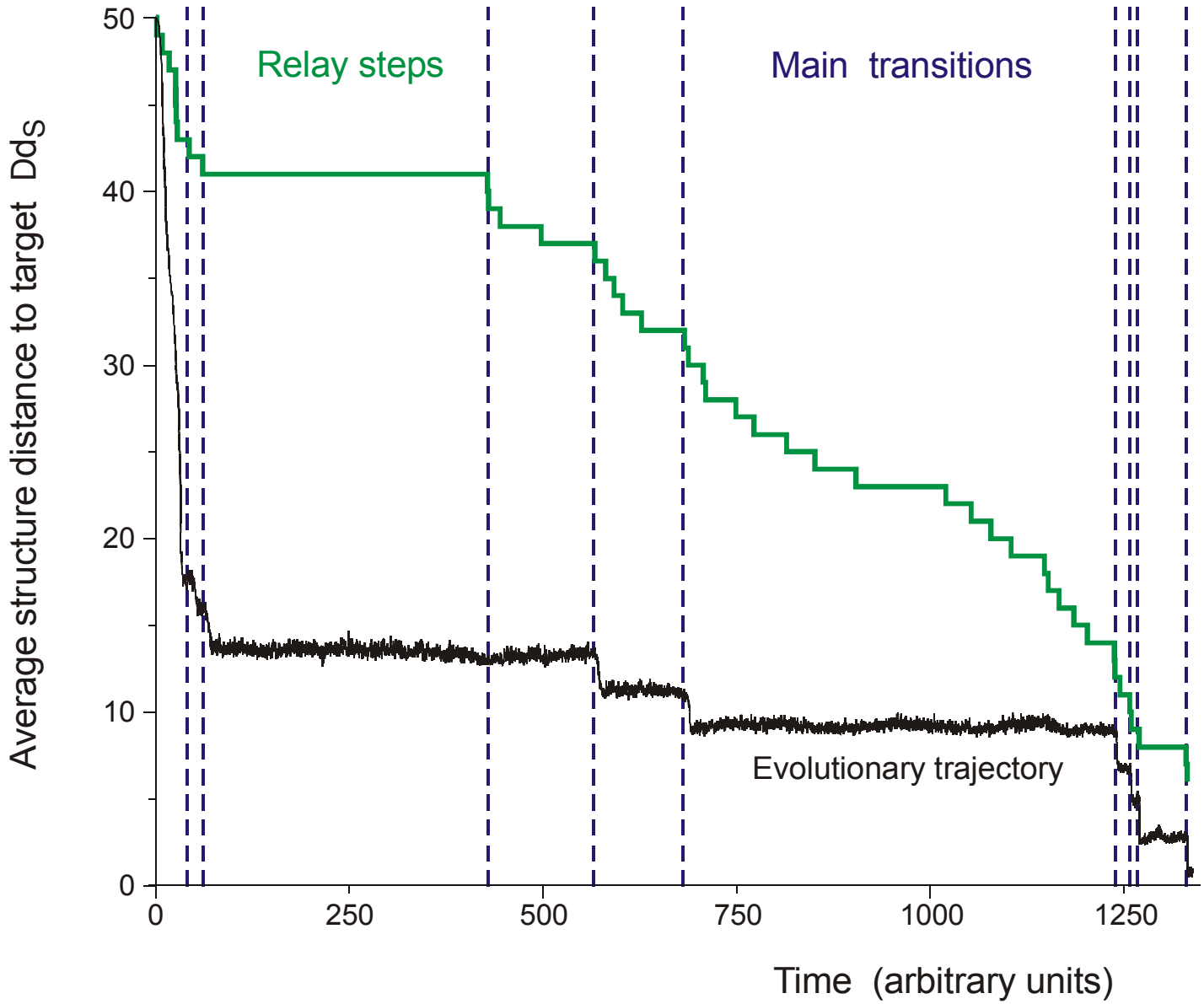


***In silico*** optimization in the flow reactor: Main transitions

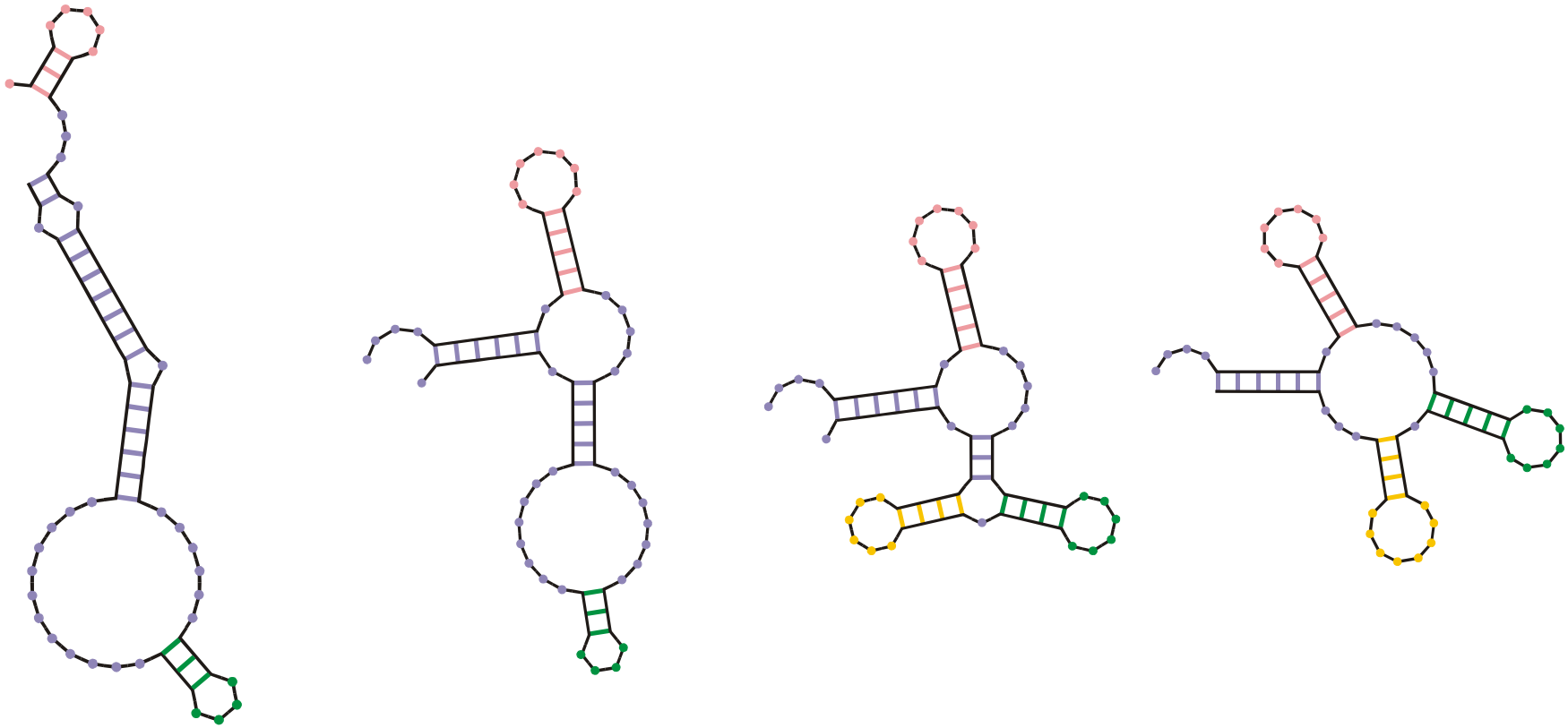


Three important steps in the formation of the tRNA clover leaf from a randomly chosen initial structure corresponding to three **main transitions**.

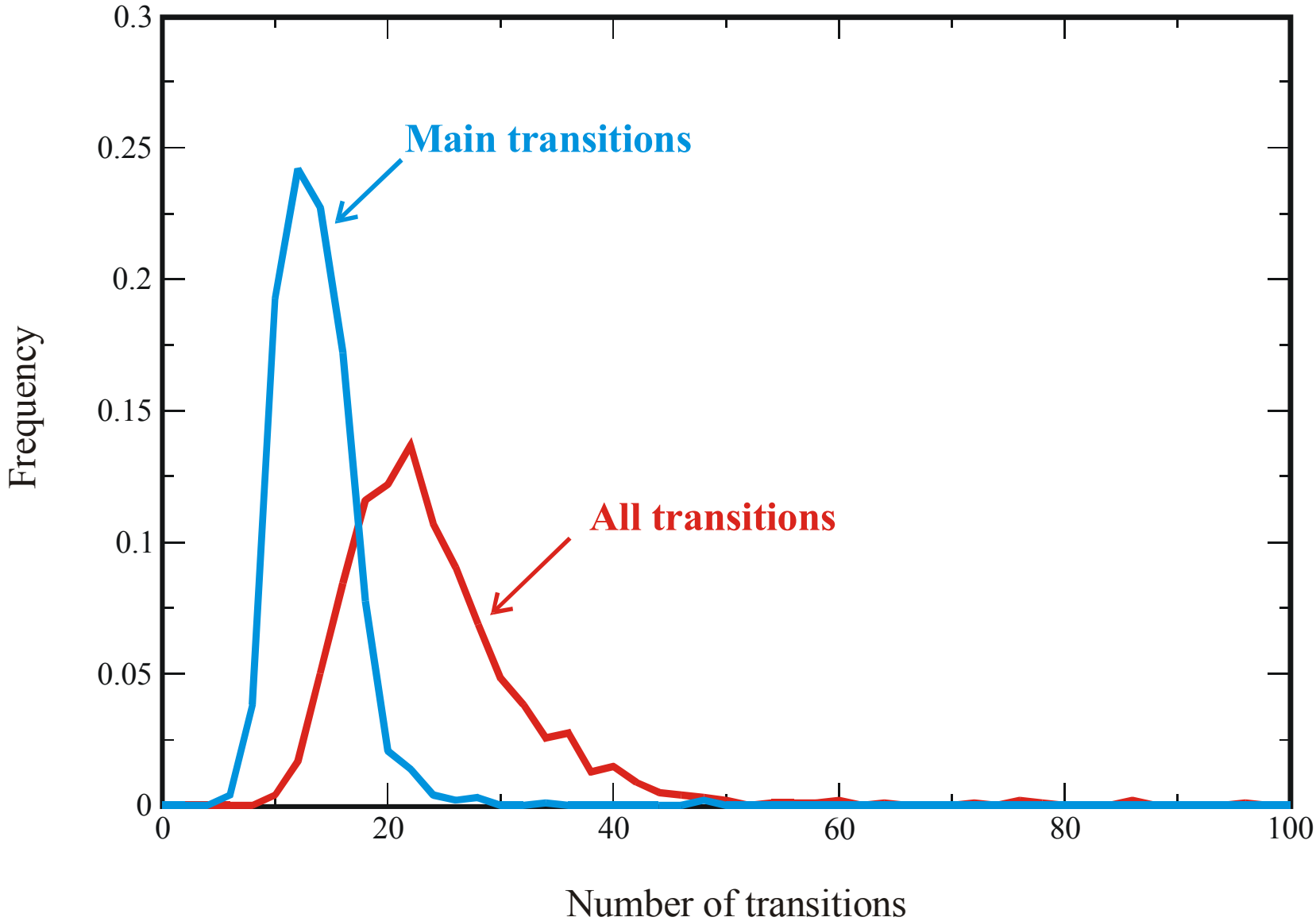


Statistics of the numbers of transitions from initial structure to target (**AUGC**-sequences)

| Alphabet | Runtime | Transitions | Main transitions | No. of runs |
|---|---|---|---|---|
| **AUGC** | 385.6 | 22.5 | 12.6 | 1017 |
| **GUC** | 448.9 | 30.5 | 16.5 | 611 |
| **GC** | 2188.3 | 40.0 | 20.6 | 107 |

Statistics of trajectories and relay series (mean values of log-normal distributions)

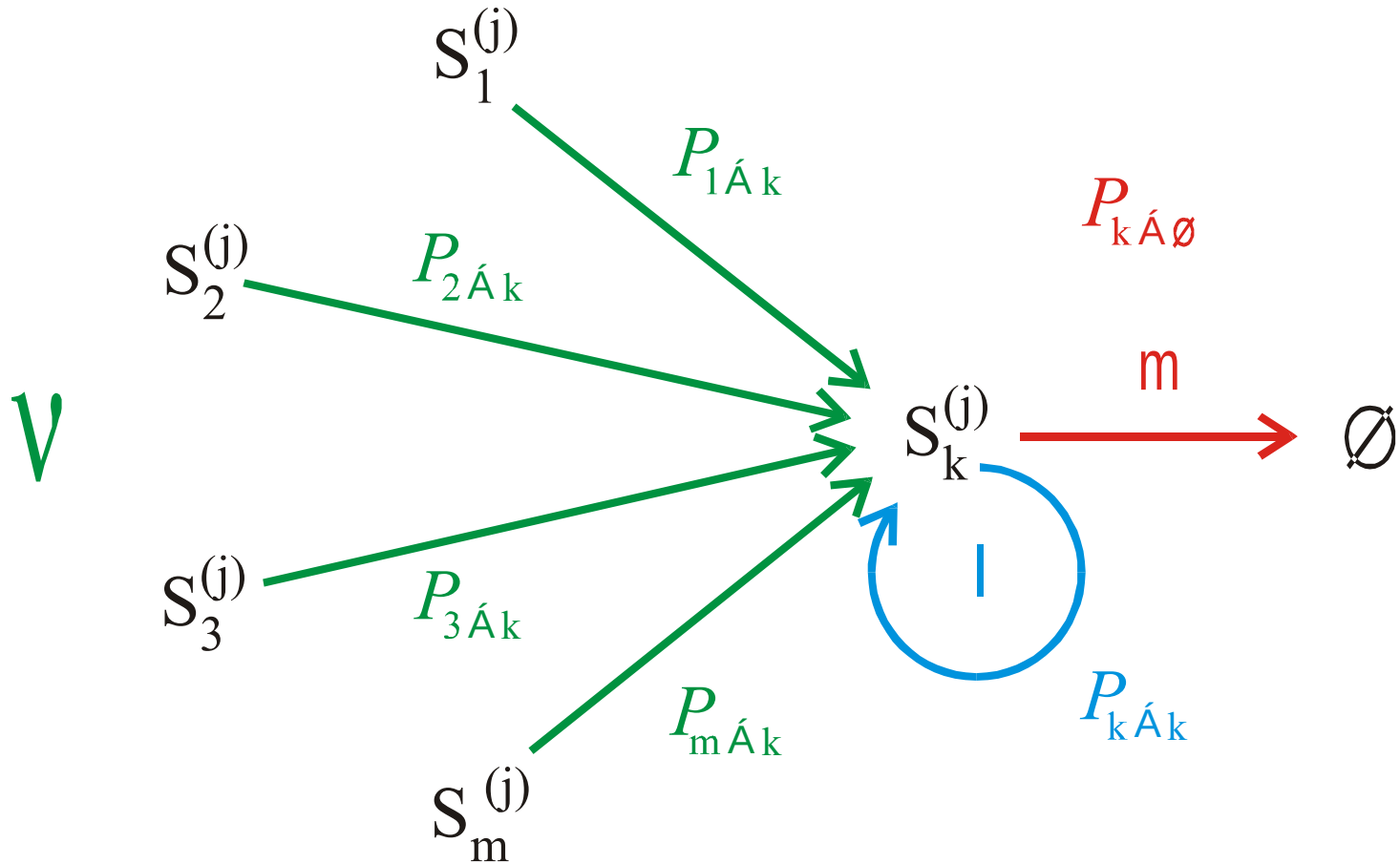


Transition probabilities determining the presence of phenotype $S_k^{(j)}$ in the population

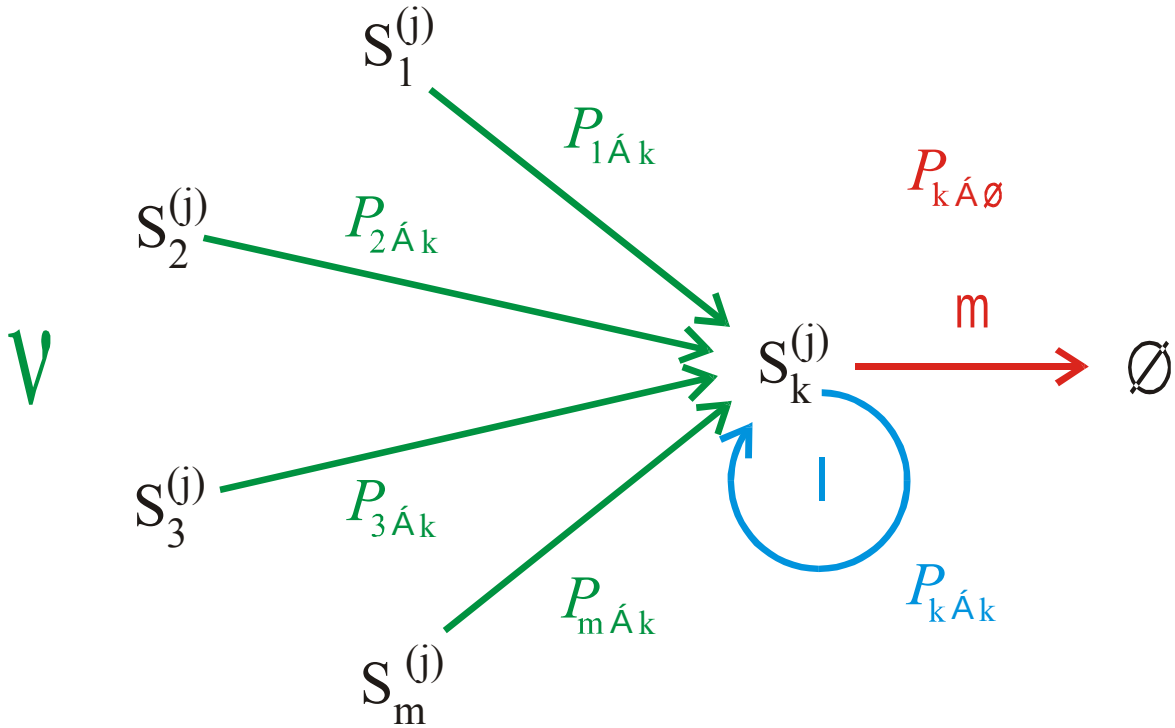


$$N_{sat}^{(j)} = \frac{1}{p \,.\, \ell \,.\, \langle r^{(j)} \rangle}$$

## Statistics of evolutionary trajectories

| Population size N | Number of replications $< n_{rep} >$ | Number of transitions $< n_{tr} >$ | Number of main transitions $< n_{dtr} >$ |
|---|---|---|---|
| 1 000 | $(5.5 \pm [6.9,3.1]) \times 10^7$ | $92.7 \pm [80.3,43.0]$ | $8.8 \pm [2.4,1.9]$ |
| 2 000 | $(6.0 \pm [11.1,3.9]) \times 10^7$ | $55.7 \pm [30.7,19.8]$ | $8.9 \pm [2.8,2.1]$ |
| 3 000 | $(6.6 \pm [21.0,5.0]) \times 10^7$ | $44.2 \pm [25.9,16.3]$ | $8.1 \pm [2.3,1.8]$ |
| 10 000 | $(1.2 \pm [1.3,0.6]) \times 10^8$ | $35.9 \pm [10.3,8.0]$ | $10.3 \pm [2.6,2.1]$ |
| 20 000 | $(1.5 \pm [1.4,0.7]) \times 10^8$ | $28.8 \pm [5.8,4.8]$ | $9.0 \pm [2.8,2.2]$ |
| 30 000 | $(2.2 \pm [3.1,1.3]) \times 10^8$ | $29.8 \pm [7.3,5.9]$ | $8.7 \pm [2.4,1.9]$ |
| 100 000 | $(3 \pm [2,1]) \times 10^8$ | $24 \pm [6,5]$ | $9 \pm 2$ |

The number of **main transitions** or evolutionary innovations is constant.

**28 neutral point mutations** during a long quasi-stationary epoch

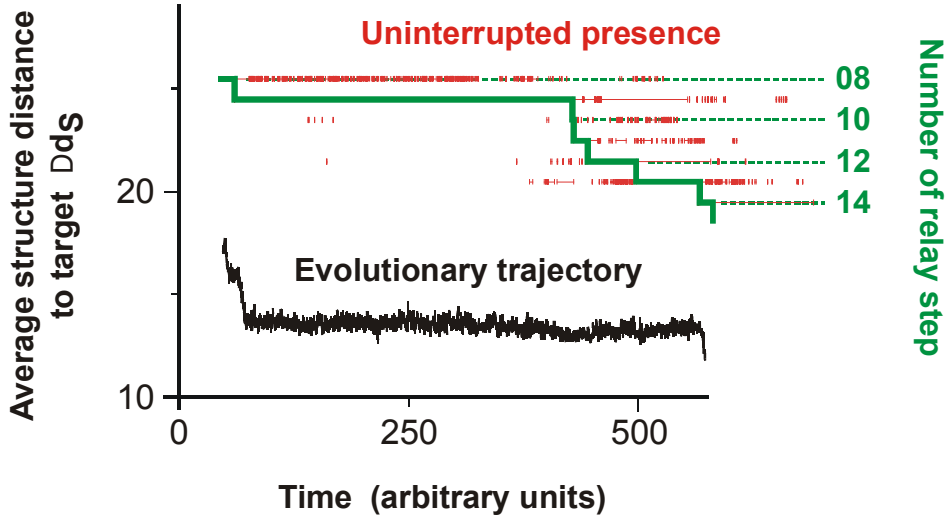


```
entry  GGUAUGGGCGUUGAAUAGUAGGGUUUAAACCAAUCGGCCAACGAUCUCGUGUGCGCAUUUCAUAUCCCGUACAGAA
8      .((((((((((((.........(((....)))........)))))).....((((.........))))))))))....
exit   GGUAUGGGCGUUGAAUAAUAGGGUUUAAACCAAUCGGCCAACGAUCUCGUGUGCGCAUUUCAUAUCCCAUACAGAA
entry  GGUAUGGGCGUUGAAUAAUAGGGUUUAAACCAAUCGGCCAACGAUCUCGUGUGCGCAUUUCAUAUACCAUACAGAA
9      .((((((.((((.........(((....)))........)))))).....((((.........))))).))))))....
exit   UGGAUGGACGUUGAAUAACAAGGUAUCGACCAAACAACCAACGAGUAAGUGUGUACGCCCCACACACCGUCCCAAG
entry  UGGAUGGACGUUGAAUAACAAGGUAUCGACCAAACAACCAACGAGUAAGUGUGUACGCCCCACACAGCGUCCCAAG
10     .(((((..((((.........(((....)))........)))))).....((((.........))))).)))))....
exit   UGGAUGGACGUUGAAUAACAAGGUAUCGACCAAACAACCAACGAGUAAGUGUGUACGCCCCACACAGCGUCCCAAG
```

**Transition inducing point mutations** **Neutral point mutations**

**Neutral genotype evolution** during phenotypic stasis

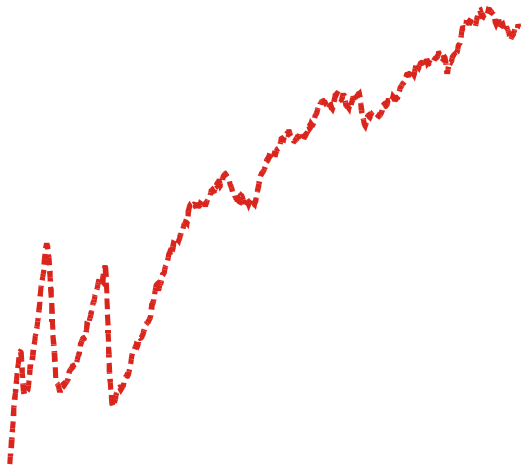

Variation in genotype space during optimization of phenotypes

**Mean Hamming distance** within the population and **drift velocity of the population center** in sequence space.

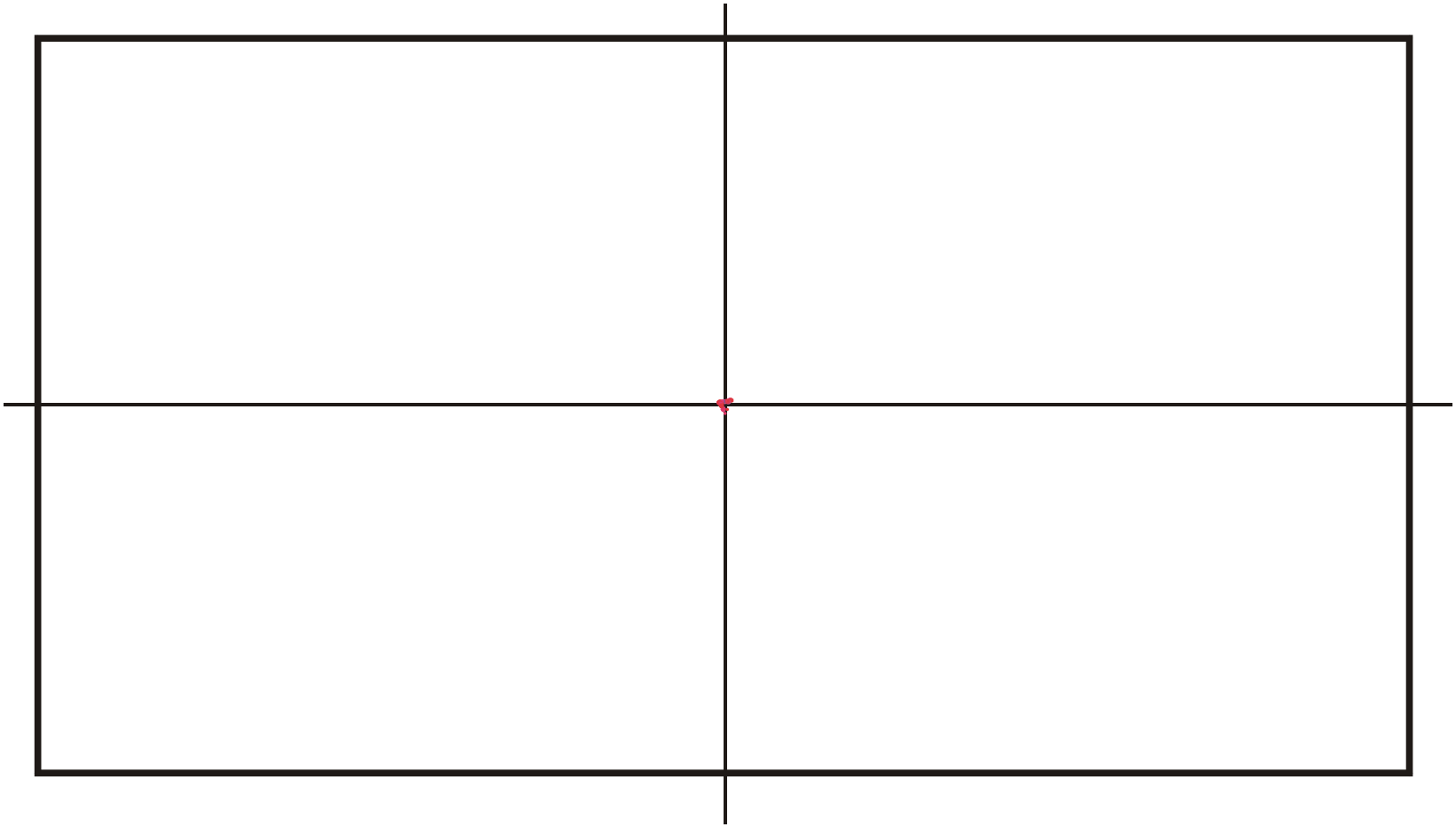

Spread of population in sequence space during a quasistationary epoch: t = 150

Spread of population in sequence space during a quasistationary epoch: t = 170

Spread of population in sequence space during a quasistationary epoch:  t = 200

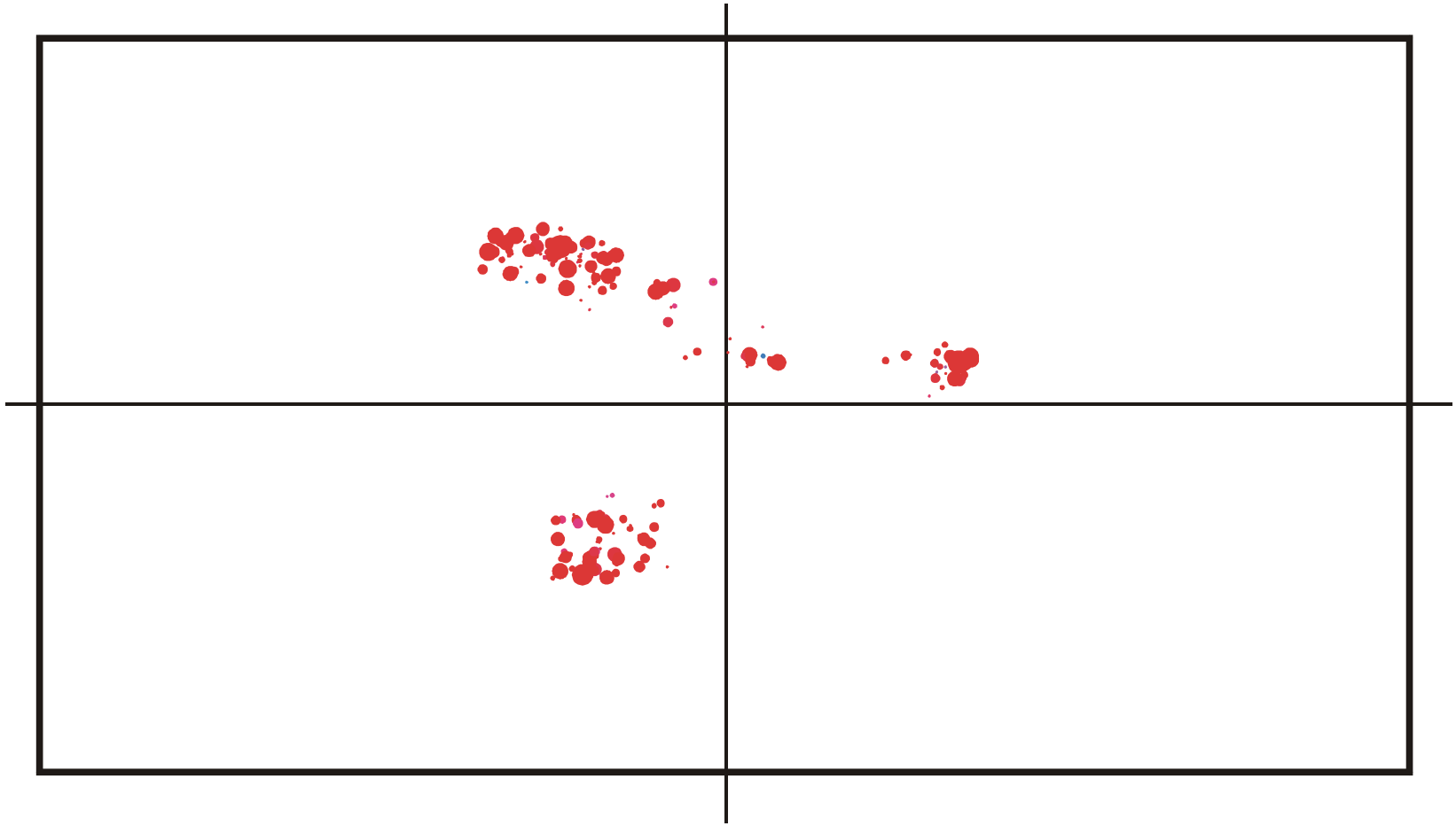

Spread of population in sequence space during a quasistationary epoch: t = 350

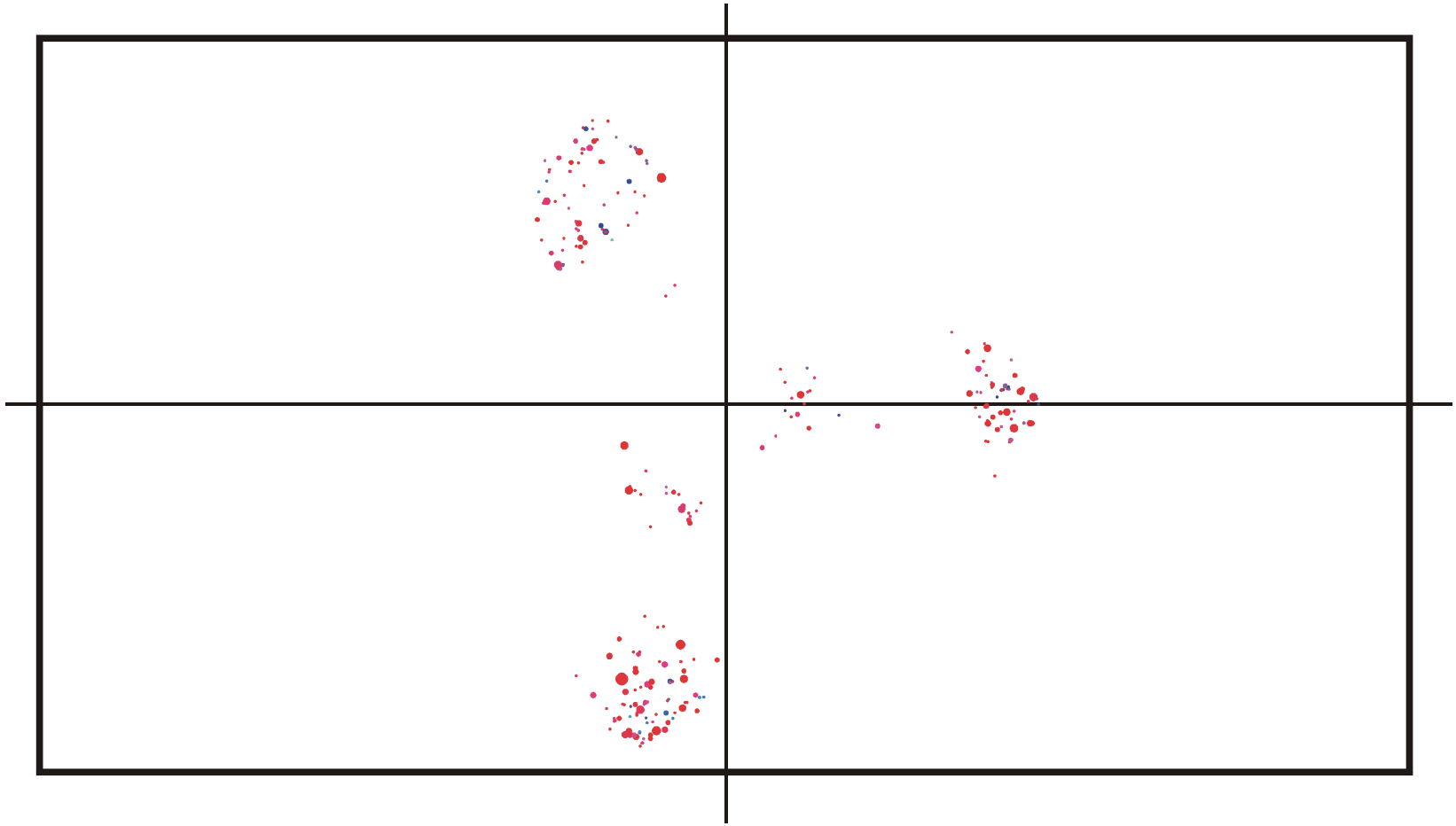

Spread of population in sequence space during a quasistationary epoch: t = 500

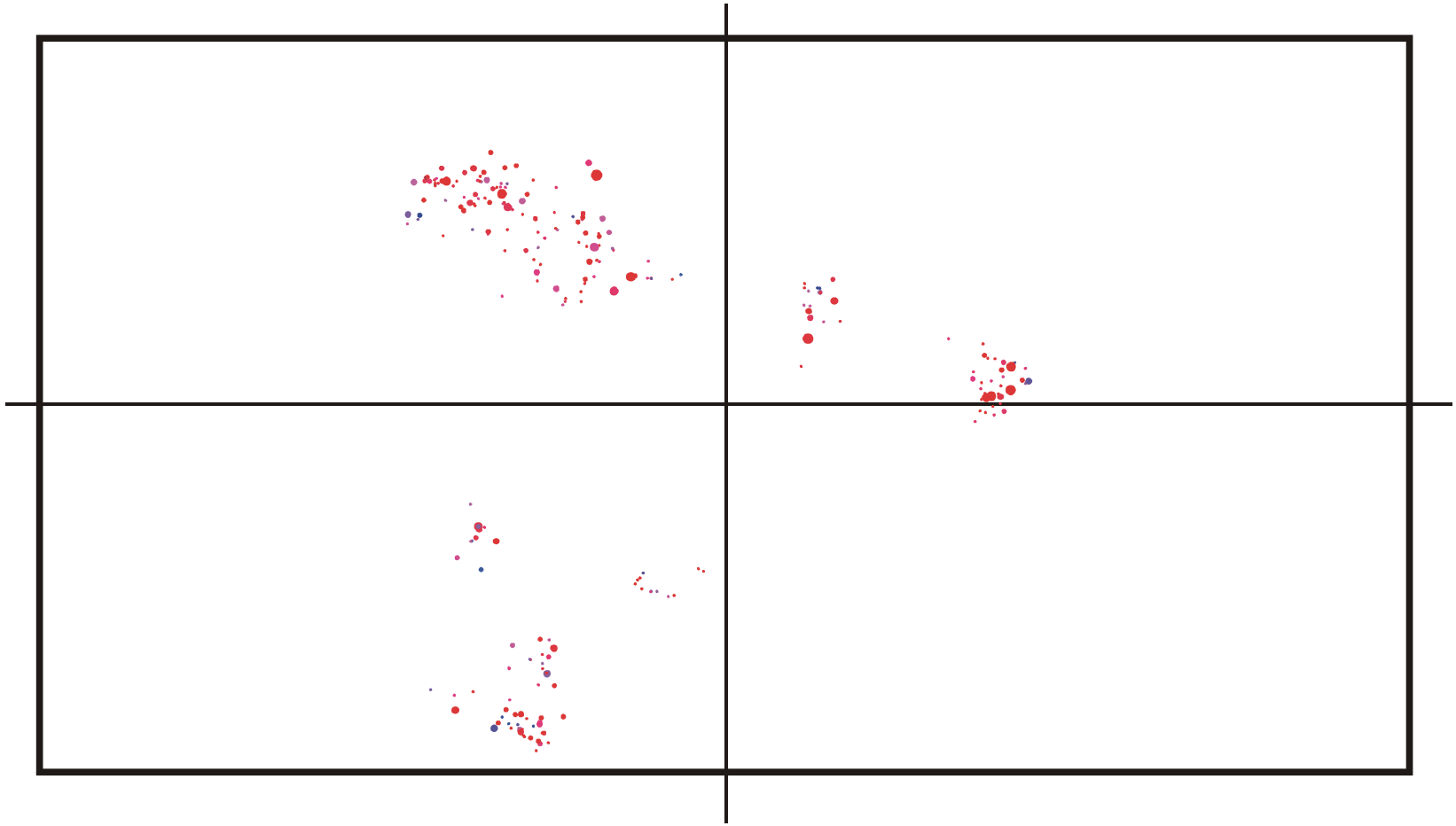

Spread of population in sequence space during a quasistationary epoch: t = 650

Spread of population in sequence space during a quasistationary epoch:  t = 820

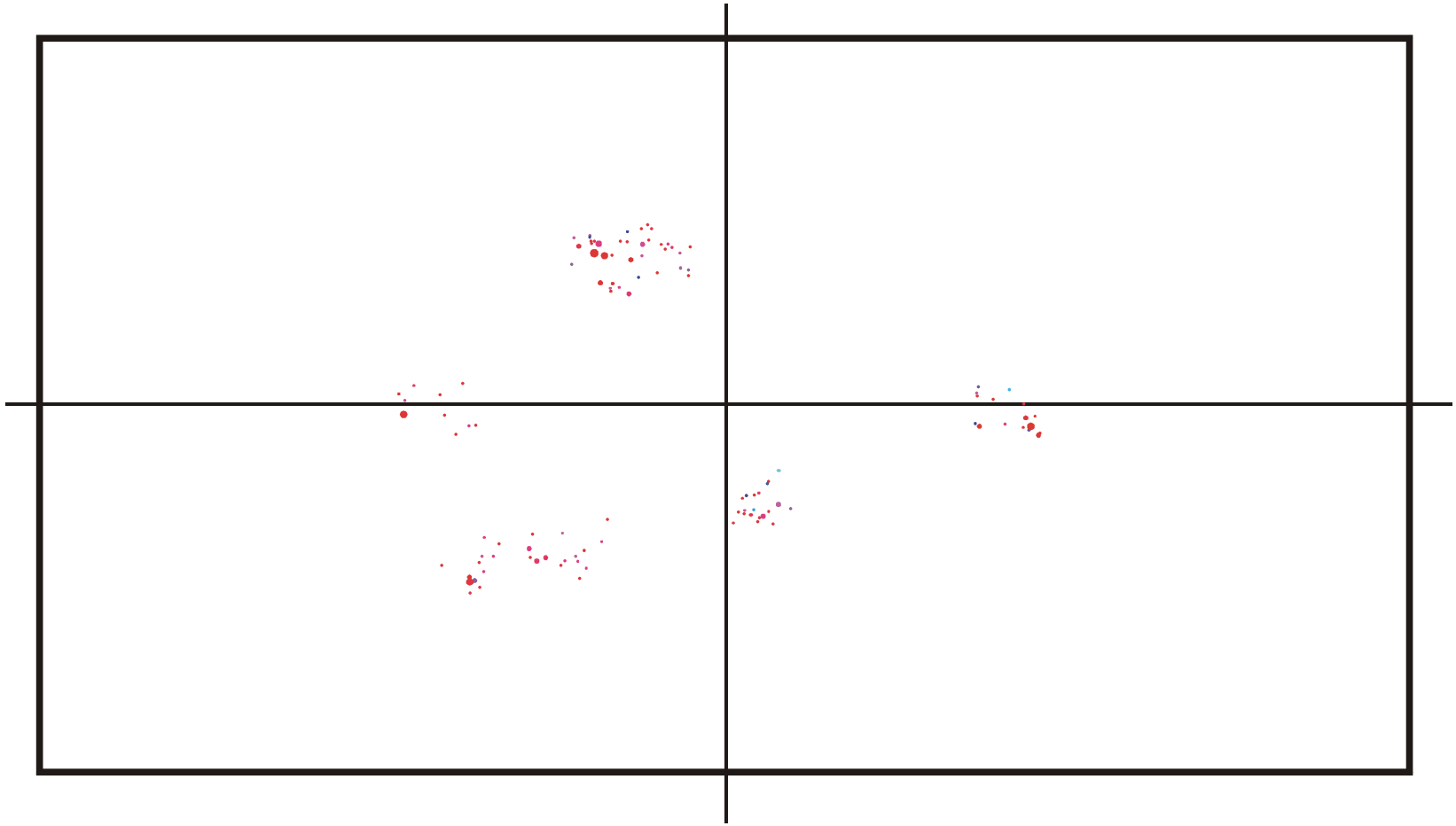

Spread of population in sequence space during a quasistationary epoch: t = 825

Spread of population in sequence space during a quasistationary epoch:  t = 830

Spread of population in sequence space during a quasistationary epoch: t = 835

Spread of population in sequence space during a quasistationary epoch:  t = 840

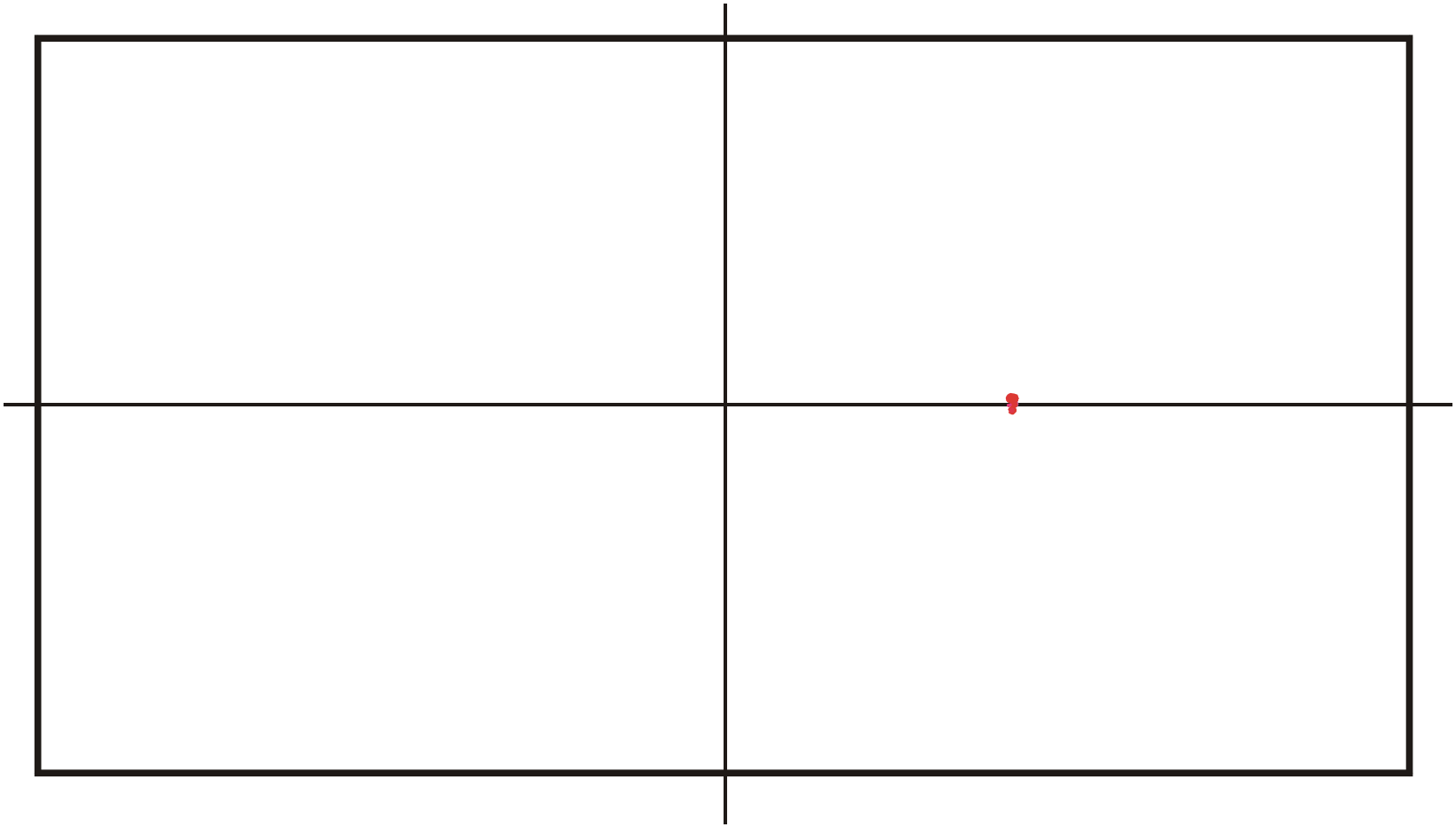

Spread of population in sequence space during a quasistationary epoch: t = 845

Spread of population in sequence space during a quasistationary epoch:  t = 850

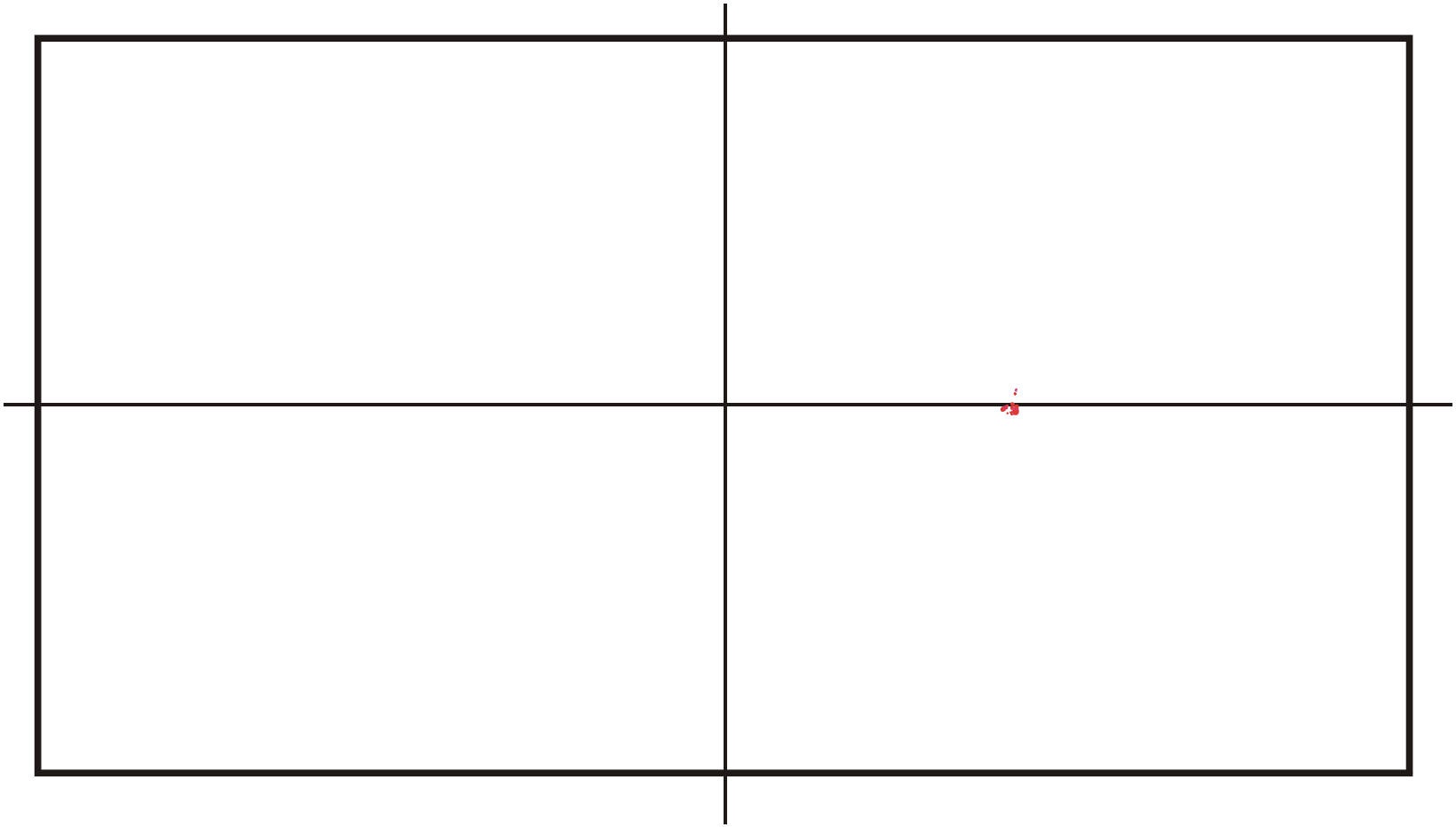

Spread of population in sequence space during a quasistationary epoch: t = 855

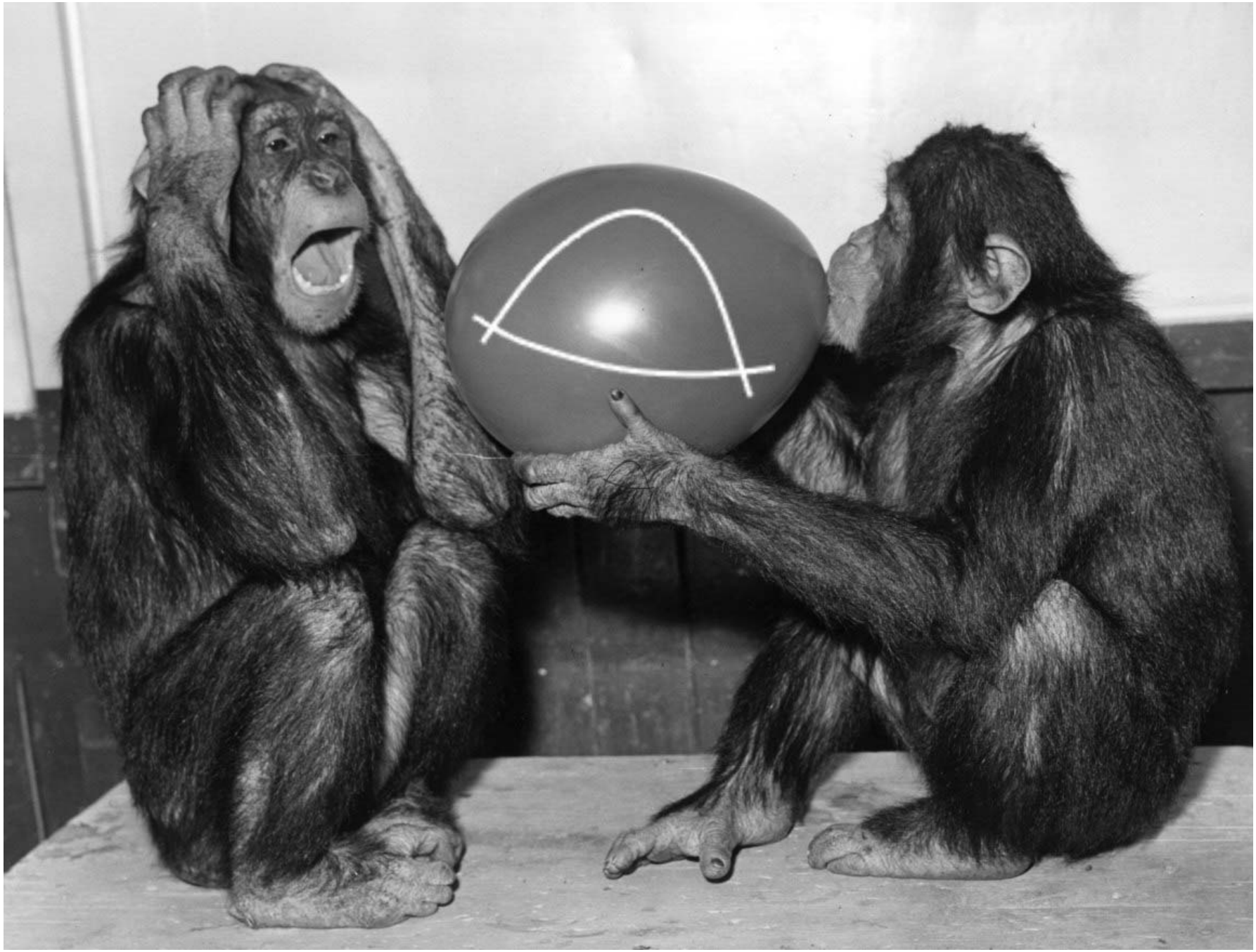

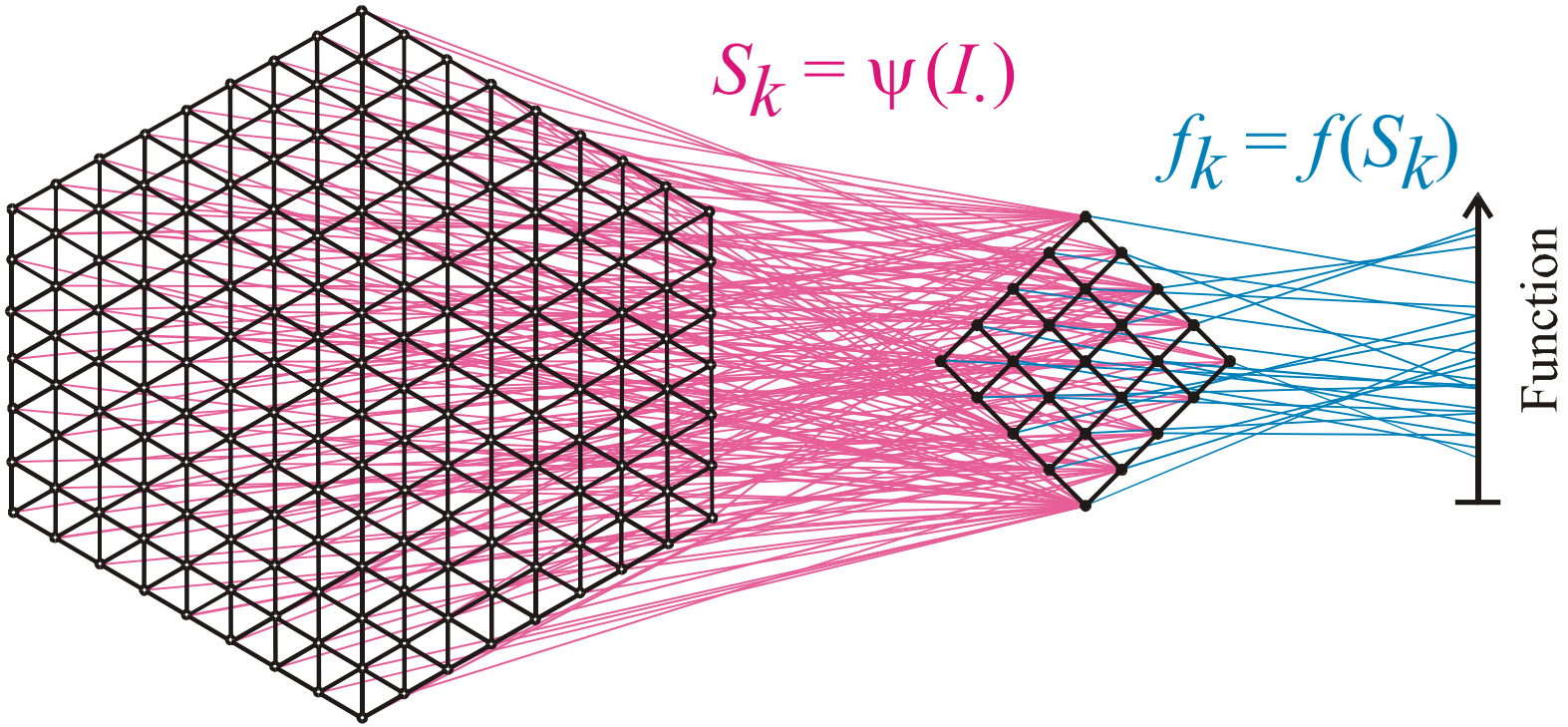


Mapping from sequence space into structure space and into function

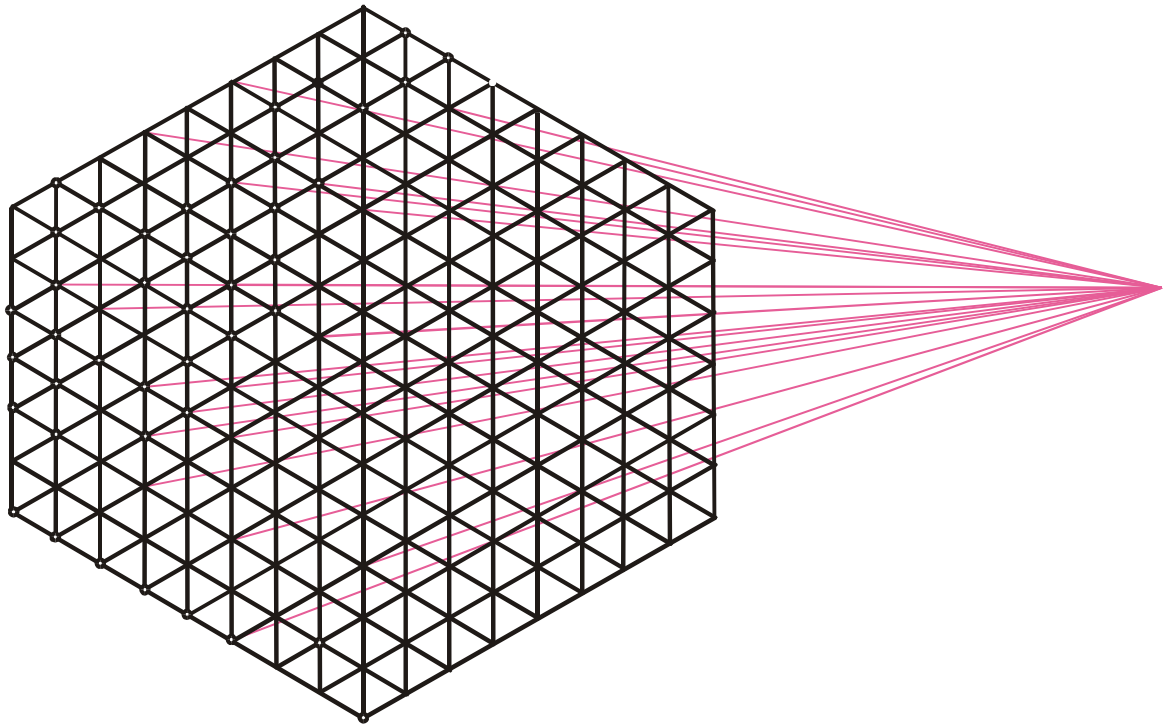

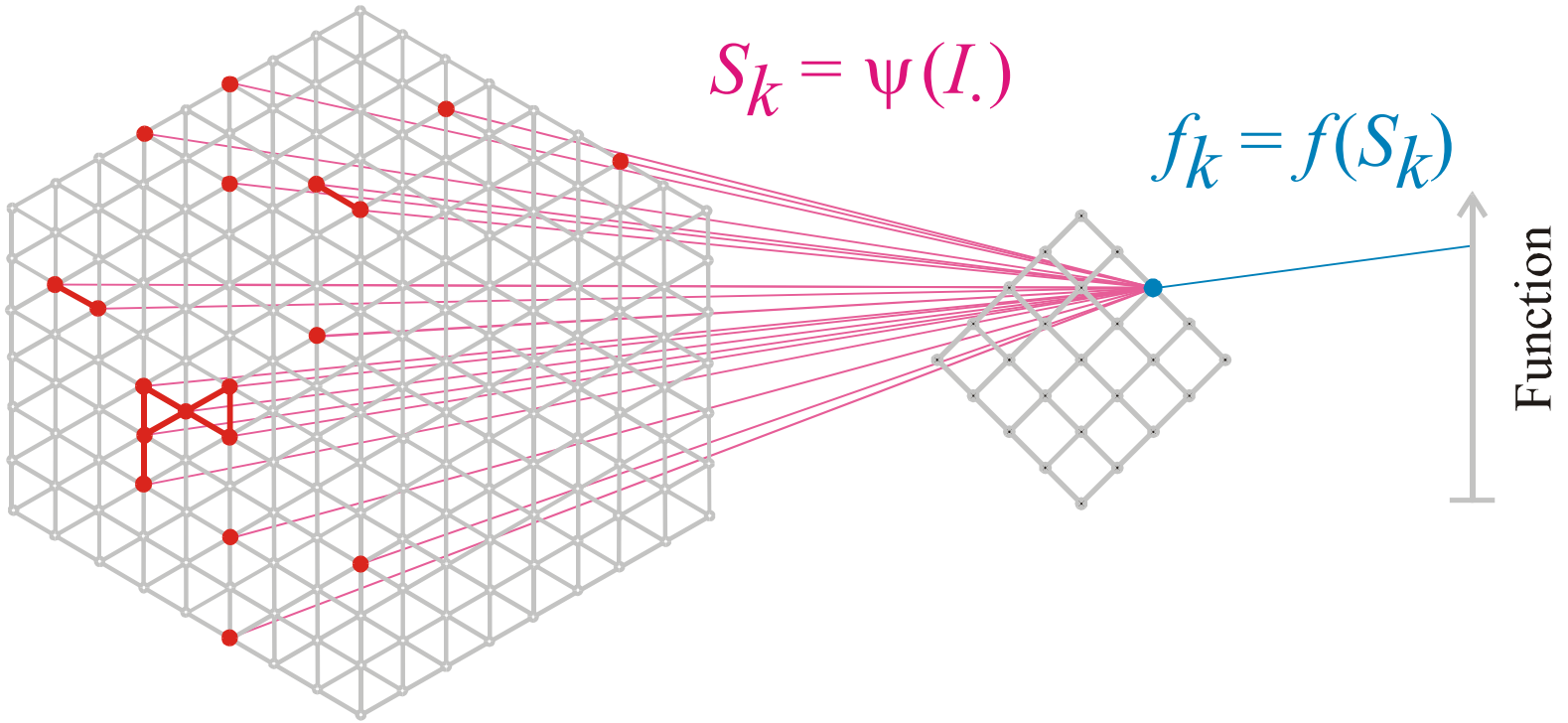


The pre-image of the structure $S_k$ in sequence space is the **neutral network $G_k$**

**Neutral networks** are sets of sequences forming the same structure. $\mathbf{G_k}$ is the pre-image of the structure $S_k$ in sequence space:

$$\mathbf{G_k} = y^{-1}(S_k)\ \pi\ \{I_j \mid y(I_j) = S_k\}$$

The set is converted into a graph by connecting all sequences of Hamming distance one.

**Neutral networks** of small RNA molecules can be computed by exhaustive folding of complete sequence spaces, i.e. all RNA sequences of a given chain length. This number, $\mathbf{N=4^n}$ , becomes very large with increasing length, and is prohibitive for numerical computations.

**Neutral networks** can be modelled by **random graphs** in sequence space. In this approach, nodes are inserted randomly into sequence space until the size of the pre-image, i.e. the number of neutral sequences, matches the neutral network to be studied.

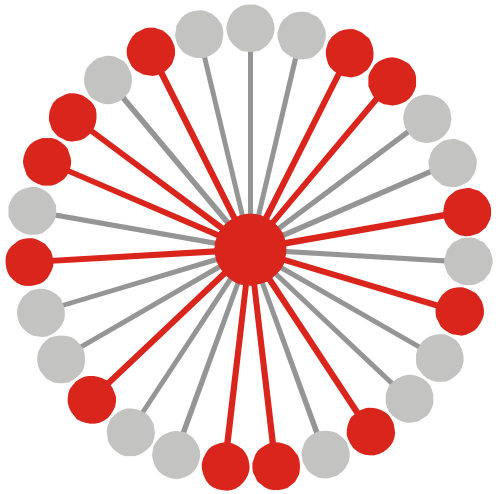

$$G_k = y^{-1}(S_k) \cup \{ I_j \mid y(I_j) = S_k \}$$

$$\lambda_j = 12 / 27 = 0.444\,, \quad \bar{\lambda}_k = \frac{\sum_{j \in |G_k|} l_j(k)}{|G_k|}$$

Connectivity threshold: $\lambda_{cr} = 1 - \kappa^{-1/(\kappa-1)}$

Alphabet size k : **AUGC** ñ k = 4

$\bar{\lambda}_k > \lambda_{cr}$ .... network $G_k$ is connected

$\bar{\lambda}_k < \lambda_{cr}$ .... network $G_k$ is **not** connected

| k | $l_{cr}$ | |
|---|---|---|
| 2 | 0.5 | **GC,AU** |
| 3 | 0.423 | **GUC,AUG** |
| 4 | 0.370 | **AUGC** |

Mean degree of neutrality and connectivity of neutral networks

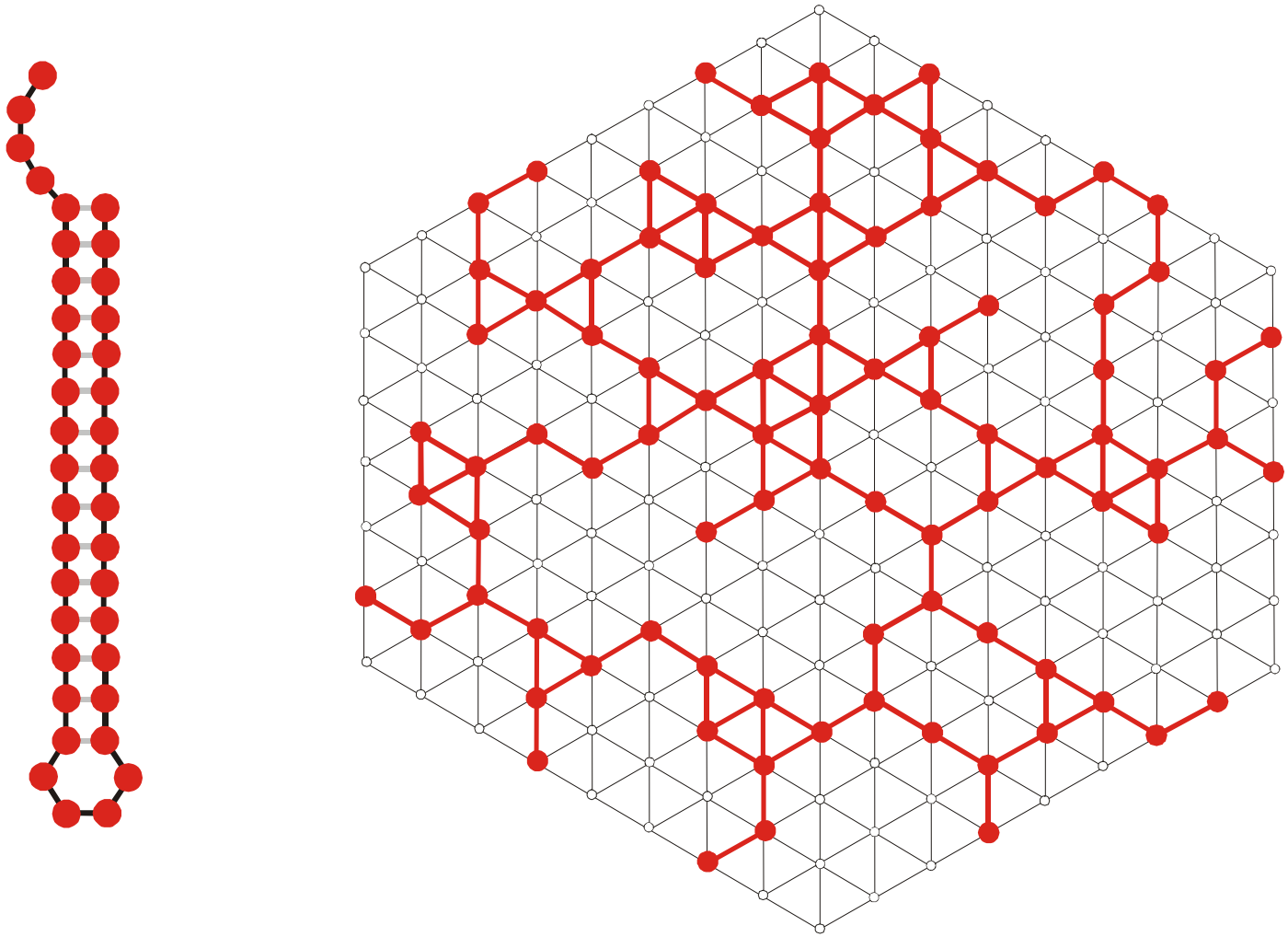

A connected neutral network

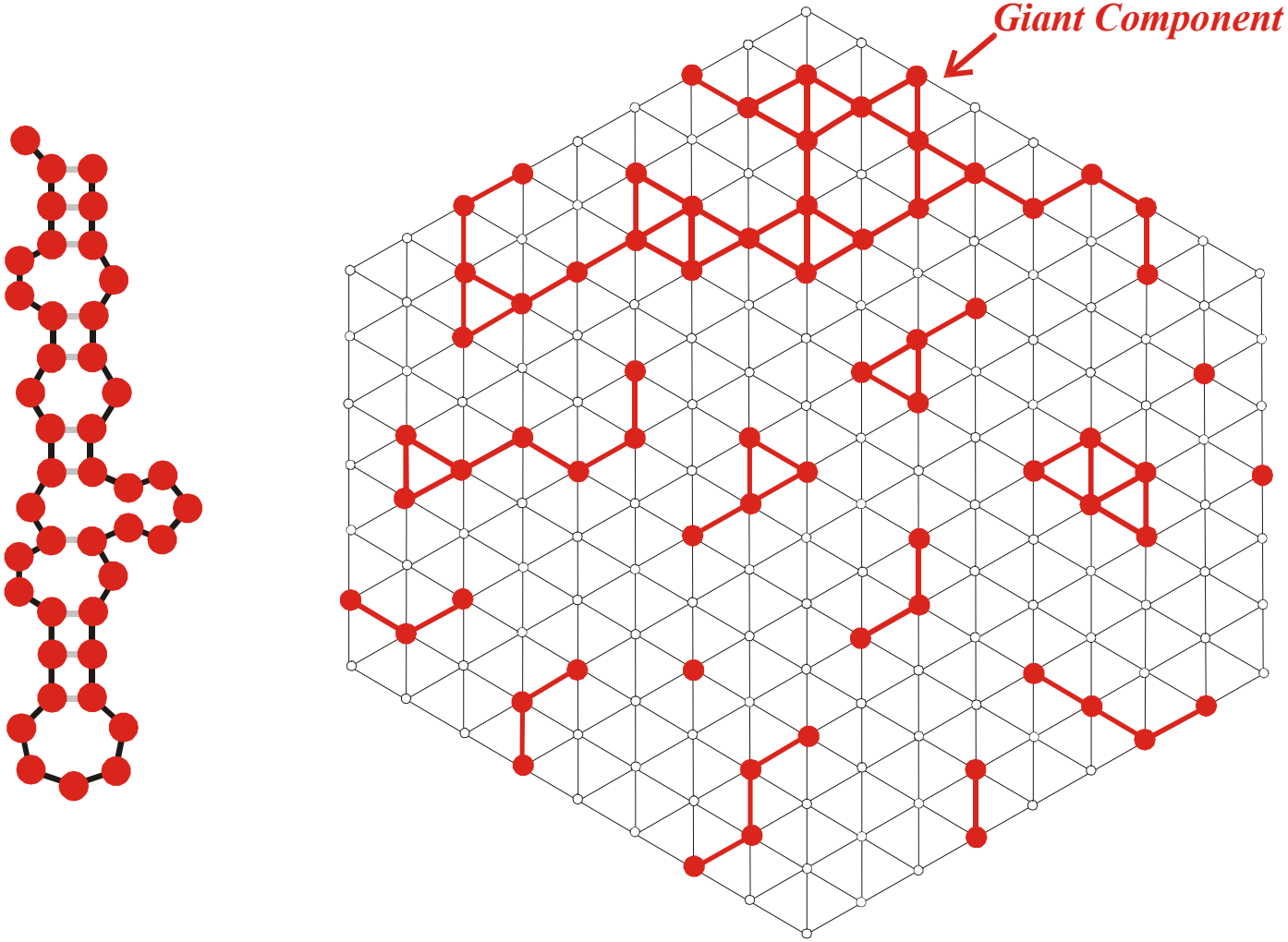


A multi-component neutral network

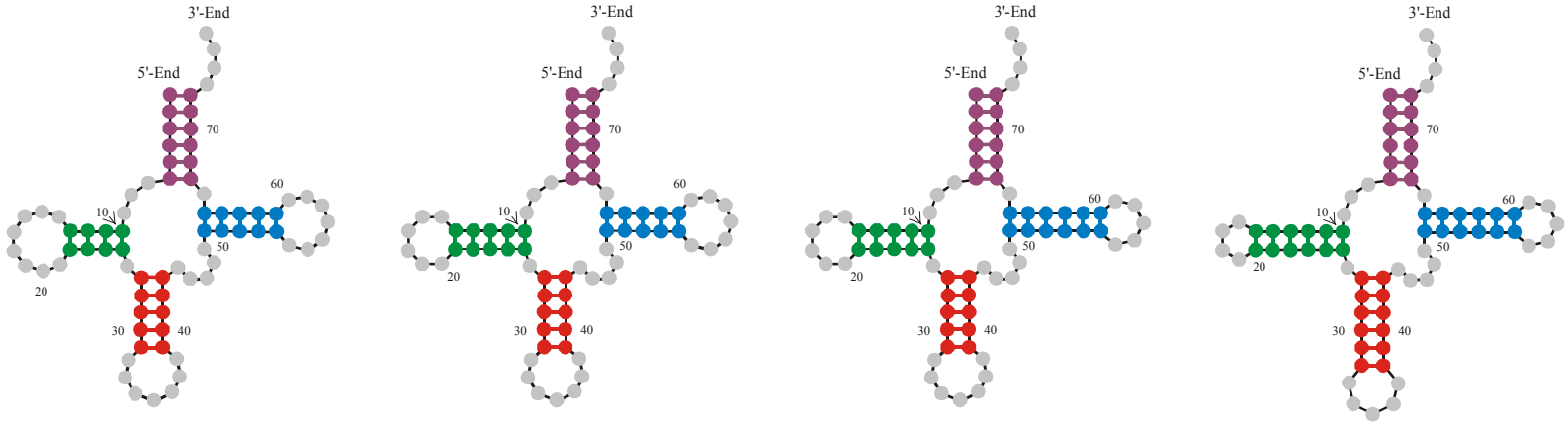


| Alphabet | Degree of neutrality ` | | | |
|---|---|---|---|---|
| AU | - - | - - | - - | 0.073 Ä 0.032 |
| AUG | - - | 0.217 Ä 0.051 | 0.207 ± 0.055 | 0.201 Ä 0.056 |
| AUGC | 0.275 Ä 0.064 | 0.279 Ä 0.063 | 0.289 ± 0.062 | 0.313 Ä 0.058 |
| UGC | 0.263 Ä 0.071 | 0.257 Ä 0.070 | 0.251 ± 0.068 | 0.250 Ä 0.064 |
| GC | 0.052 Ä 0.033 | 0.057 Ä 0.034 | 0.060 ± 0.033 | 0.068 Ä 0.034 |

Degree of neutrality of cloverleaf RNA secondary structures over different alphabets

# From sequences to shapes and back: a case study in RNA secondary structures

PETER SCHUSTER[1,2,3], WALTER FONTANA[3], PETER F. STADLER[2,3] AND IVO L. HOFACKER[2]

[1] *Institut für Molekulare Biotechnologie, Beutenbergstrasse 11, PF 100813, D-07708 Jena, Germany*
[2] *Institut für Theoretische Chemie, Universität Wien, Austria*
[3] *Santa Fe Institute, Santa Fe, U.S.A.*

SUMMARY

RNA folding is viewed here as a map assigning secondary structures to sequences. At fixed chain length the number of sequences far exceeds the number of structures. Frequencies of structures are highly non-uniform and follow a generalized form of Zipf's law: we find relatively few common and many rare ones. By using an algorithm for inverse folding, we show that sequences sharing the same structure are distributed randomly over sequence space. All common structures can be accessed from an arbitrary sequence by a number of mutations much smaller than the chain length. The sequence space is percolated by extensive neutral networks connecting nearest neighbours folding into identical structures. Implications for evolutionary adaptation and for applied molecular evolution are evident: finding a particular structure by mutation and selection is much simpler than expected and, even if catalytic activity should turn out to be sparse in the space of RNA structures, it can hardly be missed by evolutionary processes.

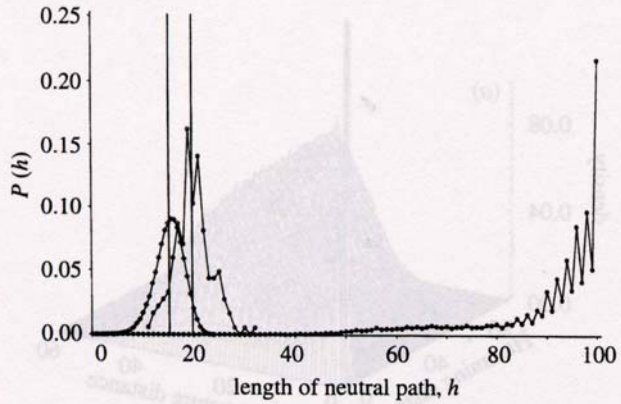


Figure 4. Neutral paths. A neutral path is defined by a series of nearest neighbour sequences that fold into identical structures. Two classes of nearest neighbours are admitted: neighbours of Hamming distance 1, which are obtained by single base exchanges in unpaired stretches of the structure, and neighbours of Hamming distance 2, resulting from base pair exchanges in stacks. Two probability densities of Hamming distances are shown that were obtained by searching for neutral paths in sequence space: (i) an upper bound for the closest approach of trial and target sequences (open circles) obtained as endpoints of neutral paths approaching the target from a random trial sequence (185 targets and 100 trials for each were used); (ii) a lower bound for the closest approach of trial and target sequences (open diamonds) derived from secondary structure statistics (Fontana *et al.* 1993*a*; see this paper, §4); and (iii) longest distances between the reference and the endpoints of monotonously diverging neutral paths (filled circles) (500 reference sequences were used).

*Proc. R. Soc. Lond.* B (1994) **255**, 279–284
*Printed in Great Britain*





Reference for postulation and ***in silico*** verification of ***neutral networks***

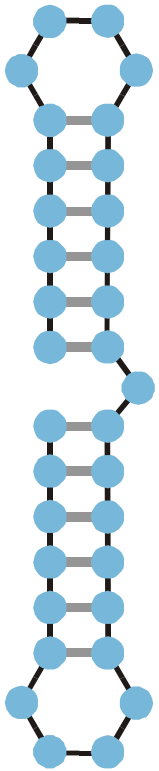

**Structure**

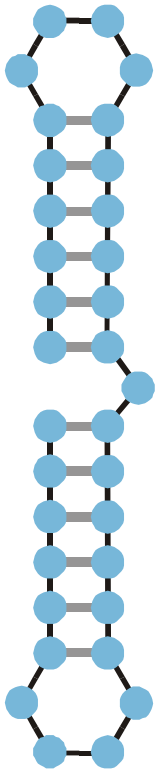

**Structure**

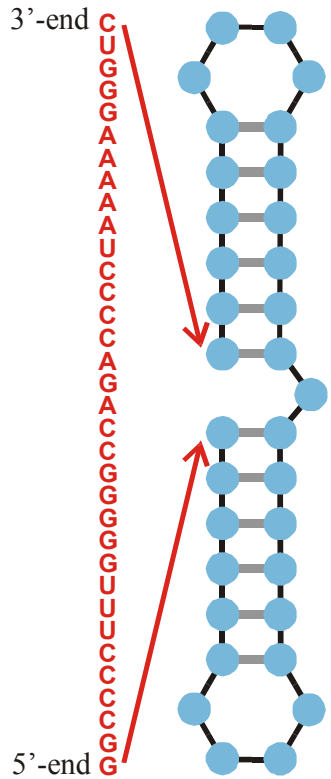


**Compatible sequence**

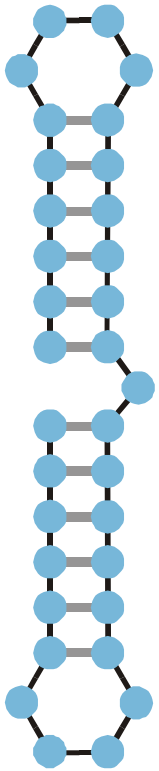

**Structure**

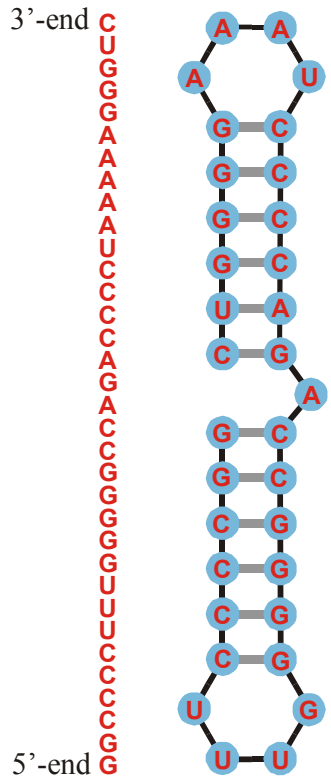


**Compatible sequence**

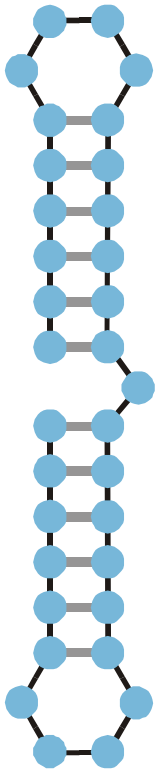

**Structure**

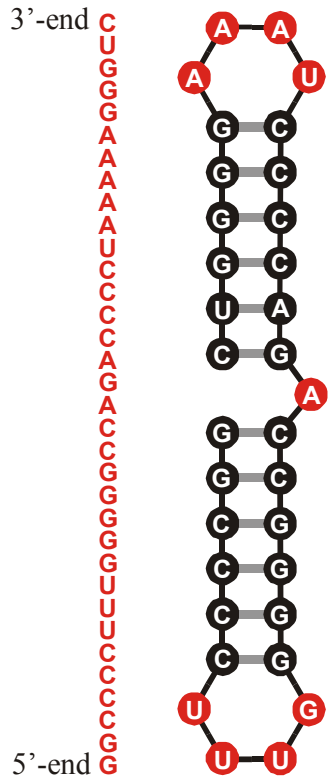


**Compatible sequence**

Single nucleotides: **A,U,G,C**

Base pairs: **AU , UA**
**GC , CG**
**GU , UG**

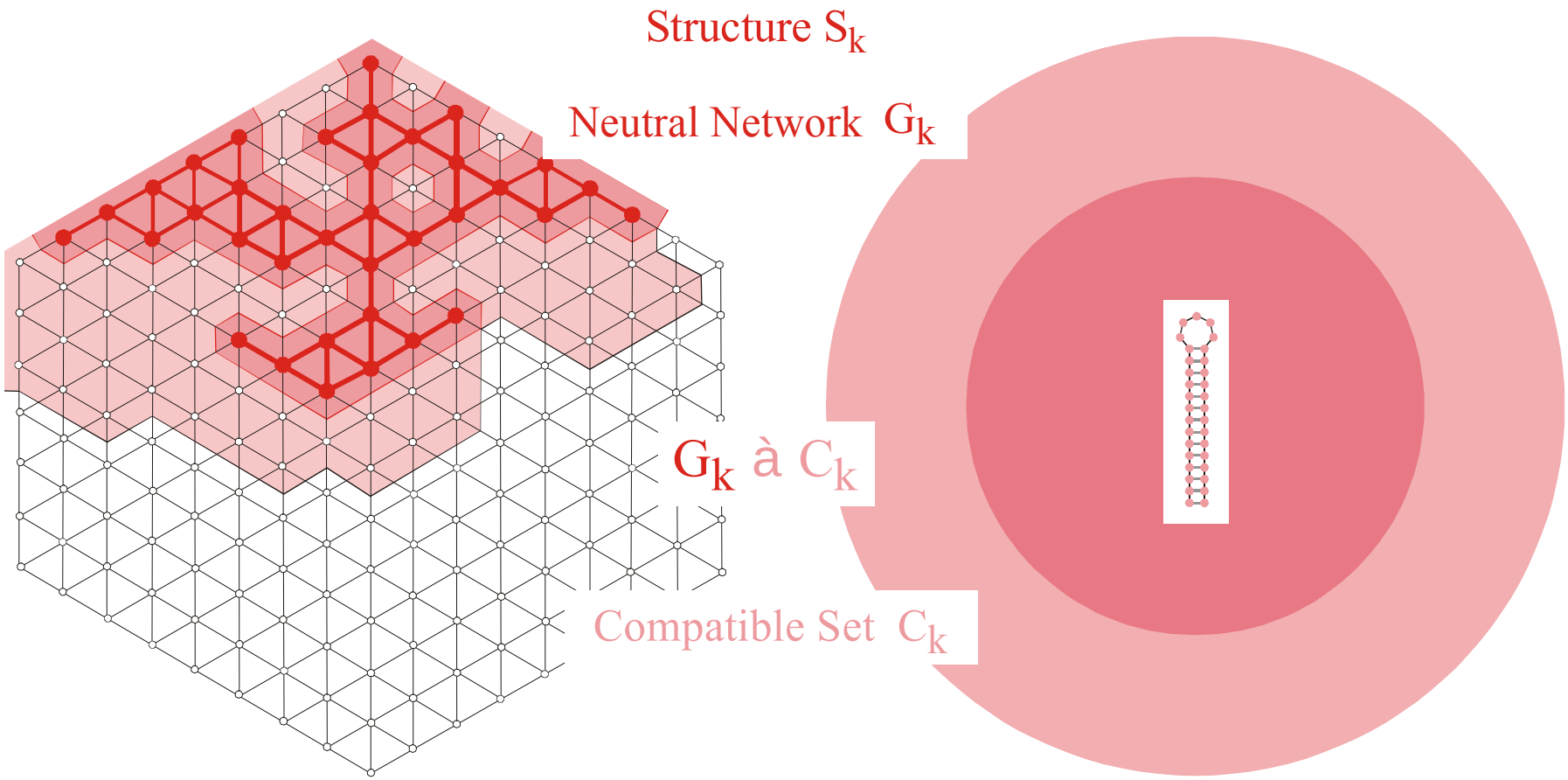


The **compatible set $C_k$** of a structure **$S_k$** consists of all sequences which form **$S_k$** as its minimum free energy structure (the neutral network **$G_k$**) or one of its suboptimal structures.

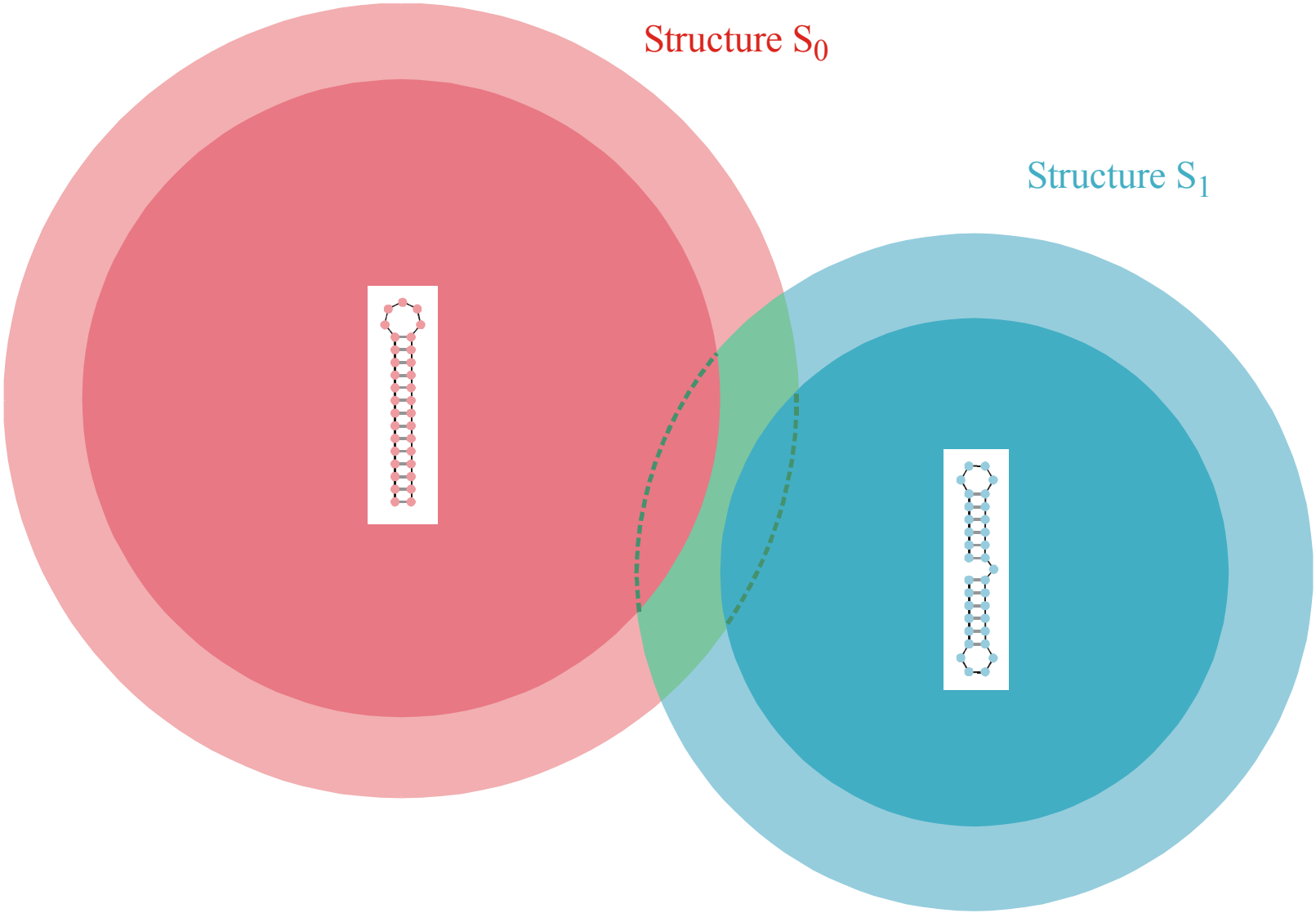


**Intersection** of two compatible sets: $C_0 \cap C_1$

The intersection of two compatible sets is always non empty: $C_0$ Ú $C_1$ â Ù

*Bulletin of Mathematical Biology*, Vol. 59, No. 2, pp. 339–397, 1997
Elsevier Science Inc.

0092-8240/97 $17.00 + 0.00

ELSEVIER

S0092-8240(96)00089-4

# GENERIC PROPERTIES OF COMBINATORY MAPS: NEUTRAL NETWORKS OF RNA SECONDARY STRUCTURES[1]

■ CHRISTIAN REIDYS*,†, PETER F. STADLER*,‡ and PETER SCHUSTER*,‡,§,[2]
*Santa Fe Institute,
Santa Fe, NM 87501, U.S.A.

†Los Alamos National Laboratory,
Los Alamos, NM 87545, U.S.A.

‡Institut für Theoretische Chemie der Universität Wien,
A-1090 Wien, Austria

§Institut für Molekulare Biotechnologie,
D-07708 Jena, Germany

(*E.mail: pks@tbi.univie.ac.at*)

Random graph theory is used to model and analyse the relationships between sequences and secondary structures of RNA molecules, which are understood as mappings from sequence space into shape space. These maps are non-invertible since there are always many orders of magnitude more sequences than structures. Sequences folding into identical structures form *neutral networks*. A neutral network is embedded in the set of sequences that are *compatible* with the given structure. Networks are modeled as graphs and constructed by random choice of vertices from the space of compatible sequences. The theory characterizes neutral networks by the mean fraction of neutral neighbors ($\lambda$). The networks are connected and percolate sequence space if the fraction of neutral nearest neighbors exceeds a threshold value ($\lambda > \lambda^*$). Below threshold ($\lambda < \lambda^*$), the networks are partitioned into a largest "giant" component and several smaller components. Structures are classified as "common" or "rare" according to the sizes of their pre-images, i.e. according to the fractions of sequences folding into them. The neutral networks of any pair of two different common structures almost touch each other, and, as expressed by the conjecture of *shape space covering* sequences folding into almost all common structures, can be found in a small ball of an arbitrary location in sequence space. The results from random graph theory are compared to data obtained by folding large samples of RNA sequences. Differences are explained in terms of specific features of RNA molecular structures. © *1997 Society for Mathematical Biology*

THEOREM 5. INTERSECTION-THEOREM. *Let* s *and* s′ *be arbitrary secondary structures and* **C**[s], **C**[s′] *their corresponding compatible sequences. Then,*

$$\mathbf{C}[s] \cap \mathbf{C}[s'] \neq \varnothing.$$

*Proof.* Suppose that the alphabet admits only the complementary base pair $[XY]$ and we ask for a sequence $x$ compatible to both $s$ and $s'$. Then $\mathcal{J}(s, s') \cong D_m$ operates on the set of all positions $\{x_1, \ldots, x_n\}$. Since we have the operation of a dihedral group, the orbits are either cycles or chains and the cycles have even order. A constraint for the sequence compatible to both structures appears only in the cycles where the choice of bases is not independent. It remains to be shown that there is a valid choice of bases for each cycle, which is obvious since these have even order. Therefore, it suffices to choose an alternating sequence of the pairing partners $X$ and $Y$. Thus, there are at least two different choices for the first base in the orbit. ■

*Remark.* A generalization of the statement of theorem 5 to three different structures is false.

Reference for the definition of the intersection and the proof of the **intersection theorem**

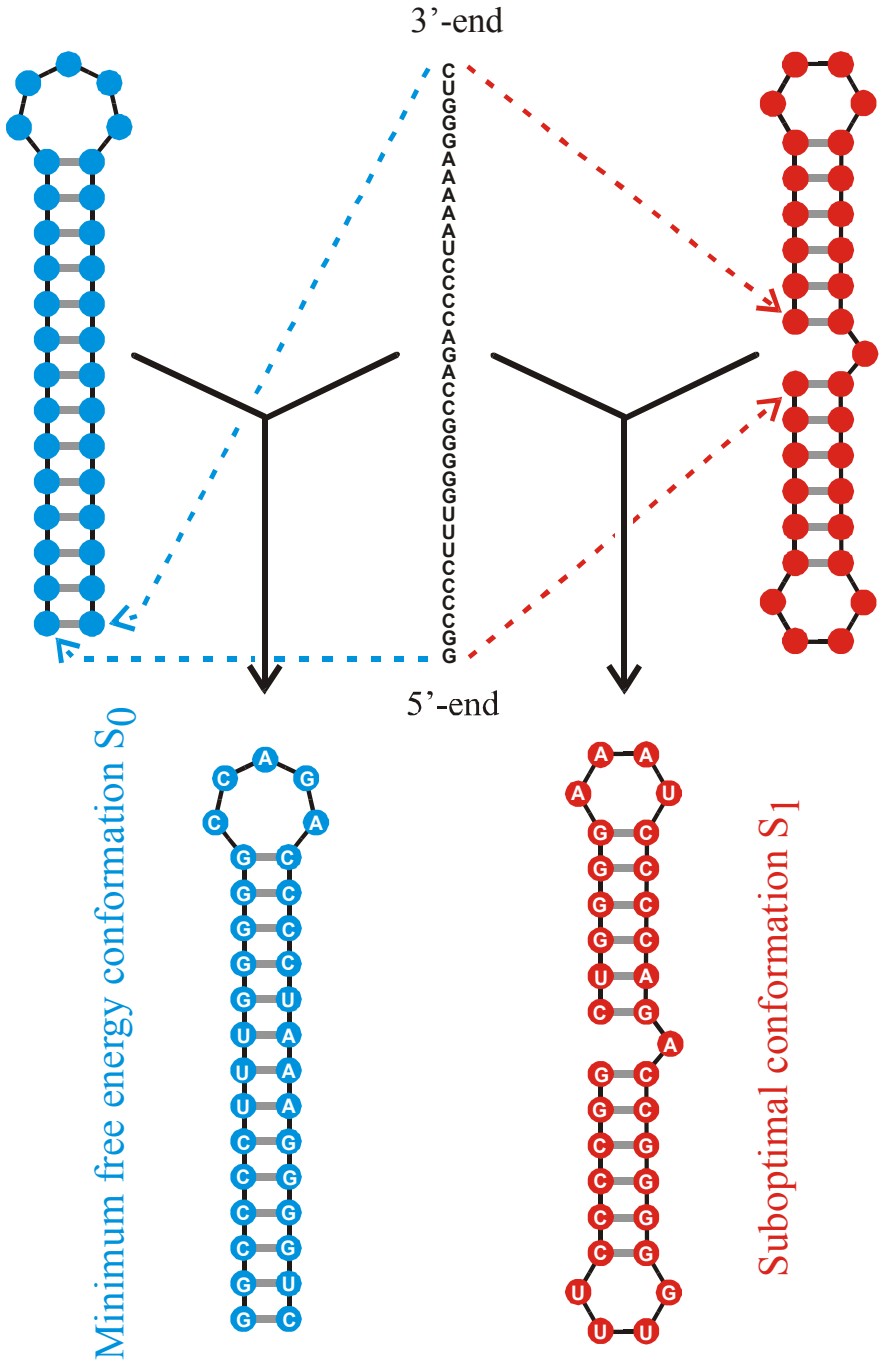


A sequence at the **intersection** of two neutral networks is compatible with both structures

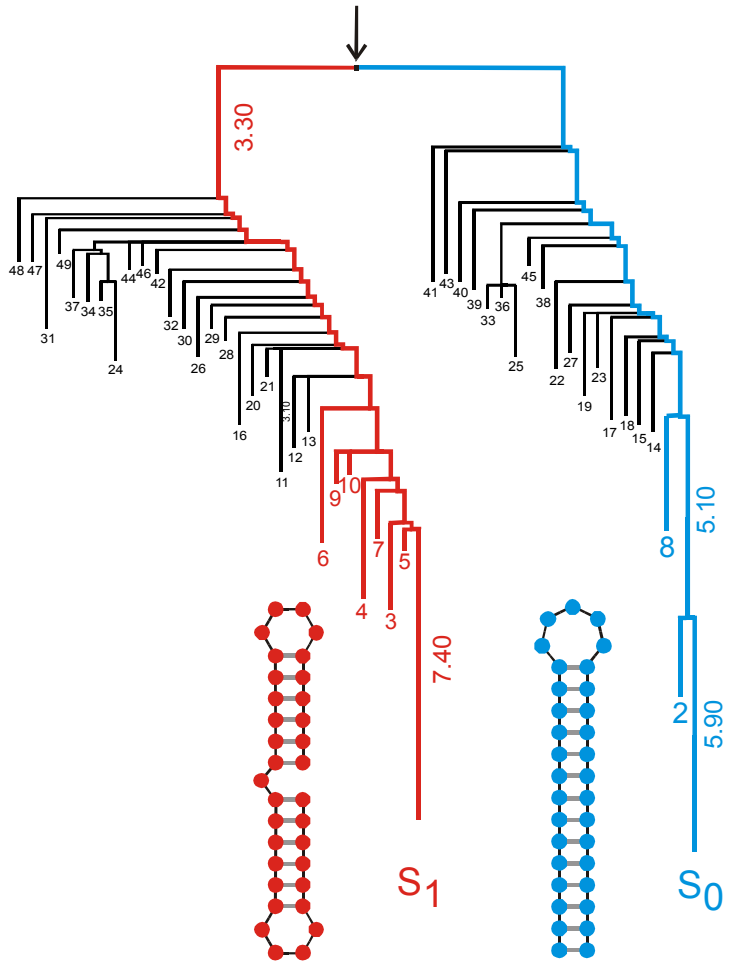


basin '1'

basin '0'

Barrier tree for two long living structures

long living metastable structure

minimum free energy structure

# A ribozyme switch

E.A.Schultes, D.B.Bartel, Science **289** (2000), 448-452



minus the background levels observed in the HSP in the control (Sar1-GDP–containing) incubation that prevents COPII vesicle formation. In the microsome control, the level of p115-SNARE associations was less than 0.1%.
46. C. M. Carr, E. Grote, M. Munson, F. M. Hughson, P. J. Novick, *J. Cell Biol.* **146**, 333 (1999).
47. C. Ungermann, B. J. Nichols, H. R. Pelham, W. Wickner, *J. Cell Biol.* **140**, 61 (1998).
48. E. Grote and P. J. Novick, *Mol. Biol. Cell* **10**, 4149 (1999).
49. P. Uetz *et al.*, *Nature* **403**, 623 (2000).
50. GST-SNARE proteins were expressed in bacteria and purified on glutathione-Sepharose beads using standard methods. Immobilized GST-SNARE protein (0.5 μM) was incubated with rat liver cytosol (20 mg) or purified recombinant p115 (0.5 μM) in 1 ml of NS buffer containing 1% BSA for 2 hours at 4°C with rotation. Beads were briefly spun (3000 rpm for 10 s) and sequentially washed three times with NS buffer and three times with NS buffer supplemented with 150 mM NaCl. Bound proteins were eluted three times in 50 μl of 50 mM tris-HCl (pH 8.5), 50 mM reduced glutathione, 150 mM NaCl, and 0.1% Triton X-100 for 15 min at 4°C with intermittent mixing, and elutes were pooled. Proteins were precipitated by MeOH/$CH_3Cl$ and separated by SDS–polyacrylamide gel electrophoresis (PAGE) followed by immunoblotting using p115 mAb 13F12.
51. V. Rybin *et al.*, *Nature* **383**, 266 (1996).
52. K. G. Hardwick and H. R. Pelham, *J. Cell Biol.* **119**, 513 (1992).
53. A. P. Newman, M. E. Groesch, S. Ferro-Novick, *EMBO J.* **11**, 3609 (1992).
54. A. Spang and R. Schekman, *J. Cell Biol.* **143**, 589 (1998).
55. M. F. Rexach, M. Latterich, R. W. Schekman, *J. Cell Biol.* **126**, 1133 (1994).
56. A. Mayer and W. Wickner, *J. Cell Biol.* **136**, 307 (1997).
57. M. D. Turner, H. Plutner, W. E. Balch, *J. Biol. Chem.* **272**, 13479 (1997).
58. A. Price, D. Seals, W. Wickner, C. Ungermann, *J. Cell Biol.* **148**, 1231 (2000).
59. X. Cao and C. Barlowe, *J. Cell Biol.* **149**, 55 (2000).
60. G. G. Tall, H. Hama, D. B. DeWald, B. F. Horazdovsky, *Mol. Biol. Cell* **10**, 1873 (1999).
61. C. G. Burd, M. Peterson, C. R. Cowles, S. D. Emr, *Mol. Biol. Cell* **8**, 1089 (1997).
62. M. R. Peterson, C. G. Burd, S. D. Emr, *Curr. Biol.* **9**, 159 (1999).
63. M. G. Waters, D. O. Clary, J. E. Rothman, *J. Cell Biol.* **118**, 1015 (1992).
64. D. M. Walter, K. S. Paul, M. G. Waters, *J. Biol. Chem.* **273**, 29565 (1998).
65. N. Hui *et al.*, *Mol. Biol. Cell* **8**, 1777 (1997).
66. T. E. Kreis, *EMBO J.* **5**, 931 (1986).
67. H. Plutner, H. W. Davidson, J. Saraste, W. E. Balch, *J. Cell Biol.* **119**, 1097 (1992).
68. D. S. Nelson *et al.*, *J. Cell Biol.* **143**, 319 (1998).
69. We thank G. Waters for p115 cDNA and p115 mAbs; G. Warren for p97 and p47 antibodies; R. Scheller for rbet1, membrin, and sec22 cDNAs; H. Plutner for excellent technical assistance; and P. Tan for help during the initial phase of this work. Supported by NIH grants GM 33301 and GM42336 and National Cancer Institute grant CA58689 (W.E.B.), a NIH National Research Service Award (B.D.M.), and a Wellcome Trust International Traveling Fellowship (B.B.A.).

20 March 2000; accepted 22 May 2000

# One Sequence, Two Ribozymes: Implications for the Emergence of New Ribozyme Folds

**Erik A. Schultes and David P. Bartel***

**We describe a single RNA sequence that can assume either of two ribozyme folds and catalyze the two respective reactions. The two ribozyme folds share no evolutionary history and are completely different, with no base pairs (and probably no hydrogen bonds) in common. Minor variants of this sequence are highly active for one or the other reaction, and can be accessed from prototype ribozymes through a series of neutral mutations. Thus, in the course of evolution, new RNA folds could arise from preexisting folds, without the need to carry inactive intermediate sequences. This raises the possibility that biological RNAs having no structural or functional similarity might share a common ancestry. Furthermore, functional and structural divergence might, in some cases, precede rather than follow gene duplication.**

Related protein or RNA sequences with the same folded conformation can often perform very different biochemical functions, indicating that new biochemical functions can arise from preexisting folds. But what evolutionary mechanisms give rise to sequences with new macromolecular folds? When considering the origin of new folds, it is useful to picture, among all sequence possibilities, the distribution of sequences with a particular fold and function. This distribution can range very far in sequence space (*1*). For example, only seven nucleotides are strictly conserved among the group I self-splicing introns, yet secondary (and presumably tertiary) structure within the core of the ribozyme is preserved (*2*). Because these disparate isolates have the same fold and function, it is thought that they descended from a common ancestor through a series of mutational variants that were each functional. Hence, sequence heterogeneity among divergent isolates implies the existence of paths through sequence space that have allowed neutral drift from the ancestral sequence to each isolate. The set of all possible neutral paths composes a "neutral network," connecting in sequence space those widely dispersed sequences sharing a particular fold and activity, such that any sequence on the network can potentially access very distant sequences by neutral mutations (*3*–*5*).

Theoretical analyses using algorithms for predicting RNA secondary structure have suggested that different neutral networks are interwoven and can approach each other very closely (*3*, *5*–*8*). Of particular interest is whether ribozyme neutral networks approach each other so closely that they intersect. If so, a single sequence would be capable of folding into two different conformations, would have two different catalytic activities, and could access by neutral drift every sequence on both networks. With intersecting networks, RNAs with novel structures and activities could arise from previously existing ribozymes, without the need to carry nonfunctional sequences as evolutionary intermediates. Here, we explore the proximity of neutral networks experimentally, at the level of RNA function. We describe a close apposition of the neutral networks for the hepatitis delta virus (HDV) self-cleaving ribozyme and the class III self-ligating ribozyme.

In choosing the two ribozymes for this investigation, an important criterion was that they share no evolutionary history that might confound the evolutionary interpretations of our results. Choosing at least one artificial ribozyme ensured independent evolutionary histories. The class III ligase is a synthetic ribozyme isolated previously from a pool of random RNA sequences (*9*). It joins an oligonucleotide substrate to its 5′ terminus. The prototype ligase sequence (Fig. 1A) is a shortened version of the most active class III variant isolated after 10 cycles of in vitro selection and evolution. This minimal construct retains the activity of the full-length isolate (*10*). The HDV ribozyme carries out the site-specific self-cleavage reactions needed during the life cycle of HDV, a satellite virus of hepatitis B with a circular, single-stranded RNA genome (*11*). The prototype HDV construct for our study (Fig. 1B) is a shortened version of the antigenomic HDV ribozyme (*12*), which undergoes self-cleavage at a rate similar to that reported for other antigenomic constructs (*13*, *14*).

The prototype class III and HDV ribozymes have no more than the 25% sequence identity expected by chance and no fortuitous structural similarities that might favor an intersection of their two neutral networks. Nevertheless, sequences can be designed that simultaneously satisfy the base-pairing requirements

Whitehead Institute for Biomedical Research and Department of Biology, Massachusetts Institute of Technology, 9 Cambridge Center, Cambridge, MA 02142, USA.

*To whom correspondence should be addressed. E-mail: dbartel@wi.mit.edu

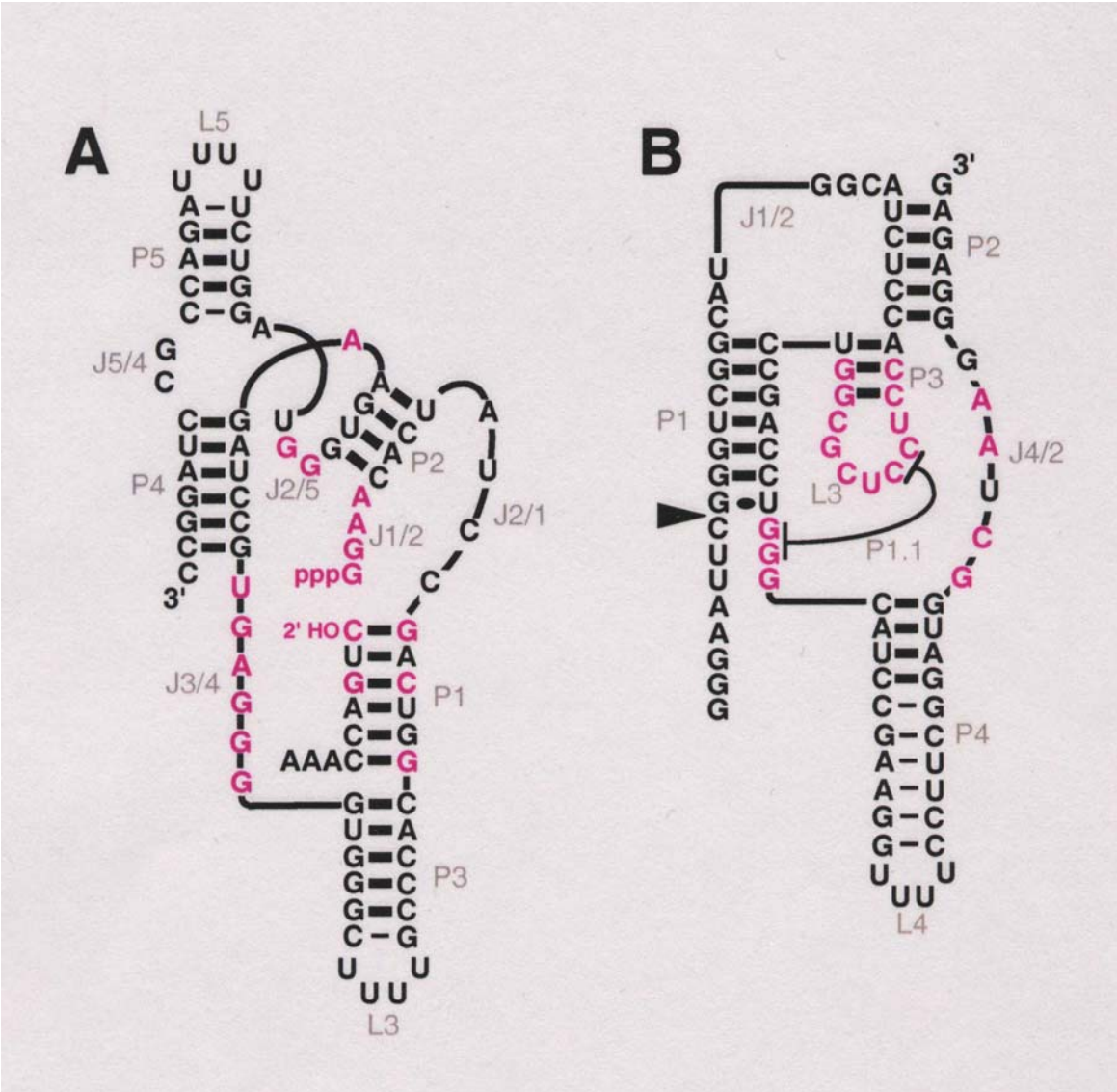


Two ribozymes of chain lengths n = 88 nucleotides: An artificial ligase (**A**) and a natural cleavage ribozyme of hepatitis-d-virus (**B**)

The sequence at the ***intersection***:

An RNA molecules which is 88 nucleotides long and can form both structures

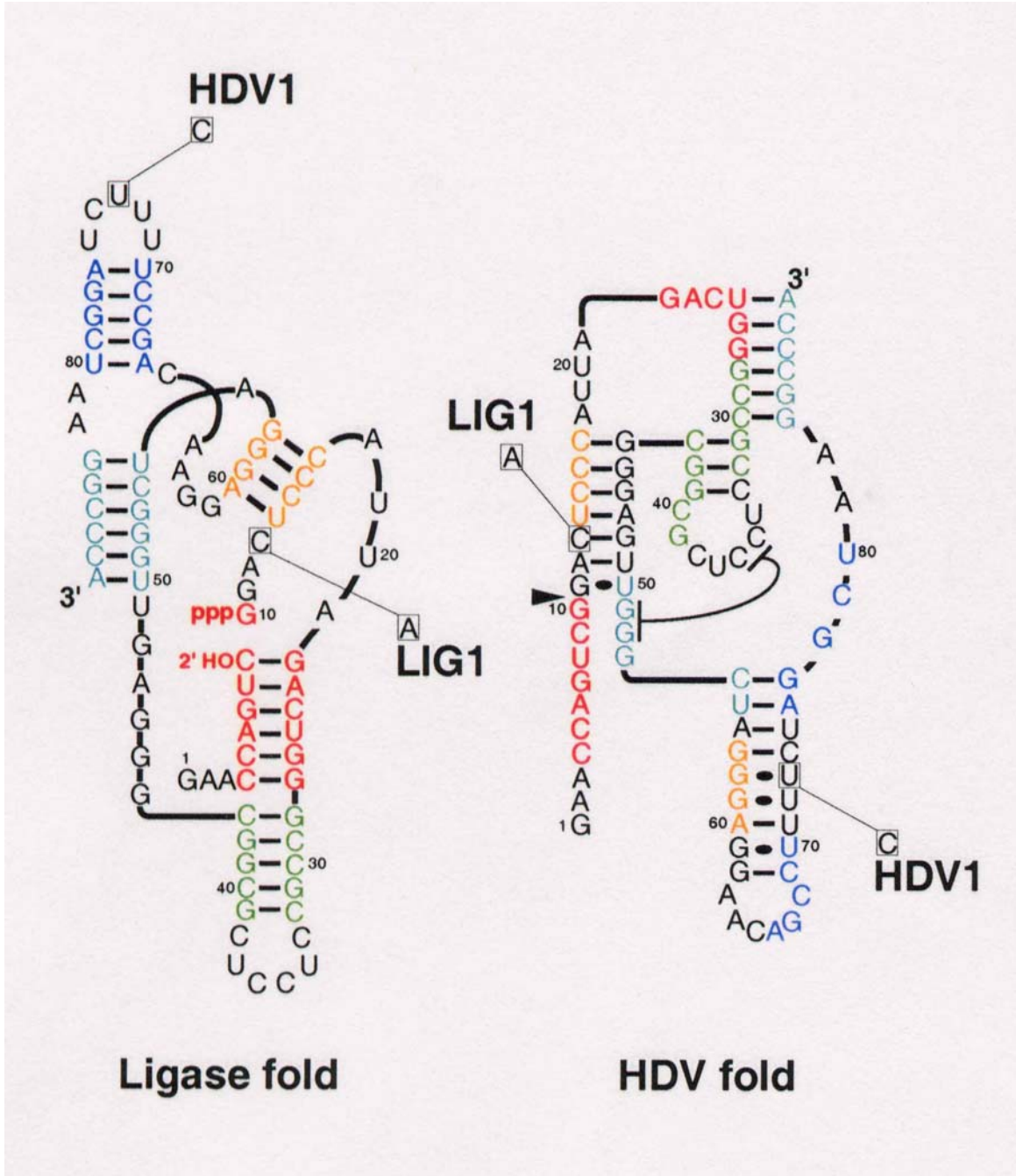

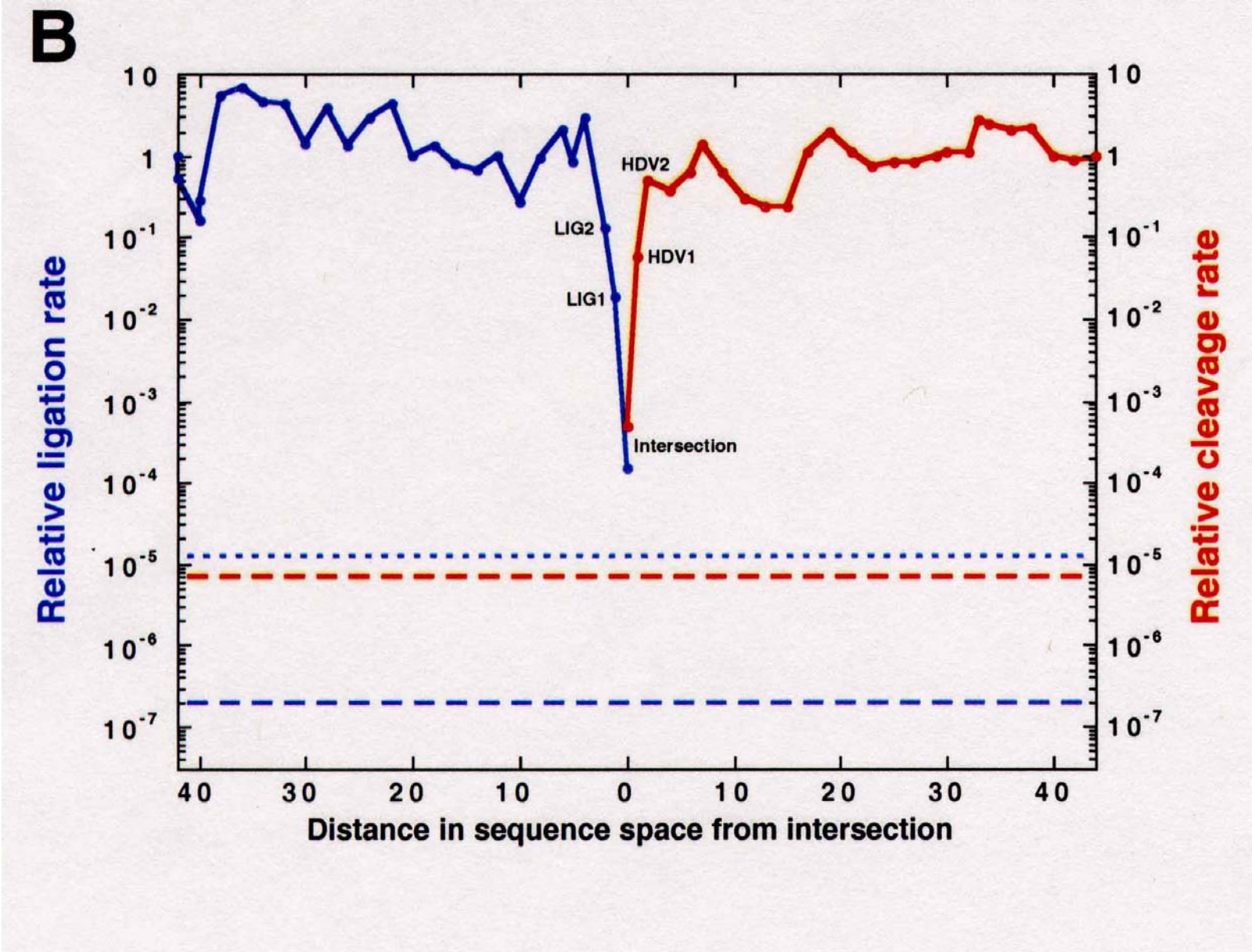


Two neutral walks through sequence space with conservation of structure and catalytic activity

Massif Central

Mount Fuji

Examples of smooth landscapes on Earth

Dolomites

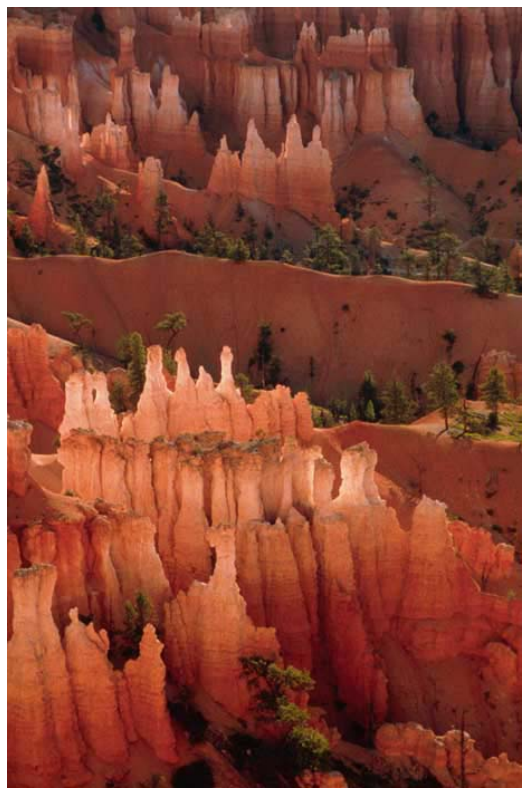

Bryce Canyon

Examples of rugged landscapes on Earth

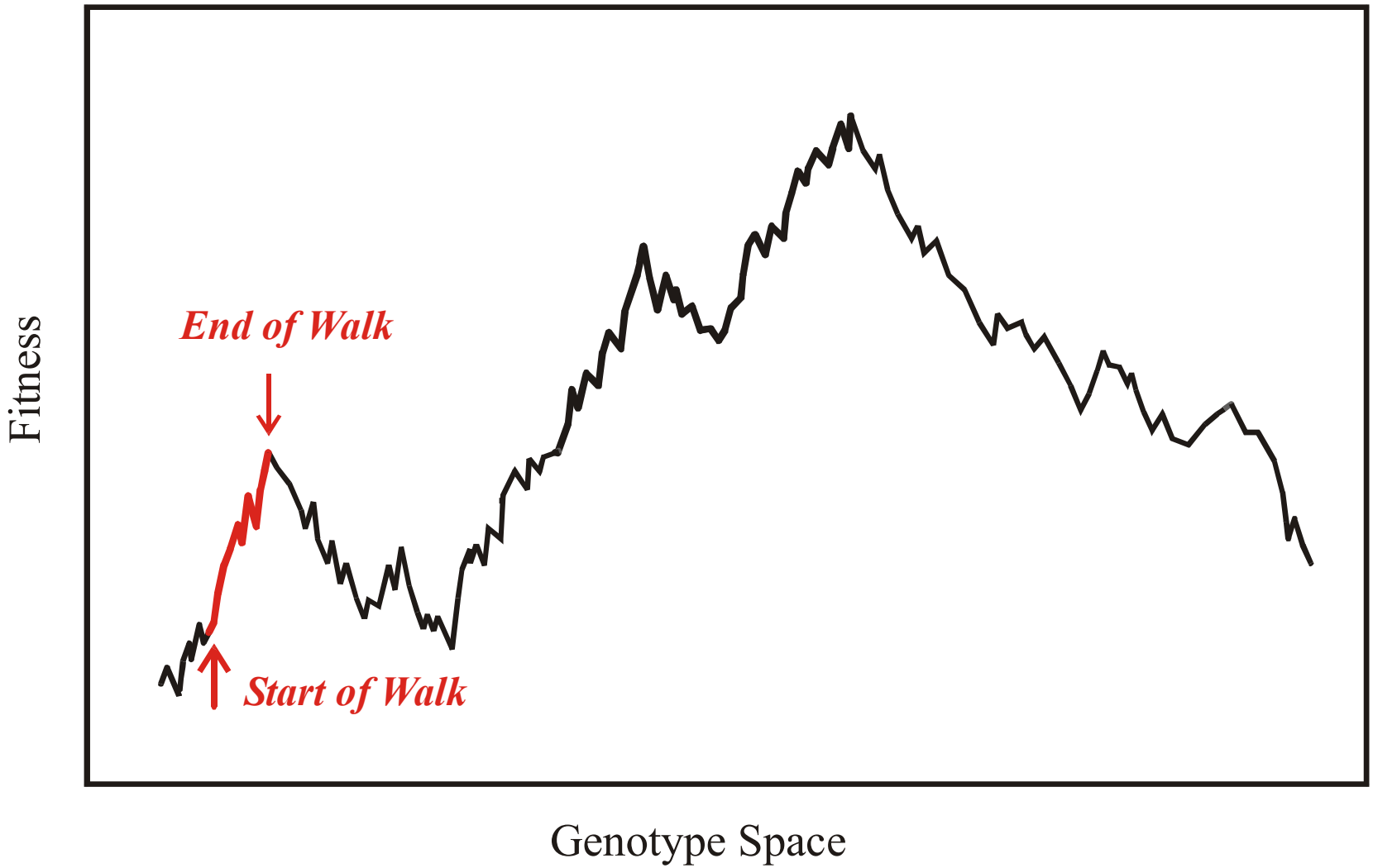


Evolutionary optimization in absence of neutral paths in sequence space

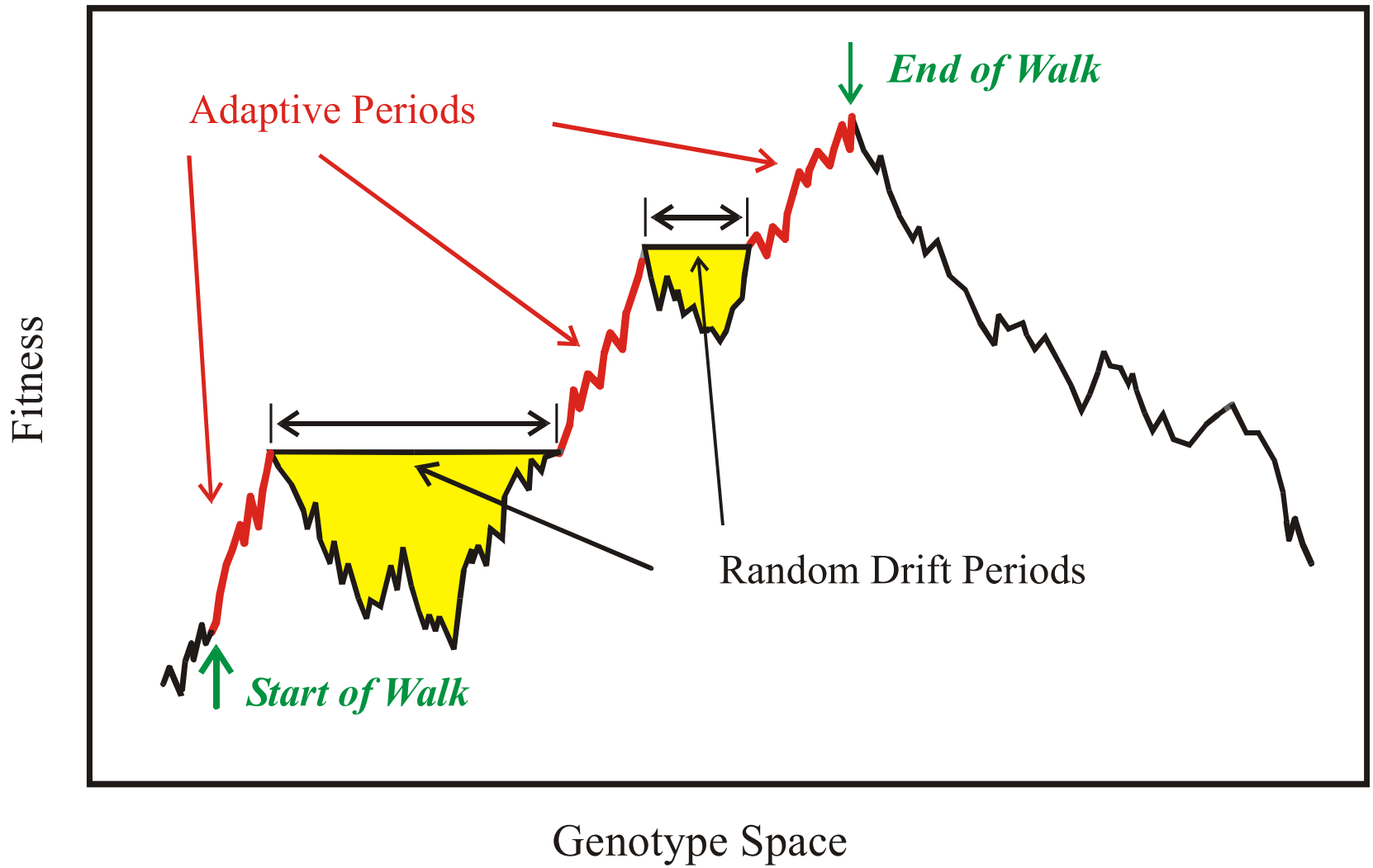


Evolutionary optimization including neutral paths in sequence space

Grand Canyon

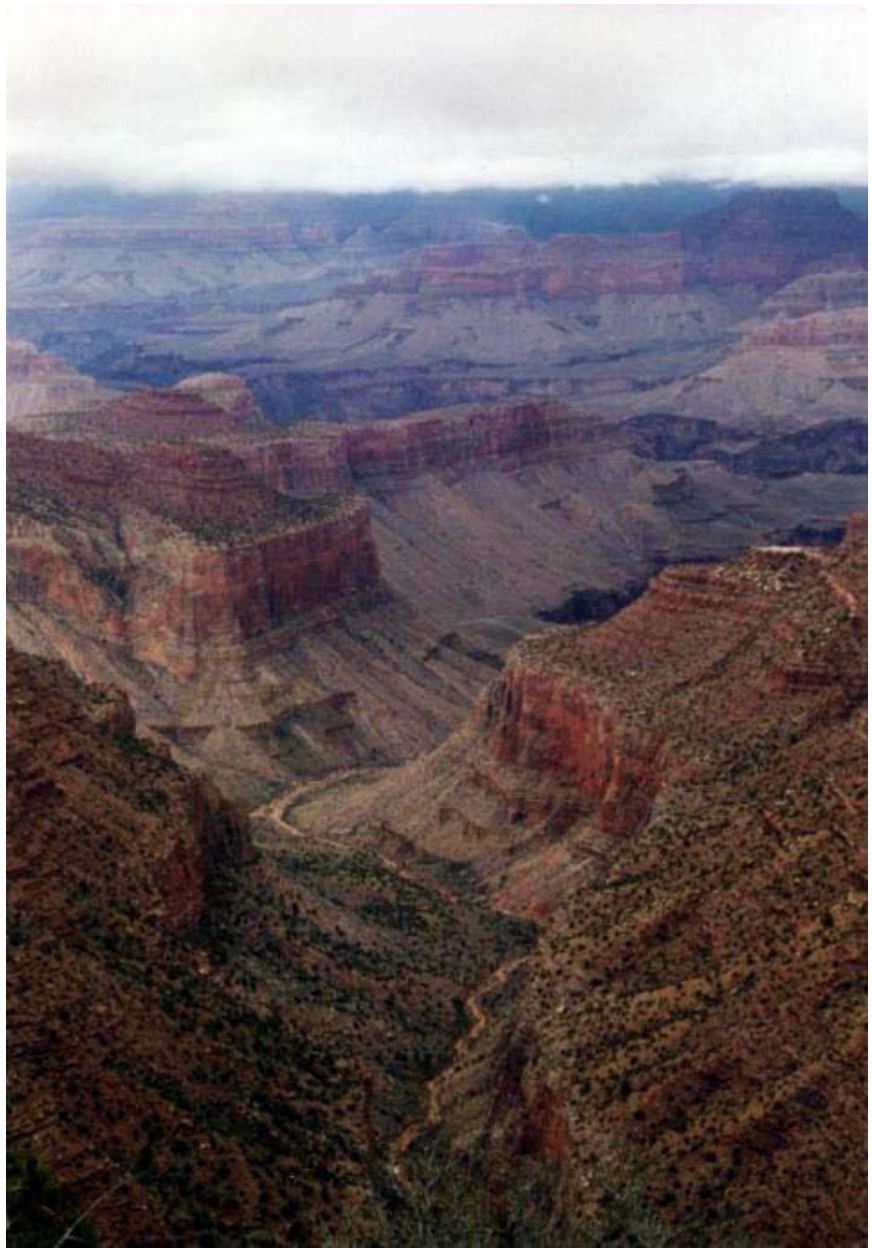

Example of a landscape on Earth with ‘neutral’ ridges and plateaus

Neutral ridges and plateus